e-ISSN 1308-8459

Official Publication of the Turkish Society of Anatomy and Clinical Anatomy

http://dergipark.org.tr/en/pub/anatomy

anatomy

An International Journal of Experimental and Clinical Anatomy

Volume 17 / Issue 1 / April 2023
Published three times a year

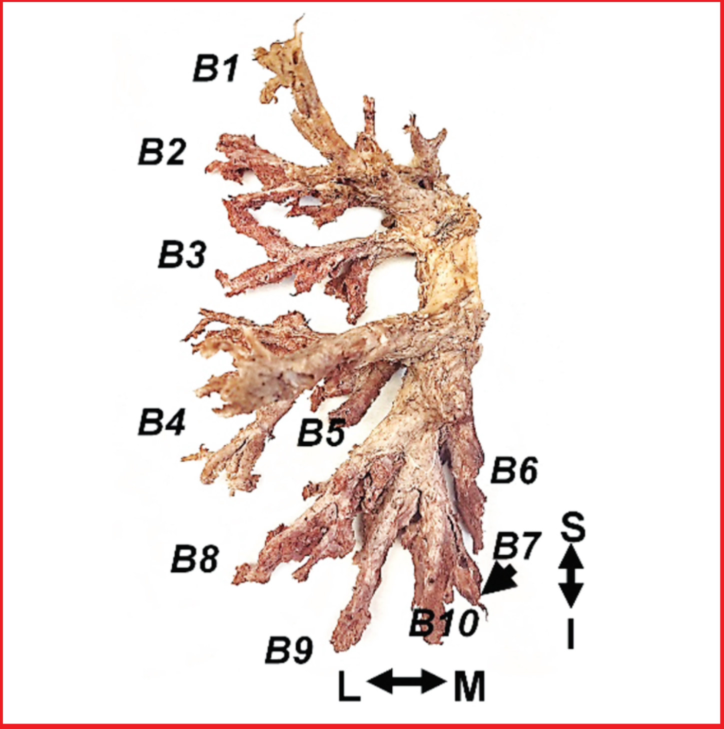

deomed®

https://dergipark.org.tr/tr/pub/anatomy

anatomy

An International Journal of Experimental and Clinical Anatomy

Official Publication of the Turkish Society of Anatomy and Clinical Anatomy

Aim and Scope

Anatomy, an international journal of experimental and clinical anatomy, is a peer-reviewed journal published three times a year with an objective to publish manuscripts with high scientific quality from all areas of anatomy. The journal offers a forum for anatomical investigations involving gross, histologic, developmental, neurological, radiological and clinical anatomy, and anatomy teaching methods and techniques. The journal is open to original papers covering a link between gross anatomy and areas related with clinical anatomy such as experimental and functional anatomy, neuroanatomy, comparative anatomy, modern imaging techniques, molecular biology, cell biology, embryology, morphological studies of veterinary discipline, and teaching anatomy. The journal is currently indexing and abstracting in TUBITAK ULAKBIM Turkish Medical Index, Proquest, EBSCO Host, Index Copernicus and Google Scholar.

Publication Ethics

Anatomy is committed to upholding the highest standards of publication ethics and observes the principles of Journal's Publication Ethics and Malpractice Statement which is based on the recommendations and guidelines for journal editors developed by the Committee on Publication Ethics (COPE), Council of Science Editors (CSE), World Association of Medical Editors (WAME) and International Committee of Medical Journal Editors (ICMJE). Fore detailed information please visit the online version of the journal which is available at https://dergipark.org.tr/tr/pub/anatomy

Authorship

All persons designated as authors should have participated sufficiently in the work to take public responsibility for the content of the manuscript. Authorship credit should be based on substantial contributions to (1) conception and design or analysis and interpretation of data, (2) drafting of the manuscript or revising it for important intellectual content and, (3) final approval of the version to be published. The Editor may require the authors to justify assignment of authorship. In the case of collective authorship, the key persons responsible for the article should be identified and others contributing to the work should be recognized with proper acknowledgment.

Copyright

Publisher

Deomed Publishing
Gür Sok. No:7/B Kadıköy, İstanbul, Türkiye
Phone: +90 216 414 83 43 (Pbx) / Fax: +90 216 414 83 42
www.deomed.com / e-mail: medya@deomed.com

deomed®

Publication Information

Anatomy (e-ISSN 1308-8459) as an open access electronic journal is published by Deomed Publishing, Istanbul, for the Turkish Society of Anatomy and Clinical Anatomy, TSACA. Due the Press Law of Turkish Republic dated as June 26, 2004 and numbered as 5187, this publication is classified as a periodical in English language.

Ownership
On behalf of the Turkish Society of Anatomy and Clinical Anatomy,
Ahmet Kağan Karabulut, MD, PhD; Konya, Türkiye

Editor-in-Chief
Nihal Apaydın, MD
Department of Anatomy,
Faculty of Medicine, Ankara University,
06100, Sıhhıye, Ankara, Türkiye
Phone: 0090 312 595 82 48
e-mail: napaydin@gmail.com; napaydin@medicine.ankara.edu.tr

Administrative Office
Güven Mah. Güvenlik Cad. Onlar Ap. 129/2 Aşağı Ayrancı, Ankara, Türkiye
Phone: +90 312 447 55 52-53

Submission of Manuscripts

Manuscripts should be submitted at our manuscript submission and information portal https://dergipark.org.tr/en/pub/anatomy

Categories of Articles

- ***Original Articles*** describe substantial original research that falls within the scope of the Journal.
- ***Teaching Anatomy*** section contains regular or all formats of papers which are relevant to comparing teaching models or to introducing novel techniques, including especially the own experiences of the authors.
- ***Reviews*** section highlights current development in relevant areas of anatomy. The reviews are generally invited; other prospective authors should consult with the Editor-in-Chief.
- ***Case Reports*** include new, noteworthy or unusual cases which could be of help for basic notions and clinical practice.
- ***Technical Note*** articles cover technical innovations and developments with a specific technique or procedure or a modification of an existing technique. They should be sectioned like an original research article but not exceed 2000 words.
- ***Viewpoint*** articles give opinions on controversial topics or future projections, some of these are invited.
- ***Historical View*** category presents overview articles about historical sections from all areas of anatomy.
- ***Terminology Zone*** category is a platform for the articles which discuss some terminological controversies or opinions.

The categories above are peer-reviewed. They should include abstract and keywords. There are also categories including Letters to the Editor, Book Reviews, Abstracts, Obituary, News and Announcements which do not require a peer review process.

For detailed instructions concerning the submission of manuscripts, please refer to the Instructions to Authors.

Advertising and Reprint Requests

Please direct to publisher. e-mail: medya@deomed.com

Editorial Board

http://dergipark.org.tr/en/pub/anatomy

anatomy
http://dergipark.org.tr/en/pub/anatomy
An International Journal of Experimental and Clinical Anatomy

Anatomy, an international journal of experimental and clinical anatomy, is the official publication of the Turkish Society of Anatomy and Clinical Anatomy, TSACA. It is a peer-reviewed e-journal that publishes scientific articles in English. For a manuscript to be published in the journal, it should not be published previously in another journal or as full text in congress books and should be found relevant by the editorial board. Also, manuscripts submitted to Anatomy must not be under consideration by any other journal. Relevant manuscripts undergo conventional peer review procedure (at least three reviewers). For the publication of accepted manuscripts, author(s) should reveal to the Editor-in-Chief any conflict of interest and transfer the copyright to the Turkish Society of Anatomy and Clinical Anatomy, TSACA.

In the Materials and Methods section of the manuscripts where experimental studies on humans are presented, a statement that informed consent was obtained from each volunteer or patient after explanation of the procedures should be included. This section also should contain a statement that the investigation conforms with the principles outlined in the appropriate version of 1964 Declaration of Helsinki. For studies involving animals, all work must have been conducted according to applicable national and international guidelines. Prior approval must have been obtained for all protocols from the relevant author's institutional or other appropriate ethics committee, and the institution name and permit numbers must be provided at submission.

Anatomical terms used should comply with Terminologia Anatomica by FCAT (1998).

No publication cost is charged for the manuscripts but reprints and color printings are at authors' cost.

Preparation of manuscripts

During the preparation of the manuscripts, uniform requirements of the International Committee of Medical Journal Editors, a part of which is stated below, are valid (*see* ICMJE. Uniform requirements for manuscripts submitted to biomedical journals. Updated content is available at www.icmje.org). The manuscript should be typed double-spaced on one side of a 21×29.7 cm (A4) blank sheet of paper. At the top, bottom and right and left sides of the pages a space of 2.5 cm should be left and all the pages should be numbered except for the title page.

Manuscripts should not exceed 15 pages (except for the title page). They must be accompanied by a cover letter signed by corresponding author and the Conflicts of Interest Disclosure Statement and Copyright Transfer Form signed by all authors. The contents of the manuscript (original articles and articles for Teaching Anatomy category) should include: 1- Title Page, 2- Abstract and Keywords, 3- Introduction, 4- Materials and Methods, 5- Results, 6- Discussion (Conclusion and/or Acknowledgement if necessary), 7- References

Title page

In all manuscripts the title of the manuscript should be written at the top and the full names and surnames and titles of the authors beneath. These should be followed with the affiliation of the author. Manuscripts with long titles are better accompanied underneath by a short version (maximum 80 characters) to be published as running head. In the title page the correspondence address and telephone, fax and e-mail should be written. At the bottom of this page, if present, funding sources supporting the work should be written with full names of all funding organizations and grant numbers. It should also be indicated in a separate line if the study has already been presented in a congress or likewise scientific meeting. Other information such as name and affiliation are not to be indicated in pages other than the title page.

Abstract

Abstract should be written after the title in 100–250 words. In original articles and articles prepared in IMRAD format for Teaching Anatomy category the abstract should be structured under sections Objectives, Methods, Results and Conclusion. Following the abstract at least 3 keywords should be added in alphabetical order separated by semicolumns.

References

Authors should provide direct references to original research sources. References should be numbered consecutively in square brackets, according to the order in which they are first mentioned in the manuscript. They should follow the standards detailed in the NLM's Citing Medicine, 2nd edition (Citing medicine: the NLM style guide for authors, editors, and publishers [Internet]. 2nd edition. Updated content is available at www.ncbi.nlm .nih.gov/books/NBK7256). The names of all contributing authors should be listed, and should be in the order they appear in the original reference. The author is responsible for the accuracy and completeness of references. When necessary, a copy of a referred article can be requested from the author. Journal names should be abbreviated as in *Index Medicus*. Examples of main reference types are shown below:

- **Journal articles:** Author's name(s), article title, journal title (abbreviated), year of publication, volume number, inclusive pages
  - *Standard journal article:* Sargon MF, Celik HH, Aksit MD, Karaagaoglu E. Quantitative analysis of myelinated axons of corpus callosum in the human brain. Int J Neurosci 2007;117:749–55.
  - *Journal article with indication article published electronically before print:* Sengul G, Fu Y, Yu Y, Paxinos G. Spinal cord projections to the cerebellum in the mouse. Brain Struct Funct Epub 2014 Jul 10. DOI 10.1007/s00429-014-0840-7.
- **Books:** Author's name(s), book title, place of publication, publisher, year of publication, total pages (entire book) or inclusive pages (contribution to a book or chapter in a book)
  - *Entire book:*
    - *Standard entire book:* Sengul G, Watson C, Tanaka I, Paxinos G. Atlas of the spinal cord of the rat, mouse, marmoset, rhesus and human. San Diego (CA): Academic Press Elsevier; 2013. 360 p.
    - *Book with organization as author:* Federative Committee of Anatomical Terminology (FCAT). Terminologia anatomica. Stuttgart: Thieme; 1998. 292 p.
    - *Citation to a book on the Internet:* Bergman RA, Afifi AK, Miyauchi R. Illustrated encyclopedia of human anatomic variation. Opus I: muscular system [Internet]. [Revised on March 24, 2015] Available from: http://www.anatomyatlases.org/AnatomicVariants/AnatomyHP.shtml
  - *Contribution to a book:*
    - *Standard reference to a contributed chapter:* Potten CS, Wilson JW. Development of epithelial stem cell concepts. In: Lanza R, Gearhart J, Blau H, Melton D, Moore M, Pedersen R, Thomson J, West M, editors. Handbook of stem cell. Vol. 2, Adult and fetal. Amsterdam: Elsevier; 2004. p. 1–11.
    - *Contributed section with editors:* Johnson D, Ellis H, Collins P, editors. Pectoral girdle and upper limb. In: Standring S, editor. Gray's anatomy: the anatomical basis of clinical practice. 29th ed. Edinburgh (Scotland): Elsevier Churchill Livingstone; 2005. p. 799–942.
  - *Chapter in a book:*
    - *Standard chapter in a book:* Doyle JR, Botte MJ. Surgical anatomy of the hand and upper extremity. Philadelphia (PA): Lippincott Williams and Wilkins; 2003. Chapter 10, Hand, Part 1, Palmar hand; p. 532–641.

Illustrations and tables

Illustrations and tables should be numbered in different categories in the manuscript and Roman numbers should not to be used in numbering. Legends of the illustrations and tables should be added to the end of the manuscript as a separate page. Attention should be paid to the dimensions of the photographs to be proportional with 10x15 cm. Some abbreviations out of standards can be used in related illustrations and tables. In this case, abbreviation used should be explained in the legend. Figures and tables published previously can only be used when necessary for a comparison and only by giving reference after obtaining permission from the author(s) or the publisher (copyright holder).

Author Contribution

Each manuscript should contain a statement about the authors' contribution to the Manuscript. Please note that authorship changes are no longer possible after the final acceptance of an article.

List each author by the initials of names and surnames and describe each of their contributions to the manuscript using the following terms:

- Protocol/project development
- Data collection or management
- Data analysis
- Manuscript writing/editing
- Other (please specify briefly using 1 to 5 words)

For example: NBA: Project development, data collection; AS: Data collection, manuscript writing; STR: Manuscript writing

Funding: information that explains whether and by whom the research was supported.

Conflicts of interest/Competing interests: include appropriate disclosures.

Ethics approval: include appropriate approvals or waivers. Submitting the official ethics approval by whom the research was approved, including the approval date, number or code is necessary.

If the submission uses cadaveric tissue, please acknowledge the donors in an acknowledgement at the end of the paper.

Control list

- Length of the manuscript (max. 15 pages)
- Manuscript format (double space; one space before punctuation marks except for apostrophes)
- Title page (author names and affiliations; running head; correspondence)
- Abstract (100–250 words)
- Keywords (at least three)
- References (relevant to *Index Medicus)*
- Illustrations and tables (numbering; legends)
- Conflicts of Interest Disclosure Statement and Copyright Transfer Form
- Cover letter

All manuscripts must contain the following declaration sections. These should be placed before the reference list at the end of the manuscript.

Original Article

http://dergipark.org.tr/en/pub/anatomy
Received: January 4, 2023; Accepted: April 11, 2023
doi:10.2399/ana.23.1349590

anatomy
An International Journal of Experimental and Clinical Anatomy

Morphological analysis of the distal femur: a radiological study

Cem Özcan

Department of Orthopedics and Traumatology, İzmir Katip Çelebi University, School of Medicine, İzmir, Türkiye

Abstract

Objectives: The morphology of the femur in both proximal and distal parts has been the subject of various studies. The dimensions of the distal femur are important in prosthesis and implant design, especially for knee joints in cases such as total knee arthroplasty. This study aims to enrich the limited literature on distal femur morphology by using computed tomography images of 100 dry femur bones obtained from the human skeleton.

Methods: Computed tomography sections were evaluated for the distal parts of 100 dry human femur bones and parameters such as mediolateral length, anteroposterior width, and medial and lateral condyle widths were measured. Measurement data were presented as means and standard deviations.

Results: As a result of the measurements, the mean mediolateral length was 76.1 mm and the mean anteroposterior width was 59.9 mm. The femoral aspect ratio was 1.27.

Conclusion: Understanding the variations in distal femur morphology will reduce the risk of bone-size mismatch in total knee replacement designs.

Keywords: computed tomography; distal femur; morphology; total knee arthroplasty

Anatomy 2023;17(1):1–4 ©2023 Turkish Society of Anatomy and Clinical Anatomy (TSACA)

Introduction

The femur is the largest bone in the human body, and its morphology in both the proximal and distal parts has been the subject of various studies.[1,2] Studies of femur morphology can be performed using techniques based on data from radiography, computed tomography (CT) , and magnetic resonance imaging (MRI). CT data can be obtained in both two-dimensional and three-dimensional formats.[3–5]

The dimensions of the distal femur are important in prosthesis and implant design, especially for knee joints in cases such as total knee arthroplasty.[6,7] For the design of the knee implant, implant geometry and size are important factors affecting the durability of the prosthesis. Optimizing the size of the implant coating surface area between the bone and the implant component may help prolong the life of prostheses as it reduces stress around the bone and wear on the tibial insert.[8] Distal femur morphology varies greatly and components are produced in a limited range of sizes and morphologies, primarily for economic reasons. Surgeons often have to compromise when choosing the size of a component, which can disrupt rotation and the stability of soft tissues. It has been reported that the components are too large for 66% to 76% of patients undergoing total knee arthroplasty.[9]

This study aims to enrich the limited literature on distal femur morphology by using CT images obtained from 100 dry femur bones from human skeletons.

Materials and Methods

The data source of our study comprised the records of 100 dry adult femur bones for which CT images had been performed in a different study. Bones with pathologies such as fractures, tumors, abnormal deformities, or previous surgeries as well as avascular necrosis, hip dysplasia, or slipped capital femoral epiphysis related to the femoral head were excluded from the study. All female and male bones that did not meet any of the exclusion criteria and exhibited no bone pathologies were included in the study. The results of

CT images (including 3D reconstructions of the femurs) were reviewed to obtain data on morphometric properties. All scans had been performed at a cross-sectional thickness of 0.6 mm (256-slice multidetector scanner; Siemens, Erlangen, Germany). All measurements were made by the author who has more than 10 years of orthopedic experience. The measurements were repeated 2 times and the arithmetic average of the 2 values was used.

Parameters noted in the CT records and their definitions are as follows (Figure 1):

- **Mediolateral length (ML-L):** The distance between the lateral epicondyle and the most prominent point of the medial epicondyle.
- **Anteroposterior width (AP-W):** The distance between the most anterior cortex point and the line connecting the most posterior point of the lateral and medial condylar.
- **Medial anteroposterior width (MAP-W):** The distance between the most anterior and posterior point of the medial condyle.
- **Lateral anteroposterior width (LAP-W):** The distance between the most anterior and posterior point of the lateral condyle.
- **Medial condyle width (MC-W):** The distance between the most medial point and the most lateral point of the medial condyle.
- **Lateral condyle width (LC-W):** The distance between the most medial point and the most lateral point of the lateral condyle.
- **Intercondylar notch width (IN-W):** Width of the intercondylar notch.
- **Femoral aspect ratio (ML-L/AP-W):** The ratio of mediolateral length to anteroposterior width.

Results

As a result of the measurements, the mean mediolateral length was 76.1 mm and the mean anteroposterior width was 59.9 mm. The femoral aspect ratio was 1.27. All measurements of distal femur morphology are shown in Table 1.

Table 1
Morphometric parameters of the distal femur.

Parameters	Mean±SD
ML-L (mediolateral length)	76.1±6.2
AP-W (anteroposterior width)	59.9±5.4
MAP-W (medial anteroposterior width)	65.2±5.4
LAP-W (lateral anteroposterior width)	67.8±5.2
MC-W (medial condyle width)	27.3±3.1
LC-W (lateral condyle width)	25.8±2.9
IN-W (intercondylar notch width)	23.8±3.0
ML-L/AP-W (femoral aspect ratio)	1.27±0.1

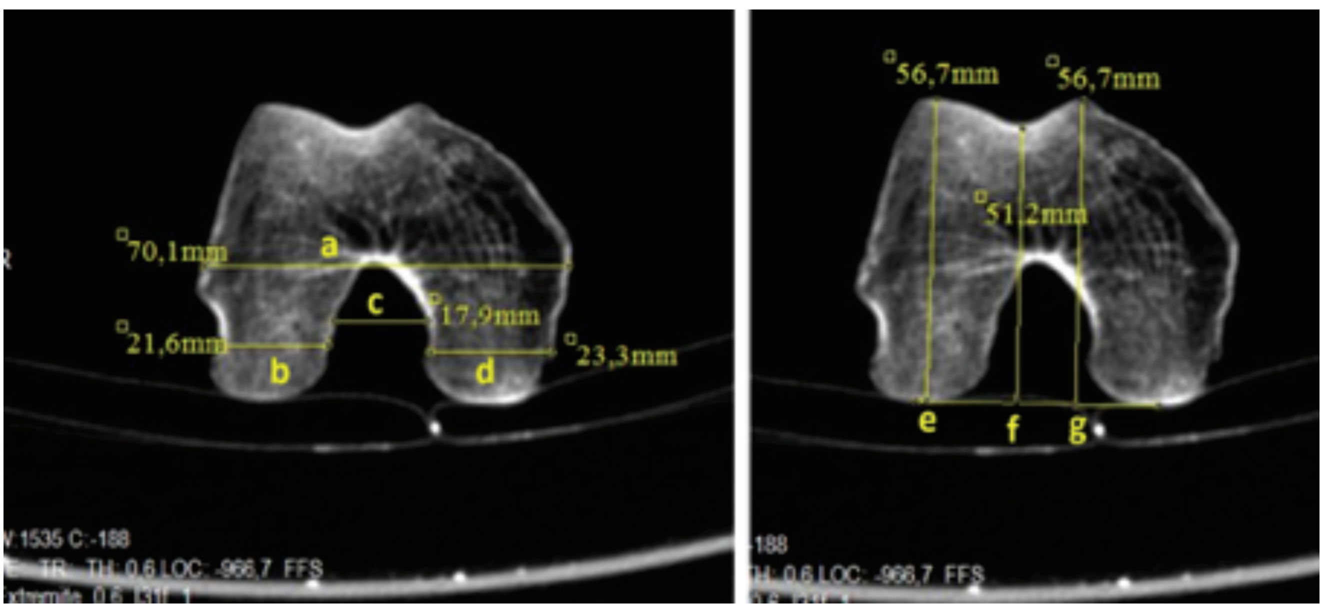

Figure 1. Measurements on CT axial section. The measurements in the figure represent the results in one case. **a:** mediolateral length, **b:** lateral anteroposterior width, **c:** intercondylar notch width, **d:** medial condyle width, **e:** lateral anteroposterior width, **f:** anteroposterior width, **g:** medial anteroposterior width.

Discussion

The morphometric parameters of the distal femur are frequently used in various applications such as gender determination, racial and ethnic identification, and determination of baseline data for the design of knee prostheses.[1,6] Our study has aimed to enrich the limited literature on distal femur morphology by analyzing CT data obtained for dry bones.

The present study showed that, the mediolateral length of the distal femur was 76.1 mm and the anteroposterior width was 59.9 mm. It was observed that the mediolateral length of the femur was greater than the anteroposterior width, and the ML-L/AP-W ratio was 1.27. This ratio was determined by Phombut et al.[10] to be 1.26, showing close similarity to our study.

With improvements in quality of life, changes in lifestyle habits, and increasing life expectancy, the incidence and detection rates of knee diseases are increasing every year. Total knee arthroplasty has made great progress in the general context of the development of orthopedic science in recent years with its wide range of indications and has come to the fore as an important treatment method to improve knee function and quality of life in patients with osteoarthritis, rheumatoid arthritis, and severe knee arthrosis. However, 20% of patients undergoing total knee arthroplasty still report dissatisfaction after surgery.[11] Postoperative outcomes after total knee arthroplasty are closely related to knee prosthesis design and prosthesis placement level. For this reason, it is very important that the intraoperatively applied prosthesis fit the patient's knee geometry. Initial designs for total knee arthroplasty included only one-dimensional femoral components, but knowledge of knee anatomy and prosthetic design have improved significantly over the years.[12] With the increase in studies indicating the differences in distal femur and proximal tibia morphology, manufacturers have introduced implants of different sizes on a wider scale.[2,13–17] Incompatibility between the prosthesis and the osteotomy surface leads to chronic knee pain, instability, and decreased range of motion and may ultimately affect the normal function of the joint.[18] An overly large femoral component causes soft tissue compression, which in turn causes painful irritation of the knee tendons and ligaments, while a small femoral component causes increased blood loss through the exposed spongiosa bone. Mueller et al.[19] reported an increase in midflexion instability in small-sized femurs and attributed this to a decrease in posterior offset. We think that anatomical studies evaluating distal femur morphology in different race, gender, and age groups should be emphasized in light of the danger of incompatibility of total knee prosthesis designs with bone morphology.

The study had some limitations. First, the study material was dry bone, and dry bone that has lost its vitality and water content may change in volume. Second, we did not have access to data such as the genders, ethnicities, or ages of the skeletons from which these bones originated, and the effects of those variables on femur morphology are well known. In spite of these limitations, however, we think that the measurements we have made based on CT images represent safer results compared to other radiographic measurements, and we anticipate that our study will contribute to the literature when evaluated together with other similar studies.

Conflict of Interest

The author declare no conflict of interest.

Ethics Approval

Since the study was conducted from our dry bone CT archive, it does not need ethics committee approval.

Funding

The author did not receive financial support from any person or institution for this study.

References

1. Kim DI, Kwak DS, Han SH. Sex determination using discriminant analysis of the medial and lateral condyles of the femur in Koreans. Forensic Sci Int 2013;233:121–5.
2. Mahfouz M, Abdel Fatah EE, Bowers LS, Scuderi G. Three-dimensional morphology of the knee reveals ethnic differences. Clin Orthop Relat Res 2012;470:172–85.
3. Pinskerova V, Nemec K, Landor I. Gender differences in the morphology of the trochlea and the distal femur. Knee Surg Sports Traumatol Arthrosc 2014;22:2342–9.
4. Cavaignac E, Ancelin D, Reina N, Telmon N, Chiron P. Geometric morphometric analysis reveals ethnic group related differences in the distal femur. Journal of Orthopedic and Trauma Surgery 2016;102: S181.
5. Bansal V, Mishra A, Verma T, Maini D, Karkhur Y, Maini L. Anthropometric assessment of tibial resection surface morphology in total knee arthroplasty for tibial component design in Indian population. J Arthrosc Jt Surg 2018;5:24–8.
6. Cheng FB, Ji XF, Lai Y, Feng JC, Zheng WX, Sun YF, Fu YW, Li YQ. Three dimensional morphometry of the knee to design the total knee arthroplasty for Chinese population. Knee 2009;16:341–7.
7. Yue B, Varadarajan KM, Ai S, Tang T, Rubash HE, Li G. Gender differences in the knees of Chinese population. Knee Surg Sports Traumatol Arthrosc 2011;19:80–8.
8. Koh YG, Jung KH, Hong HT, Kim KM, Kang KT. Optimal design of patient-specific total knee arthroplasty for improvement in wear performance. J Clin Med 2019;8:2023.
9. Mahoney OM, Kinsey T. Overhang of the femoral component in total knee arthroplasty: risk factors and clinical consequences. J Bone Joint Surg Am 2010;92:1115–21.

10. Phombut C, Rooppakhun S, Sindhupakorn B. Morphometric analysis and three-dimensional computed tomography reconstruction of Thai distal femur. Applied Sciences 2021;11:1052.
11. Gunaratne R, Pratt DN, Banda J, Fick DP, Khan RJK, Robertson BW. Patient dissatisfaction following total knee arthroplasty: a systematic review of the literature. J Arthroplasty 2017;32:3854–60.
12. Insall JN, Hood RW, Flawn LB, Sullivan DJ. The total condylar knee prosthesis in gonarthrosis. A five to nine-year follow-up of the first one hundred consecutive replacements. J Bone Joint Surg Am 1983;65:619–28.
13. Hitt K, Shurman 2nd JR, Greene K, McCarthy J, Moskal J, Hoeman T, Mont MA. Anthropometric measurements of the human knee: correlation to the sizing of current knee arthroplasty systems. J Bone Joint Surg Am 2003;85:115–22.
14. Lonner JH, Jasko JG, Thomas BS. Anthropomorphic differences between the distal femora of men and women. Clin Orthop Relat Res 2008;466:2724–9.
15. Barrett WP. The need for gender-specific prostheses in TKA: does size make a difference? Orthopedics 2006;29:S53–5.
16. MacDonald SJ, Charron KD, Bourne RB, Naudie DD, McCalden RW, Rorabeck CH. The John Insall Award: gender-specific total knee replacement: prospectively collected clinical outcomes. Clin Orthop Relat Res 2008;466:2612–6.
17. Merchant AC, Arendt EA, Dye SF, Fredericson M, Grelsamer RP, Leadbetter WB, Post WR, Teitge RA. The female knee: anatomic variations and the female-specific total knee design. Clin Orthop Relat Res 2008;466:3059–65.
18. Kawahara S, Okazaki K, Okamoto S, Iwamoto Y, Banks SA. A lateralized anterior flange improves femoral component bone coverage in current total knee prostheses. Knee 2016;23:719–24.
19. Mueller JKP, Wentorf FA, Moore RE. Femoral and tibial insert downsizing increases the laxity envelope in TKA. Knee Surg Sports Traumatol Arthrosc 2014;22:3003–11.

ORCID ID:
C. Özcan 0000-0002-1541-2484

deomed®

Correspondence to: Cem Özcan, MD
Department of Orthopedics and Traumatology, İzmir Katip Çelebi University, School of Medicine, İzmir, Türkiye
Phone: +90 532 623 18 20
e-mail: cemozca@gmail.com

Conflict of interest statement: No conflicts declared.

 How to cite this article: Özcan C. Morphological analysis of the distal femur: a radiological study. Anatomy 2023;17(1):1–4.

Original Article

http://dergipark.org.tr/en/pub/anatomy
Received: January 11, 2023; Accepted: April 12, 2023
doi:10.2399/ana.23.1348742

http://dergipark.org.tr/en/pub/anatomy
anatomy
An International Journal of Experimental and Clinical Anatomy

Renal vascular and ureteral variations in patients with kidney transplantation

Atilla Satır[1], Meriç Yıldız Yılmaz[2], Murat Öztürk[1], Erdoğan Şendemir[3], Hakan Demirci[4]

[1]*Department of Urology, Bursa Yüksek İhtisas Training and Research Hospital, University of Health Sciences, Bursa, Türkiye*
[2]*Specialist of Anatomy, Private Office, Bursa, Türkiye*
[3]*Department of Anatomy, Faculty of Medicine, Bursa Uludağ University, Bursa, Türkiye*
[4]*Department of Family Medicine, Bursa Yüksek İhtisas Training and Research Hospital, University of Health Sciences, Bursa, Türkiye*

Abstract

Objectives: To investigate the renal vascular and ureteral variations in patients subjected to kidney transplantation.

Methods: This retrospective study was conducted between January 2018 and December 2021. A total of 233 donors who underwent cadaveric harvesting were included in the study. By using the operation records, the numbers of the participants' right and left renal arteries, right and left renal veins and right and left ureters were evaluated.

Results: The mean age of participants was 54.41±17.76 years, and 58.8% were males. Multiple renal vessels were detected in 77 (33%) donors, and ureter duplication was detected in 3 (1.2%) donors. No significant difference was observed between the right and left kidneys and between sexes regarding the incidence of supernumerary renal vessels and ureters. There was a substantial relationship between the supernumerary renal artery and vein count on the right side (p=0.024 when dichotomized for artery count, p=0.004 when dichotomized for vein count).

Conclusion: Anatomical differences in vascular structures and ureters may create risks that will affect the outcome of kidney surgeries and transplants. During kidney transplantation, interventional radiological procedures or other retroperitoneal surgeries, surgeons and radiologists are advised to remember that supernumerary renal arteries and veins are likely to be concurrent, especially on the right side.

Keywords: kidney surgery; supernumerary renal vessels; transplantation; ureter duplication; harvesting

Anatomy 2023;17(1):5–12

Introduction

Morphological kidney variations can be seen frequently, although frequency varies according to ethnic and racial differences.[1,2] These variations may be related to the kidney itself, such the presence of ectopic kidney[3] or horseshoe kidney,[4] and may also be directly associated with variations in the renal artery, renal vein and ureters.[1] The most common variations related to the renal artery are supernumerary renal artery (SRA) and early bifurcation of renal artery.[1,5] Supernumerary renal vein (SRV),[6] retroaortic left renal vein,[7] plexiform renal vein[8] and late confluence of renal vein[9] can be counted among the well-known variations of the renal vein. Ureteral duplication and dilatation are anatomical variations of the ureter.[10]

Anatomical variations in arteries, veins and ureters can create extra risks for the donor, recipient and graft during kidney transplantation. Additionally, missing such structural differences during intra-abdominal operations and radiological interventions may cause bleeding, pyeloureteral necrosis, increased complications, and may even necessitate conversion of laparoscopic operations to open surgery.[1,8,11] Moreover, especially SRV presence has been associated with increased spread of cancer cells throughout the body and these vessels are critical for the placement of caval filters.[8,12] It is also known that multiple ureter complicates renal transplantation surgeries and increase the risk of complications after transplantation.[13] The prevalence of SRA is estimated to be 2–56% and 2–67% in the right and left sides, respectively.[14,15] SRV frequency on the right and left sides has been reported between 7–38% and 0–9%, respectively.[12,16,17] Finally, multiple ureter has been detected in 0.1–1.1% of individuals.[10,18,19] The incidence of these variations may show ethnic and racial differences.[1,20] Therefore, knowing population- and sex-specific frequencies and type of multiplicity on the right and left sides (arteries, veins and ureters) can provide important advantages in diagnostic imaging, interventional radiological procedures, retroperitoneal surgical procedures and renal transplantation.[1,12,21,22] There are many studies in the literature which have examined renal vessel variations.[1,9,11] However, the number of studies in which both renal vessels and ureters are evaluated with respect to sex and side are limited.[18]

In this study, we aimed to investigate the renal vascular and ureteral variations in patients subjected to kidney transplantation harvesting.

Materials and Methods

This study is a retrospective study evaluating the operations performed by Bursa Regional Organ and Tissue Transplant Coordination Center between January 2018 and December 2021 in Turkey. A total of 233 donors who underwent kidney harvesting for donor kidney vessels assessment before renal transplantation were included in the study. All samples and information were recorded anonymously. Donors whose anatomy of the artery, vein, and ureter of both kidneys could not be clearly evaluated by any reason, and donors who did not have one and have ectopic kidney were excluded from the study (n=18).

The primary outcome was to evaluate whether there were significant differences in the number of renal arteries, renal veins and ureters between the right and left kidneys. The secondary outcomes were to investigate whether there were significant differences in the numbers of right and left kidney renal arteries, renal veins and ureters between males and females and to ascertain whether there was a significant relationship between the number of SRA and SRV in the right and left kidneys, separately.

All analyses were performed on IBM SPSS Statistics for Windows, Version 25.0 (IBM Corp., Armonk, NY, USA), and with a statistical significance threshold of $p<0.05$. Mean±standard deviation was used to summarize continuous variables, while absolute and relative frequency were used for categorical variables. Age was analyzed with the independent samples t-test. Analyses between right and left side were performed with the McNemar test or marginal homogeneity test depending on number of categories. For the analysis of relationships between artery and vein counts, variables were dichotomized for both artery and vein count (n=1 vs. n≥2) with relative assessment according to exact numbers (n=1, n=2, n=3). Between-groups analysis of categorical variables was performed with the Fisher's exact test or the Fisher-Freeman-Halton test.

Results

Overall mean age was 54.41±17.76 years and 58.8% of the participants were males. Multiple renal vessels were detected in 77 (33%) donors and ureter duplication was detected in 3 (1.2%) donors (**Figure 1**). SRA anomalies were present in 68 (29.1%) donors and 8 (3.4%) of them had concomitant SRV. Right-sided SRA was detected in 40 donors (17.1%), left-sided in 40 donors (17.1%), and bilateral SRA in 12 (5.1%) donors. SRV was present in 17 (7.3%) donors, of which 11 (4.7%) were on the right, 6 (2.6%) were on the left, while none of the participants had bilateral SRV anomalies. Bilateral ureteral duplication was not detected in any donor. No significant difference was observed between the right and left kidneys in terms of the number of renal arteries (p=0.808), the number of renal veins (p=0.180), and the number of ureters (p=1.000) (**Table 1**) and (**Figure 2**).

The mean age of females was significantly higher than male (p=0.005). There was no significant difference between the sexes in terms of the numbers of right and left renal arteries (p=0.179 and 0.247, respectively), renal veins (p=0.603 and 1.000, respectively) and ureters (p=1.000 for both sides) (**Table 2**). There was a significant relationship between SRA count and SRV count on the right side (p=0.024 when dichotomized for artery count, p=0.004 when dichotomized for vein count) (**Table 3**).

Figure 1. Double artery kidney. **Black arrows:** arteries.

Table 1
Summary of the numbers of arteries, veins and ureters with regard to side.

		Right (n=233)	Left (n=233)	p-value
Number of arteries	1	193 (82.8%)	193 (82.8%)	
	2	39 (16.7%)	37 (15.9%)	0.808
	3	1 (0.4%)	3 (1.3%)	
Number of veins	1	222 (95.3%)	227 (97.4%)	
	2	10 (4.3%)	6 (2.6%)	0.180
	3	1 (0.4%)	0 (0.0%)	
Number of ureters	1	232 (99.6%)	231 (99.1%)	1.000
	2	1 (0.4%)	2 (0.9%)	h

Data are given as frequency (percentage).

Discussion

Morphological variations of renal vessels and ureter are mostly asymptomatic and diagnosed incidentally. The importance of these clinically silent conditions emerges especially in retroperitoneal surgeries, renal transplantations and interventional radiological procedures.[8] Since the prevalence of these variations may show ethnic differences[1,2] and considering that the most common variations are additional vessel(s) or ureter(s), we aimed to determine the frequencies of multiple-renal vessels and ureters with respect to the right and left kidneys and sexes in a population from Turkey. There was no significant difference between the right and left kidneys and between males and females in terms of supernumerary vessels and ureters. It was observed that there was a significant positive correlation between the number of SRA and the number of SRV on the right side.

The importance of accessory arteries is evident in many clinical situations.[1] It is especially important to detect SRAs in kidney transplant, since these variations

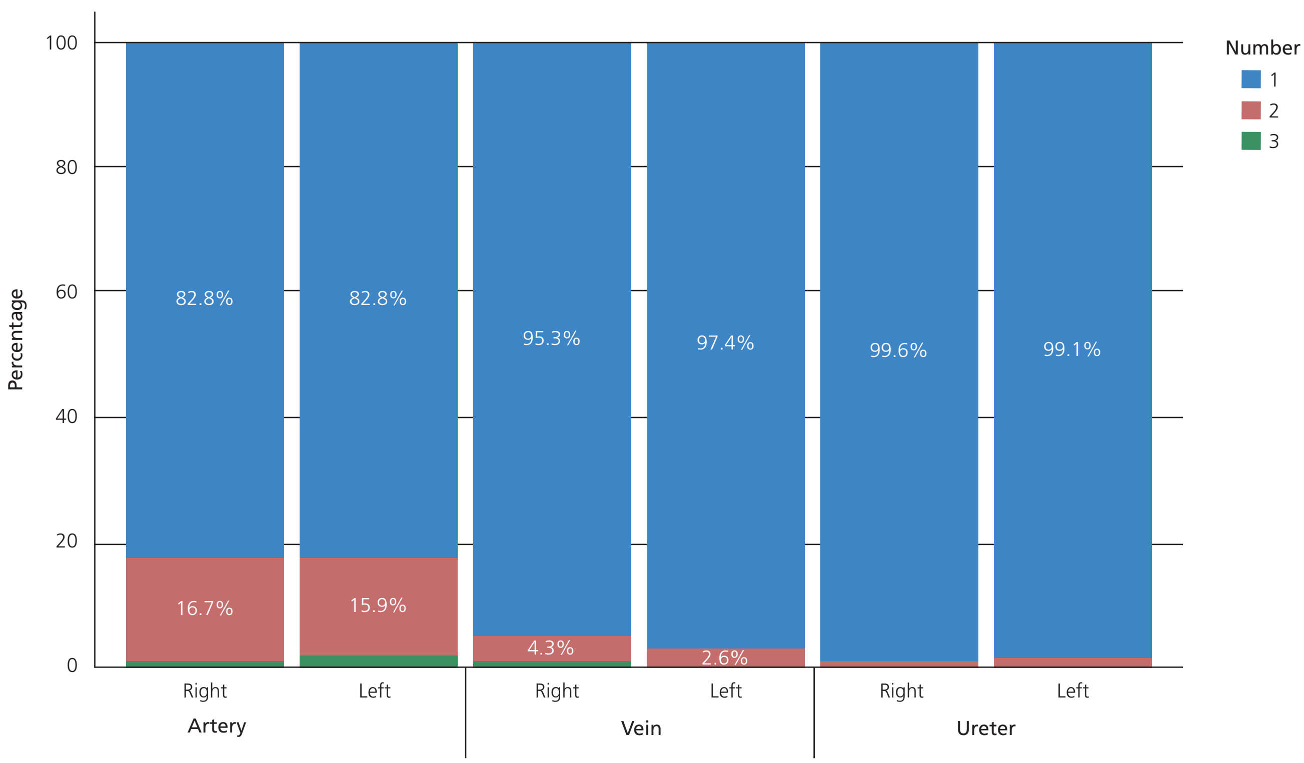

Figure 2. Distribution of the numbers of arteries, veins and ureters.

Table 2
Summary of the numbers of arteries, veins and ureters with regard to sex.

		Female (n=96)	Male (n=137)	p-value
Number of arteries, right	1	84 (87.5%)	109 (79.6%)	0.179
	2	12 (12.5%)	27 (19.7%)	
	3	0 (0.0%)	1 (0.7%)	
Number of arteries, left	1	78 (81.3%)	115 (83.9%)	0.247
	2	18 (18.8%)	19 (13.9%)	
	3	0 (0.0%)	3 (2.2%)	
Number of veins, right	1	91 (94.8%)	131 (95.6%)	0.603
	2	4 (4.2%)	6 (4.4%)	
	3	1 (1.0%)	0 (0.0%)	
Number of veins, left	1	94 (97.9%)	133 (97.1%)	1.000
	2	2 (2.1%)	4 (2.9%)	
	3	0 (0.0%)	0 (0.0%)	
Number of ureters, right	1	96 (100.0%)	136 (99.3%)	1.000
	2	0 (0.0%)	1 (0.7%)	
Number of ureters, left	1	95 (99.0%)	136 (99.3%)	1.000
	2	1 (1.0%)	1 (0.7%)	

Data are given as mean±standard deviation for continuous variables and as frequency (percentage) for categorical variables.

Table 3
Relationships between numbers of arteries and veins.

		Number of arteries, right		
		1 (n=193)	≥2 (n=40)	p-value
Number of veins, right	1	187 (96.9%)	35 (87.5%)	**0.024**
	2	5 (2.6%)	5 (12.5%)	
	3	1 (0.5%)	0 (0.0%)	
		Number of arteries, left		
		1 (n=193)	**≥2 (n=40)**	**p-value**
Number of veins, left	1	188 (97.4%)	39 (97.5%)	1.000
	2	5 (2.6%)	1 (2.5%)	
	3	0 (0.0%)	0 (0.0%)	
		Number of veins, right		
		1 (n=222)	**≥2 (n=11)**	**p-value**
Number of arteries, right	1	187 (84.2%)	6 (54.5%)	**0.004**
	2	35 (15.8%)	4 (36.4%)	
	3	0 (0.0%)	1 (9.1%)	
		Number of veins, left		
		1 (n=227)	**≥2 (n=6)**	**p-value**
Number of arteries, right	1	188 (82.8%)	5 (83.3%)	1.000
	2	36 (15.9%)	1 (16.7%)	
	3	3 (1.3%)	0 (0.0%)	

Data are given as frequency (percentage).

may create special conditions for both the donor and the recipient. Their potential effects include the transplant decision, nephrectomy method, operation side, selection of donor, graft ischemia duration, and greater risk of complications.[1,11] In addition to kidney transplant, these variations or anomalies should be considered during other intraabdominal operations.[1,22,23] SRVs may cause undesirable consequences and difficulties for both the donor/recipient and surgeons during kidney transplant and other surgeries.[23] In the presented study, we determined the rate of supernumerary renal vessels as 33%, SRA rate as 29.1% (17.1% on the right and left), and SRV rate as 7.3% (4.7% on the right, 2.6% on the left). Bilateral SRA ratio was 5.1%, and bilateral SRV was not detected in any donor. There was no significant difference between the right and left sides in terms of the incidence of SRA and SRV. In the computed tomography angiography (CTA) study of Gupta et al.,[1] renal vessel variations were investigated and the frequency of overall SRA was found to be 43.5% (28.70% on the right side, 29.62% on the left side, 14.81% bilateral). The frequency of SRV was 8.3%, and interestingly, all of these variations were right-sided. In another study conducted in Turkey, the renal vessels of 70 kidney donors were evaluated by CTA. SRA was detected in 40 (29.6%) of the 140 kidneys and SRV was identified in 3 (2.1%). In this study, no significant difference was found between the right and left kidneys in terms of SRA.[11] In another study from Turkey, the incidence of SRV and SRA on the right and left sides also was found to be similar.[24] Our findings in this study were similar to the data reported in the Turkish population.[11,24] SRV anomaly was reported at higher rates in our study. This difference may have arisen because the data evaluated in our study was higher and the venous anatomy was more variable.[11,24]

Although many studies on the subject report varying frequencies, it can be said that the frequency of SRA is higher than that of SRV in the majority of literature,[11,25] and that SRVs are seen more frequently on the right side.[8,12,17] The literature concerning the comparison of SRA and SRV frequencies on the right and left sides is inconsistent. While there are those who argue that the frequency is similar.[11,26–28] there are also studies that argue that these variations are more common on the right[24,29] or on the left.[1,30] The fact that SRV is more common on the right side is thought to be due to the different embryological origins and developmental processes of the right and left renal veins.[1,8,12,31] There are also studies that do not conform to this generalization.[5,26,27] But, whatever the reason for these differences, with regard to the reasons outlined above, surgeons and radiologists need to consider the risk and frequency of abnormalities in right and left renal vessels in their population. For instance, the presence of the inferior vena cava on the right causes the left renal vein to be longer, making the left kidney a better transplant candidate than the right due to ease of anastomosis. However, if there are multiple arteries in the left kidney, this may result in preference of the right kidney (even though the vein is shorter) in order to reduce the risk of vascular injury and to shorten ischemia duration.[11,23]

In the current study, we also evaluated the relationship between the number of SRA and the number of SRV for the right and left kidneys separately. According to our results, there was a significant relationship between the number of SRA and the number of SRV on the right side, but no such relationship on the left side. In addition, we also observed that the donor who had 3 renal veins on the right side had 1 renal vein on the left and 1 renal artery on each side. In the observational study of Ikidag et al.,[11] it was reported that a patient with 3 renal veins on the right had 1 renal artery on the right, 2 renal arteries and 2 polar arteries on the left. Deshpande et al.[32] published a case report presenting a patient with 3 renal arteries on the right, 2 renal arteries on the left, and 2 renal veins on the right. We did not come across any other study in which this relationship was investigated. Although CTA scan performed before renal transplantation can accurately detect renal vessel abnormalities with a highly-respectable sensitivity, it should be kept in mind that the sensitivity is not 100%, especially if such variations are not suspected.[5,24] In one study, CTA findings were found to be correlated well with the intraoperative findings in only 72.7% of patients.[5] Therefore, we recommend that when SRA or SRV anomaly is encountered both during renal transplantation and other intra-abdominal operations as well as during interventional radiological procedures, it should be considered that there may be other accompanying supernumerary opposite vessels, especially on the right side. The limitations of imaging methods in radiological studies increase the importance of surgical and cadaver studies. Anomalies of position, rotation, and duplication of the collection system are rarely encountered compared to renal vessel variations. They are caused by anomalies in the morphogenesis of the urinary system.[10] Ureter duplication frequency has been reported to be around 1%.[18,19] Depending on the type and severity of duplication, it may be asymptomatic, or it may be a cause of vesicoureteral reflux, incontinence, ureterocele, obstructive uropathy, renal parenchymal scarring, dysplasia and decreased renal function.[33] In this study, we detected ureteral duplication in only 3 donors (1.2%). None of these had bilateral duplications. One of the donors also had 2 renal arteries on both sides. In a study of 254 deceased donors, ureteral duplication was found in 3 subjects (2 left- and 1 right-sided).[18] Ureteral duplication may also accompany renal vascular anomalies. Other studies have also presented cases with ureteral duplication concurrent with multiple renal vessel anomalies.[19,34] Therefore, when radiologists and surgeons detect ureteral duplication, they should make extra evaluations and be more careful for other accompanying collector system or vessel anomalies. Additionally, when incidental accessory vessels are detected preoperatively or intraoperatively, it should be taken into account that undetected ureteral duplication may be present. This will allow the surgeon to approach the pedicle more carefully, especially during renal graft removal. In addition, since presence of multiple ureter may also be effective in donor selection, its detection is of particular importance. Indeed, high complication rates have been reported in kidney transplants with multiple ureters.[13]

Our investigation did not reveal any difference between a significant difference between males and females in terms of the number of renal arteries, renal veins and ureters on either the right or left side. The studies by Ferhatoglu et al.[24] and Ikidag et al.[11] also found no significant differences between the sexes in terms of SRA and SRV frequencies. These findings are also supported by other literature.[27,28,35] However, in a retrospective evaluation of CTA images of 820 patients, Gumus et al.[36] found the incidence of SRA to be significantly higher in males on both sides. Another retrospective study reported that the overall rate of renal vascular variation was significantly higher in male.[37] In the same study, it was reported that the percentage of males with SRA was higher than females (31.1% vs 15.2%), and the percentage of females with SRV was higher than male (10.2% vs 8.2%), but the significance of these differences was not given.[37] It is also important to note that urinary tract duplication is encountered more frequently in females.[33]

In our study, no significant effect of sex on the frequency of ureteral duplication was observed, but this may be due to the low number of cases. Sex does not seem to have a clear effect on numerical anomalies of the renal vessels; however, more studies that are comprehensive are required to reach a definite conclusion.

This study has considerable advantages over others, including the fact that SRA, SRV and multiple ureters were evaluated together. Additionally, cross-sectional analysis of these abnormalities between the right and left sides and between the sexes was performed. The numerical relationship between SRA and SRV was also investigated. The number of cases included is higher than in many similar studies conducted in Turkey. However, some critical limitations should be noted. It is a single-center study, so its results cannot be generalized to the entire population. The retrospective design prevented the inclusion of prospective data, which may have been valuable in cases where additional imaging may have been required. Also, other anomalies that may be important in radiological interventions and surgeries such as polar vessels, vessel and ureter diameters, early branching arteries, complete or incomplete ureteral duplication[1,5] were not investigated. Evaluation was made only on CTA data, and although CTA and visual detection are usually consistent,[11,24] some studies have reported that there may be differences in the rates of radiologically-detected variations and intraoperatively-detected variations.[5,24] Finally, despite high patient count, multicenter studies with more cases are needed to provide data on a national scale.

Conclusion

The incidence of SRA, SRV, and duplicated ureter did not differ significantly between the right and left sides and between males and females. There was a significant positive correlation between the incidence of SRA and SRV on the right side. We also found that SRA was more frequent compared to SRV and ureter duplication. During interventional radiological procedures, kidney transplantation or other retroperitoneal surgeries, both surgeons and radiologists are advised to keep in mind that SRA and SRV are likely to be concurrent, especially on the right side.

Conflict of Interest

There is no competing interest.

Author Contributions

AS: protocol/project development, data collection or management, literature review, manuscript writing/editing; MYY: protocol/project development, data collection or management, literature review manuscript writing/editing; MÖ: protocol/project development, literature review, supervision; EŞ: protocol/project development, literature review, supervision; HD: protocol/project development, literature review, supervision.

Ethics Approval

The protocol of this study was approved by the Ethics Committee of the Health Sciences Bursa Yüksek İhtisas Training and Research Hospital, with the date: May 12, 2021, no: 2011-KAEK-25 and conducted by the ethical standards as laid down in the 1964 Declaration of Helsinki and its later amendments. Since the study is retrospective, the Medical Ethics Committee did not require written informed consent from donors. All samples and information were recorded anonymously.

Funding

The authors received no financial support for the research, authorship, and publication of this article.

References

1. Gupta M, Kaul NV, Shukla AK. A contrast-enhanced MDCT study on the morphology of renal vessels, their variations and clinical implications. International Journal of Anatomy and Research 2022; 10:8275–82.
2. Gulas E, Wysiadecki G, Szymański J, Majos A, Stefańczyk L, Topol M, Polguj M. Morphological and clinical aspects of the occurrence of accessory (multiple) renal arteries. Arch Med Sci 2018;14:442–53.
3. Rosenblum ND, Baskin LS. Renal ectopic and fusion anomalies. [Internet]. [Retrieved on February 12, 2023]. Available from: https://medilib.ir/uptodate/show/6107
4. Agarwal S, Yadav RN, Kumar M, Sankhwar S. Horseshoe kidney with unilateral single ectopic ureter. BMJ Case Rep 2018;2018: bcr2017223913.
5. Jose N, Jayaprakash V, Deiva A, Sai V, Jayakumar M. Renal angiographic evaluation of prospective renal donors: Single-center data and outcome analysis from South India – A retrospective observational study. Indian Journal of Transplantation 2021;15:24–8.
6. Abas R, Asri SFM, Nor NHM, Basir R, Subramaniam SD. A case report of superior bilateral aberrant renal arteries with accessory left renal vein. Journal of Health and Translational Medicine 2022;25:5–8.
7. Madhunarayana B, Rao S, Rajagopalan R. Retro-aortic left renal vein draining into left common iliac vein: a rare renal vein anomaly and its significance. International Journal of Anatomical Variations 2019; 12:1.
8. Gupta A, Gupta R, Singal R. Congenital variations of renal veins: embryological background and clinical implications. Journal of Clinical and Diagnostic Research 2011;5:1140–3.
9. Agarwal S, Aiyappan SK, Mathuram AC, Raveendran NH, Valsala VS. Prevalence of renal vascular variations in patients subjected to contrast CT abdomen. International Journal of Contemporary Medicine Surgery and Radiology 2019;4:B114–9.
10. Dodeja A, Mane R, Mukherjee A, Dodeja A. A rare case report of bilateral duplication of ureter along with presence of accessory renal vein: embryological basis and clinical implication. International Journal of Medical Science and Current Research 2020;3:94.
11. Ikidag MA, Uysal E. Evaluation of vascular structures of living donor kidneys by multislice computed tomography angiography before transplant surgery: is arterial phase sufficient for determination of both arteries and veins? Journal of the Belgian Society of Radiology 2019;103:23.
12. Kumaresan M, Pk S, Gunapriya R, Karthikeyan G, Priyadarshini A. Morphometric study of renal vein and its variations using CT. Indian Journal of Medical Research and Pharmaceutical Sciences 2016;3: 41–9.
13. Haferkamp A, Dörsam J, Möhring K, Wiesel M, Staehler G. Ureteral complications in renal transplantation with more than one donor ureter. Nephrol Dial Transplant 1999;14:1521–4.
14. Palmieri BJ, Petroianu A, Silva LC, Andrade LM, Alberti LR. Study of arterial pattern of 200 renal pedicle through angiotomography. Rev Col Bras Cir 2011;38:116–21.
15. Hlaing K, Das S, Sulaiman IM, Abd-Latiff A, Abd-Ghafar N, Suhaimi FH, Othman F. Accessory renal vessels at the upper and lower pole of the kidney: a cadaveric study with clinical implications. Bratisl Lek Listy 2010;111:308–10.
16. Satyapal KS, Rambiritch V, Pillai G. Additional renal veins: incidence and morphometry. Clin Anat 1995;8:51–5.
17. Mishall PL. Renal arteries. In: Tubbs RS, Shoja MM, Loukas M, editors. Bergman's comprehensive encyclopedia of human anatomic variation. Chapter 55. Haboken, NJ: Wiley-Blackwell; 2016. p. 682–93.
18. Costa H, Moreira R, Fukunaga P, Fernandes R, Boni R, Matos A. Anatomic variations in vascular and collecting systems of kidneys from deceased donors. Transplant Proc 2011;43:61–3.
19. Stojadinovic D, Zivanovic-Macuzic I, Sazdanovic P, Jeremic D, Jakovcevski M, Minic M, Kovacevic M. Concomitant multiple anomalies of renal vessels and collecting system. Folia Morphol 2020;79:627–33.
20. Gulas E, Wysiadecki G, Cecot T, Majos A, Stefańczyk L, Topol M, Polguj M. Accessory (multiple) renal arteries - differences in frequency according to population, visualizing techniques and stage of morphological development. Vascular 2016;24:531–7.
21. Deák P, Doros A, Lovró Z, Toronyi E, Kovács JB, Végsö G, Piros L, Tóth S, Langer RM. The significance of the circumaortic left renal vein and other venous variations in laparoscopic living donor nephrectomies. Transpl Proc 2011;43:1230–2.
22. Aragão JA, Santos RM, Aragão FMSA, Aragão ICSA, Carvalho HDG, Matos ÍQ, Reis FP. Multiple renal vessels: a case report. International Journal of Anatomy and Research 2017;5:4460–62.
23. Arévalo Pérez J, Gragera Torres F, Marín Toribio A, Koren Fernández L, Hayoun C, Daimiel Naranjo I. Angio CT assessment of anatomical variants in renal vasculature: its importance in the living donor. Insights Imaging 2013;4:199–211.
24. Ferhatoglu MF, Atli E, Gürkan A, Kebudi A. Vascular variations of the kidney, retrospective analysis of computed tomography images of ninety-one laparoscopic donor nephrectomies, and comparison of computed tomography images with perioperative findings. Folia Morphol (Warsz) 2020;79:786–92.
25. Raman SS, Pojchamarnwiputh S, Muangsomboon K, Schulam PG, Gritsch HA, Lu DS. Utility of 16-MDCT angiography for comprehensive preoperative vascular evaluation of laparoscopic renal donors. AJR Am J Roentgenol 2006;186:1630–8.
26. Turba UC, Uflacker R, Bozlar U, Hagspiel KD. Normal renal arterial anatomy assessed by multidetector CT angiography: are there differences between men and women? Clin Anat 2009;22:236–42.
27. Hassan SS, El-Shaarawy E, Johnson JC, Youakim MF, Ettarh R. Incidence of variations in human cadaveric renal vessels. Folia Morphol (Warsz) 2017;76:394–407.
28. Natsis K, Paraskevas G, Panagouli E, Tsaraklis A, Lolis E, Piagkou M, Venieratos D. A morphometric study of multiple renal arteries in Greek population and a systematic review. Rom J Morphol Embryol 2014;55:1111–22.
29. Ozkan U, Oguzkurt L, Tercan F, Kizilkilic O, Koc Z, Koca N. Renal artery origins and variations: angiographic evaluation of 855 consecutive patients. Diagn Interv Radiol 2006;12:183–6.

30. Zagyapan R, Pelin C, Kürkçüoğlu A. A retrospective study on multiple renal arteries in Turkish population. Anatomy 2009;3:35–9.

31. Kumar S, Neyaz Z, Gupta A. The utility of 64 channel multidetector CT angiography for evaluating the renal vascular anatomy and possible variations: a pictorial essay. Korean J Radiol 2010;11:346–54.

32. Deshpande SH, Bannur BM, Patil BG. Bilateral multiple renal vessels: a case report. J Clin Diagn Res 2014;8:144–5.

33. Didier RA, Chow JS, Kwatra NS, Retik AB, Lebowitz RL. The duplicated collecting system of the urinary tract: embryology, imaging appearances and clinical considerations. Pediatr Radiol 2017;47:1526–38.

34. Madhyastha S, Suresh R, Rao R. Multiple variations of renal vessels and ureter. Indian Journal of Urology 2001;17:164–5.

35. Majos M, Stefańczyk L, Szemraj-Rogucka Z, Elgalal M, De Caro R, Macchi V, Polguj M. Does the type of renal artery anatomic variant determine the diameter of the main vessel supplying a kidney? A study based on CT data with a particular focus on the presence of multiple renal arteries. Surg Radiol Anat 2018;40:381–8.

36. Gumus H, Bükte Y, Özdemir E, Çetinçakmak MG, Tekbaş G, Ekici F, Onder H, Uyar A. Variations of renal artery in 820 patients using 64-detector CT-angiography. Ren Fail 2012;34:286–90.

37. Gebremickael A, Afework M, Wondmagegn H, Bekele M. Renal vascular variations among kidney donors presented at the national kidney transplantation center, Addis Ababa, Ethiopia. Transl Res Anat 2021;25:100145.

ORCID ID:
A. Satır 0000-0001-7628-1935; M. Yıldız Yılmaz 0000-0003-3086-8727; M. Öztürk 0000-0002-5660-2022; E. Şendemir 0000-0001-9699-4342; H. Demirci 0000-0003-0434-4807

deomed

Correspondence to: Atilla Satır, MD
Department of Urology, Bursa Yüksek İhtisas Training and Research Hospital, University of Health Sciences, Bursa, Türkiye
Phone: +90 533 221 49 21
e-mail: atillasatir@gmail.com

Conflict of interest statement: No conflicts declared.

 How to cite this article: Satır A , Yıldız Yılmaz M, Öztürk M, Şendemir E, Demirci H. Renal vascular and ureteral variations in patients with kidney transplantation. Anatomy 2023;17(1):5–12.

Original Article

http://dergipark.org.tr/en/pub/anatomy
Received: April 10, 2022; Accepted: February 14, 2023
doi:10.2399/ana.23.1308824

anatomy
An International Journal of Experimental and Clinical Anatomy

Perforator flaps based on the pectoral branch of the thoracoacromial artery: anatomical basis using 24 dissections

Philippe Manyacka Ma Nyemb[1,2], **Christian Fontaine**[3], **Véronique Duquennoy-Martinot**[4], **Xavier Demondion**[3,5]

[1]*Department of Anatomy and Organogenesis, School of Medicine, Gaston Berger University, Route de Ngallèlle, Saint-Louis, Senegal*
[2]*Department of General Surgery, Regional Hospital, Saint-Louis, Senegal*
[3]*Department of Anatomy and Organogenesis, Henri Warembourg Faculty of Medicine, Université de Lille 2, Lille, France*
[4]*Department of Plastic, Esthetic and Reconstructive Surgery, Roger Salengro Hospital, Lille University Hospital, Lille, France*
[5]*Department of Musculoskeletal Imaging, Roger Salengro Hospital, Lille University Hospital, Lille, France*

Abstract

Objectives: A perforator flap based on the pectoral branch of the thoracoacromial artery (TAA) is an attractive option, both in terms of the regional coverage possibilities and the reduced donor site morbidity. And yet this technique has been little documented in the literature. The authors report a series of dissections in order to understand the realization and the indications of this surgical technique.

Methods: We dissected 24 perforator flaps based on the pectoral branch of the TAA in cadaver specimens preserved in a glycerin-rich, formalin-free solution. The TAA was first injected with methylene blue. The vascular territory, location of perforators relative to known landmarks, along with the flap's potential amplitude and arc of rotation were studied.

Results: The main perforator arteries were in the middle of the deltopectoral groove length; they were surrounded by adipose tissue in 80% of specimens. Two perforator arteries were found in two specimens: one was in the middle of the deltopectoral groove length and the other was more proximal. The flap's arc of rotation made it possible to reach the anterior cervical region, the sternal region and the axillary region in every specimen.

Conclusion: Through an anatomical study of perforator flaps based on the TAA, we reviewed the principles and landmarks that can be used by plastic surgeons to easily carry out this surgical technique.

Keywords: dissection; pectoral branch; perforator flap; thoracoacromial artery

Anatomy 2023;17(1):13–21 ©2023 Turkish Society of Anatomy and Clinical Anatomy (TSACA)

Introduction

For several decades, complex surgical techniques have been used to cover soft tissue defects in the head and neck region. Two advances expanded the options for head and neck reconstruction: the deltopectoral flap technique developed by Bakamjian in 1968[1] for pharynx reconstruction and the pectoralis major flap described by Ariyan in 1979.[2] However, the deltopectoral flap's pedicle is short and a skin graft is often required to close the donor site. The presence of muscle in the pectoralis major flap results in excess flap volume and increases morbidity at the donor site. More recently, the advent of perforator flaps has changed how head and neck reconstruction is done.[3–5] These flaps are based on musculocutaneous perforator arteries that perforate the muscle and terminate on the skin paddle by a vascular territory or perforasome, without vascularizing the muscle itself. They are better suited to these tissue defects, due to their lower morbidity and larger variety of donor sites.

This study was a poster presentation at the 102nd Congress of the French Association of Morphologists, 11th–12th March 2021, Montpellier, France.

The TAA arises from the anterior side of the axillary artery, between the middle and lateral thirds of the clavicle. Its origin from the axillary artery is hidden by the pectoralis minor muscle.[6–8] It gives off deltoid and pectoral branches that are always present. It also gives off a clavicular branch that arises directly from the thoracoacromial artery and an acromial branch which arises directly from the deltoid branch. However these branches are not always present.[6–8] The branches of TAA arise immediately below the clavicle; they then penetrate the pectoralis major through its internal surface immediately below the midpoint of the clavicle. The veins are accompanying the arteries. The deltoid and acromial branches supply the clavicular part of the pectoralis major medially and the clavicular branch laterally.[6,8] The latter two branches give off musculocutaneous perforators that vascularize the integuments located in the superior part of the pectoral wall. The deltoid branch often gives off the acromial branch directly. The acromial branch also provides a musculoskeletal perforator towards the integuments covering the deltoid muscle and the acromial end of the clavicle.[6,8] The pectoral branch supplies the sternocostal part of the pectoralis major muscle.[6,8] It then gives off a lateral branch that courses towards the lateral thoracic artery, one medial and one caudal branch directed towards the 4th intercostal space that anastomose with the anterior intercostal arteries and the perforators of the internal thoracic artery (ITA).[6,9,10] The pectoral branch generally courses along a line joining the acromion with the xiphoid process. However, there are several anatomical variations have been described.[11] Several small musculocutaneous perforators arise from this pectoral branch but they can not be used surgically.[6] Injections have shown the cutaneous vascular territory of the pectoral branch extending from the axillary fossa in transverse plane as far as the nipple, laterally beyond the margin of the pectoralis major muscle.[8]

A perforator flap based on the pectoral branch of the thoracoacromial artery (TAA) corresponds to the perforator variant of the pectoralis major musculocutaneous flap. Hence, it has the same advantages but not necessarily the same drawbacks, which makes it a good option for head and neck reconstruction. The authors performed a series of injections and dissections to study the feasibility of developing and using perforator flaps based on the pectoral branch of the TAA to cover tissue defects in the head and neck area.

Materials and Methods

Twenty-four sides (12 right and 12 left upper limbs) of 12 BIOMET embalmed cadavers were dissected in this study. The mean age of the cadavers was 69 years (range: 47–88); there were 9 males (range: 47–88) and 3 females (range: 69–87). The cadavers had no history of surgery or deformity around the shoulder region. “BIOMET Solution” is a glycerin-rich, formalin-free solution to preserve tissue suppleness and usually used in the anatomy laboratory of the University of Lille (France) for conservation of the cadavers. The composition for obtaining 13.7 liters of BIOMET Solution is as follows: 4.75 liters of methanol+4.75 liters of distilled water+3 liters of glycerin+1.2 liters of phenol. Prior to our work, all the institutional procedures concerning cadaveric dissection were respected, as well as the ethical framework. From an ethical point of view, our work was based on the legislation at the time of the study.

First, the cadavers were placed in supine position and the clavicles were removed from the lateral triangle of the neck. The subclavian artery and its collateral branches were dissected, identified and marked. The dissection was extended to expose the origin of the TAA on the anterior side of the first part of the axillary artery. The TAA was injected with a mixture of gelatin, methylene blue and iron powder (**Figures 1a** and **b**). The cadaver was then frozen for 24 hours.

In the second phase, the cadaver was thawed out at room temperature and then placed in supine position to dissect the integuments. For this dissection, a superficial incision was made on the lateral, caudal and cranial margins of the cutaneous perforasome, making sure not to breach the muscle layer. Next, the superficial plane was separated from the muscle layer from the periphery to the center of the perforasome (**Figure 2**). This dissection was performed meticulously so as to prevent damaging the satellite veins accompanying each perforator artery. During this procedure, the perforators were dissected and inventoried based on their location, dimensions, orientation, frequency, and size of the cutaneous perforasome (**Figure 3**). Perforasome area was calculated based on a circular shape (radius X radius X π) or elliptical shape (long radius X small radius X π). Dissection of perforators was then continued through the muscle while preserving the integrity of the pectoralis major muscle. The superficial layer (perforator flap) was then harvested completely with its pedicle.

Results

The TAA had an average diameter of 2 mm. An average of 2.4 perforators were found (range: 1–4) on the perforasome corresponding to the territory of the TAA’s pectoral branch. The average diameter of each perfora-

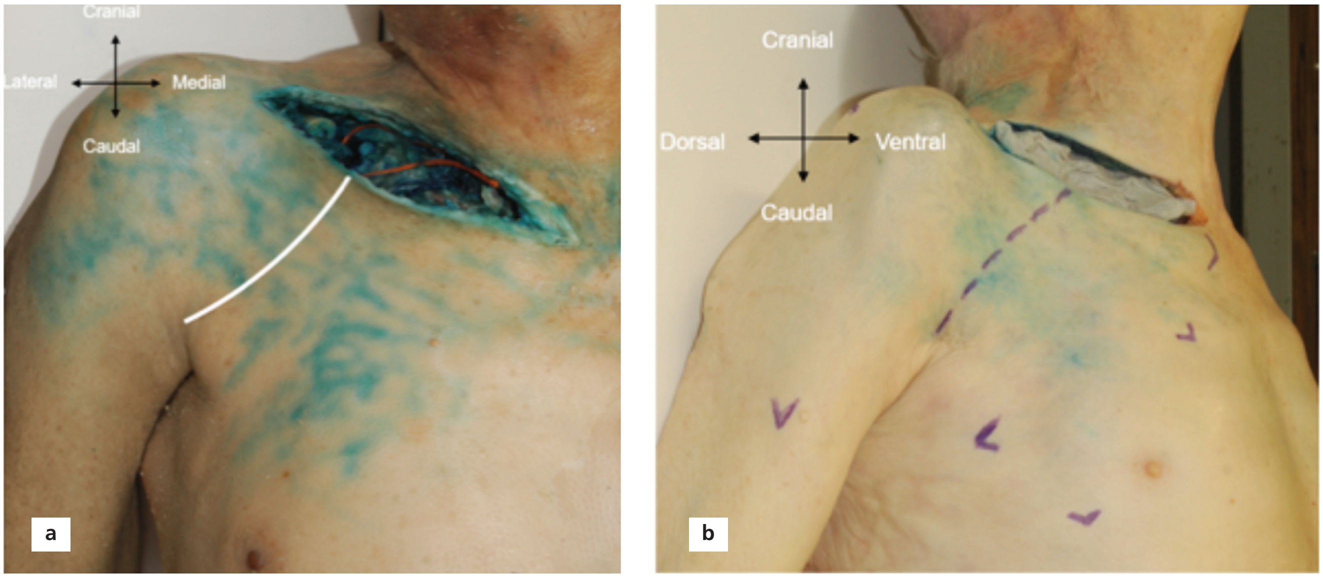

Figure 1. Injecting and coloring of the branches of the thoraco-acromial artery in two subjects (**right side**). The deltopectoral groove is represented as a white line (**a**) and in blue dotted lines (**b**), as the limit of the cutaneous perforasome. Specimens numbers 7 and 14 (*see* **Table 1**).

tors was 0.9 mm (range: 0.3–1.8). The average dimensions of the perforasome was 5×9 cm, corresponding to a mean area of 35.3 cm^2 (range: 22–80). Its general orientation was caudal and medial. The extramuscular pedicle had an average length of 1.5 cm (range: 0.5–4) and the transmuscular pedicle had an average length of 8 cm (range: 5–12). A 180° arc of rotation of the perforator artery was possible from the pivot point. In 21 of the 24 specimens, the pectoral branch of the TAA and its perforators converged over the middle third of the deltopectoral groove (pivot point) (**Figures 4** and **5**).

The following topographic boundaries can be used when dissecting this flap, although the perforasome area often extends beyond these boundaries: the nipple and 4th intercostal space caudally; lateral margin of the pectoralis major muscle and anterior axillary line laterally; vertical line through the medial third of the clavicle medially; the tip of the perforator flap is located at its pedicle over the deltopectoral groove (**Figure 4**). More detailed findings are given in **Table 1** and **Figure 4**.

Discussion

The pectoralis major musculocutaneous flap has long been the workhorse flap in head and neck reconstruction.[12] Little research has been carried out up to now on the perforator variant of this flap–a perforator flap based on the TAA's pectoral branch. Anatomical studies performed on the TAA show that its perforators are small in diameter and that several variations exist in their origin.[6,8] While there is little known about perforator flaps based on the TAA's pectoral branch, its perforators have already been used for axillary wound contractures[13] and in facial and cervical reconstruction.[7,14–16] Most of the injection studies done on the pectoralis major muscle showed these muscle perforators originate either medially from the anterior intercostal and internal mammary arteries, or laterally from the lateral thoracic artery.[6,8,17] However, particularly in the cranial part of the muscle, distinct perforators have been found that originate in the TAA, although this has been obscured by numerous authors.[9,17] In the 1960s, Bakamjian[1] used axial flaps for

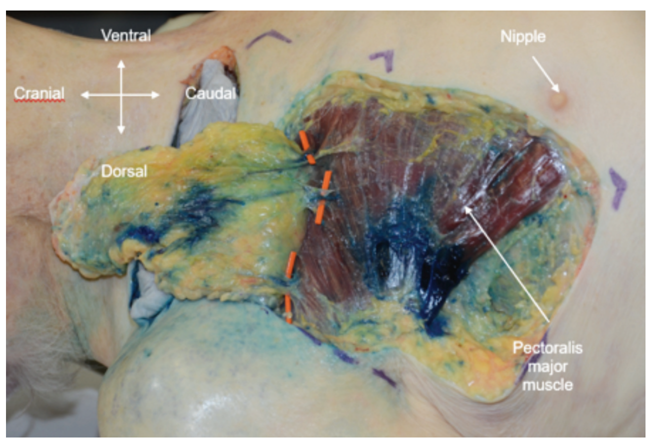

Figure 2. Dissecting the perforasome of the pectoral branch of the thoraco-acromial artery on the right side. Specimen number 13 (*see* **Table 1**).

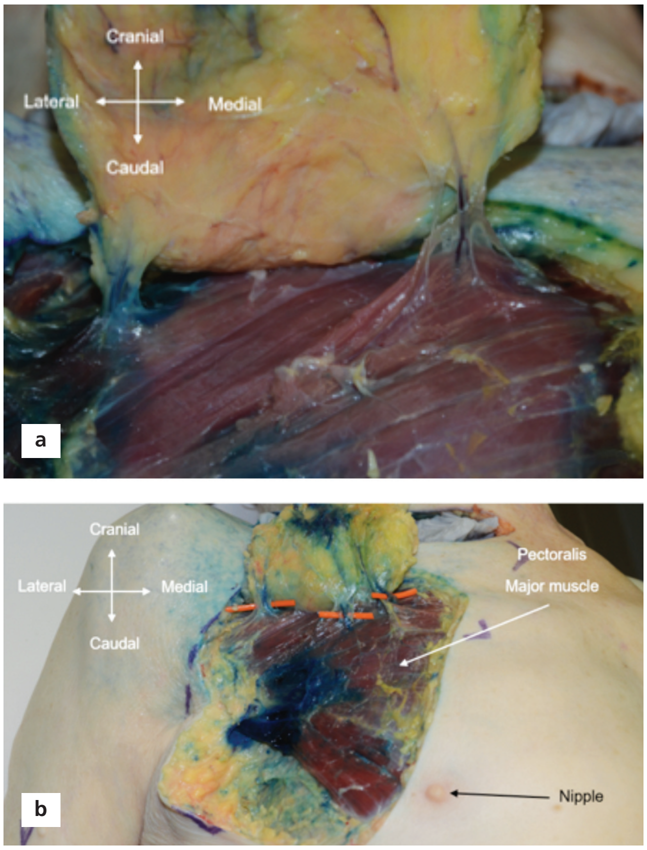

Figure 3. Identification and dissection of perforators of the pectoral branch of the thoracoacromial artery, in close-up (**a**) and in panoramic view (**b**). Specimen number 13, right side (*see* **Table 1**).

cervicofacial reconstruction. He went on to describe the deltopectoral flap, which has a wide medial base at the cranial part of the thorax and shoulder. Then, several pioneers understood that including an axial pedicle within a flap improves its vascular pedicle.[3] Since perforators have anatomical variations, their location may need to be defined preoperatively. This is most often done through a computed tomography scan with contrast and/or Doppler ultrasonography.

The anterior thoracic wall has long been used as a donor site for head and neck reconstruction because of its proximity to the cervicofacial area and its similar color, texture and thickness. Traditionally, the primary choices for head and neck reconstruction are the pectoralis major musculocutaneous flap and the deltopectoral flap.[2] Despite the benefits of these two types of flaps, functional and esthetic requirements limit their use. Research has shifted towards flaps with characteristics that correspond exactly to the recipient site, with less donor site morbidity. The main drawbacks of deltopectoral flaps are the high necrosis rate, the need for a skin graft to cover the donor site, and the small arc of rotation due to the short pedicle.[6] Our study shows that a perforator flap based on the TAA's pectoral branch does not have such drawbacks. As for pectoralis major musculocutaneous flaps, its perforator variant corresponds to TAA perforator flaps. Hence, the latter shares its advantages but not its disadvantages. Like the ITA perforator flap, the perforator flap based on the TAA's pectoral branch is a good option for exploiting the pectoral teguments for head and neck tissue defects. The benefits include acceptable color, texture and suppleness.[7,16] Moreover, a perforator flap based on the TAA's pectoral branch has the same topographic advantages as the pectoralis major flap, along with being thinner (avoiding excess volume at the defect site), having a longer vascular pedicle and preserving the function of a major trunk muscle.[7,16] This result is close to what we found in our work. We defined the limits of the area in which the perforator branches of the pectoral branch of the TAA usually project. In addition, inside the described area, the orientation of the perforator branches was mediocaudal.

Geddes et al.[6] reported that the TAA arises in an isolated manner from the axillary artery in all specimens he dissected. The average diameter of the TAA was 2.5±0.5 mm in his study. The average external diameter was 2 mm in our study, although it varied greatly. We also found that the TAA is the primary vascular source for the pectoralis major muscle and that is courses deeply in the adipose tissue dividing the pectoralis major muscle from other muscles. He showed the TAA gives off three main branches: pectoral, clavicular and deltoid. The acromial branch could also be considered a main branch; however, he found it to be supplied by the deltoid branch of TAA in 18 of 20 specimens and by the TAA in the other 2. The pectoral branch of the TAA supplies the largest vascular territory. Geddes et al.[6] revealed its average diameter as 1.7±0.6 mm. In most cases, it gives off three secondary branches that course obliquely, medially and caudally against the internal surface of the pectoralis major muscle. The medial and caudal branches anastomose with perforators from the ITA. These arteries are issued from small diameter (less than 0.5 mm) musculoskeletal perforators. The lateral ramus of the pectoral branch anastomoses with the terminal branches of the lateral thoracic artery inside the pectoralis major muscle. We found the pectoral branch can give off three or four viable perforators in 50% of specimens that are 1 mm in diameter.

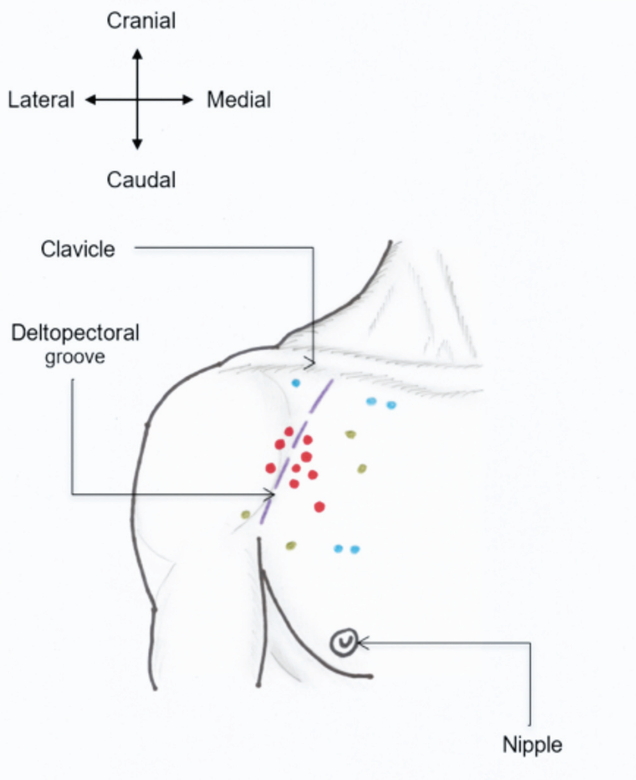

Figure 4. Distribution of perforator arteries of the pectoral branch of TAA based on incidence. **Blue:** <40%; **green:** between 40 and 70%; **red:** >70%.

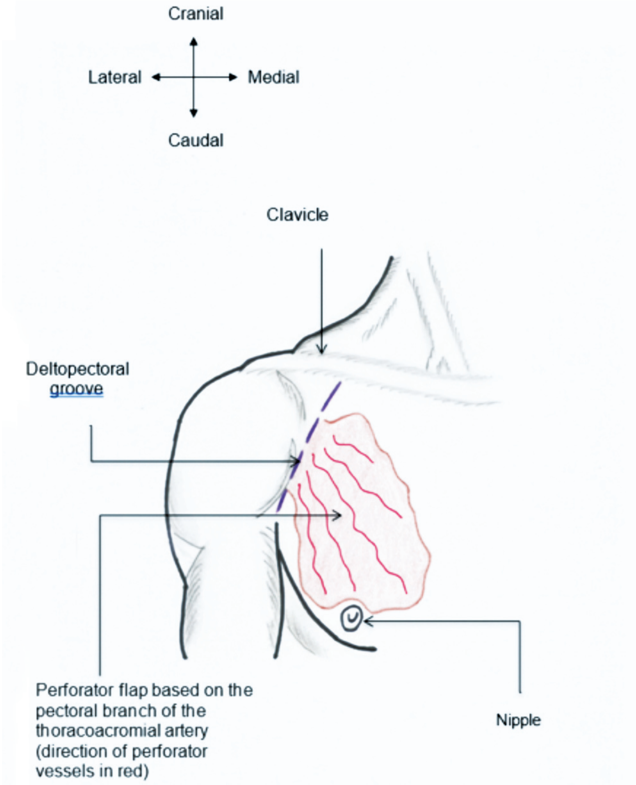

Figure 5. Drawing of the perforator flap based on the pectoral branch of TAA.

It appears from Salmon's works that the TAA represents the main integumentary artery of the anterior deltoid region, and that it quickly branches into an acromial branch and a thoracic branch.[18,19] He found that the thoracic branch largely irrigates the pectoralis major muscle. Our work also shows that the pectoral branch of TAA supplies a large area of the pectoralis major muscle. However, we find that TAA is constantly divided into a deltoid branch and a thoracic branch. The clavicular and sternocostal parts of the pectoralis major muscle receive independent vascularization.[6] The sternocostal part receives the pectoral branch of the TAA, while the clavicular part is supplied medially by the clavicular branch and laterally by the deltoid and acromial arteries. The integuments located cranially are supplied by musculocutaneous perforators of the deltoid and clavicular branches, a few branches from the transverse cervical artery, and by the suprascapular arteries. According to Geddes et al.,[6] the musculocutaneous perforators of the TAA's pectoral branch are limited to small perforators in the laterocaudal and intermediate areas of the pectoralis major muscle.

Contrary to what we found in our study, Geddes et al.[6] has not consistently identified large musculocutaneous perforators from the pectoral branch of TAA. However, when the dissection is completed by an angiography, there appears a significant variability in the vascular network of the pectoralis major muscle. Our work shows that it is possible to dissect the perforators of the pectoral branch of the TAA, including through the muscle. The arc of rotation and the dimensions of the pedicles would facilitate the mobility of a perforator flap. However, the inconsistent nature of this artery between individuals and from one side to the other limits its use according to Geddes et al.[6] On the contrary, we found that two potential pedicled perforator flaps can be developed from large, consistent musculocutaneous perforators from the clavicular and deltoid branches. The proximity of these flaps to the head and neck region provides them with an additional advantage in terms of color and texture for tissue defects in this region. The absence of hair is also a strong point. Our study found that–despite the considerable variations in arterial territories–the trajectory of the various perforators is more consistent, at both the integument and the muscle level.

Table 1
Summary of the findings in the 24 dissected specimens.

Specimen number and side	Age	Sex	Diameter of thoracoacromial artery (mm)	Number of pectoral perforators	Average (min–max) diameter of pectoral perforators (mm)	Dimensions of pectoral branch's perforasome (cm)	Length of extrafascial pedicle (cm)	Length of pedicle after transmuscular dissection (cm)	Arc of rotation from pivot point (°)
1 L	72	H	2	3	0.8 (0.5–1.2)	8×5	0.5	7	180
2 R	72	H	2	3	1.2 (0.3–1.5)	8×4	0.5	10	180
3 L	58	H	2	1	0.8 (0.8–0.8)	7×6	1.5	12	180
4 R	58	H	1 .5	3	0.8 (0.5–1.2)	8×8	2	10	180
5 L	63	H	2	2	1.2 (0.8–1.5)	7×7	1	6	180
6 R	63	H	2.5	2	0.8 (0.6–1.0)	5×7	1.5	8	180
7 L	88	H	1	1	0.8 (0.8–0.8)	5×8	2	11	180
8 R	88	H	1	2	1.2 (0.8–1.6)	5×8	0.5	9	180
9 L	67	H	2	3	0.7 (0.5–0.8)	5×8	0.5	7	180
10 R	67	H	2	2	1.3 (0.9–1.8)	7×10	2.5	10	180
11 L	64	H	2	4	0.9 (0.8–1.8)	4×7	1	11	180
12 R	64	H	1.5	3	1 (0.7–1.5)	5×7	0.5	8	180
13 L	75	F	1.5	1	0.9 (0.9–0.9)	6×10	1.5	6	180
14 R	75	F	1.5	2	0.8 (0.5–1.0)	5×8	1	5	180
15 L	87	F	2	3	1 (0.8–1.2)	6×10	2	7	180
16 R	87	F	2	2	0.7 (0.5–1.0)	8×8	3.5	5	180
17 L	82	H	2.5	1	0.8 (0.8–0.8)	6×10	1.5	6	180
18 R	82	H	2.5	3	1 (0.8–1.5)	6×10	2	8	180
19 L	69	F	2.5	4	1.2 (0.8–1.8)	5×8	1.5	9	180
20 R	69	F	2	2	0.9 (0.6–1.2)	5×8	1	10	180
21 L	57	H	3	3	0.9 (0.8–1.2)	8×12	4	6	180
22 R	57	H	3	3	0.9 (0.6–1.0)	8×10	3	6	180
23 L	47	H	1.5	2	0.8 (0.8–0.8)	5×8	0.5	5	180
24 R	47	H	2	3	0.9 (0.7–1.2)	6×7	0.5	6	180

Contrary to Geddes et al.,[6] our study's findings were similar to those of the study by Zhang et al.[16] The latter group found at least one perforator from the TAA's pectoral branch in a 4 cm2 area around the intersection of two lines: one is the xipho-acromial line and the other perpendicular to the first line and passing through the mid-point of the ipsilateral clavicle. We also found a consistent perforator ramus from the TAA's pectoral branch. However, in our study, this perforator was generally projected on the middle third of the deltopectoral groove. Although we used different anatomical landmarks than Zhang et al.,[16] the areas on which the TAA's pectoral branch is projected, as defined in the respective studies, are similar.

In the study by Zhang et al.[16] at least one perforator was always present at the septum between the clavicular and sternocostal insertions of the pectoralis major muscle in 87% of flaps (21 of 24). Two musculocutaneous perforators were found in 13 of their 21 specimens and only one in the other 8 flaps. Each perforator had two satellite veins. Our study found an average of 2.4 perforators arising from the TAA's pectoral branch (range: 1–4); one perforator in 4 specimens, two perforators in 8 specimens, three perforators in 10 specimens and four perforators in 2 specimens. Zhang et al.[16] reported the perforator diameter ranged from 0.4 to 1.1 mm (average: 0.7 mm). We found slightly larger diameters ranging from 0.3 to 1.8 mm with an average of 0.9 mm. The vascular pedicle after dissection to the TAA's origin at the axillary artery was 7.1 cm long (range: 6.1 to 8.3 cm) in the study by Zhang et al.[16] versus 8 cm in our study (range: 5 to 12 cm). In the study by Zhang et al.,[16] the perforasome supplied by the TAA's pectoral branch had a different medial boundary comparing to our study. Despite the TAA's pectoral branch giving off a consistent number of perforators that supply the integuments of the lateral region of the nipple up to the lateral margin of the pectoralis major muscle, none of these perforators were found below the 4th intercostal space, and they were rarely found medial to a vertical line passing through the medial one-third the clavicle.

A perforator flap based on the TAA's pectoral branch is thinner and has a longer vascular pedicle than the pectoralis major musculocutaneous flap. While the donor site can reclose itself, or can be closed with prior expansion, it can induce breast deformity or areolar attraction, particularly in women. The 12-cadaver study performed by Zhang et al.[16] showed the potential clinical application of perforators flaps based on the TAA's pectoral branch. The authors found perforators in almost all of their dissections. In this way, the findings of the Zhang et al. study[16] contradict those of the Geddes et al.[6] who demonstrated that TAA's pectoral branch was inconsistent and had only tiny musculocutaneous perforators. This reduced the feasibility of a pedicled perforator flap with the pectoral branch, contrary to flaps using the deltoid and clavicular branches of the TAA. Our findings are most like those of Zhang et al.[16] When we performed a retrograde dissection of the perforasome and then the perforator artery while using the middle third of the deltopectoral groove as a landmark, the pedicle from the TAA's pectoral branch to its axillary origin was up to 12 cm long, versus 8 cm in the study by Zhang et al.[16]

Our findings are also consistent with the two clinical cases described by Hallock[7] and the four cases described by Nishi et al.,[14] although the latter included fibers from the pectoralis major muscle in the perforator pedicles. Hallock[7] raised and applied two perforator flaps based on the TAA's pectoral branch for two reconstruction cases (cervical and facial). As in our study, they separated the pectoralis major muscle fibers to increase the length of the pedicle and the arc of rotation. Muscle function was preserved in both patients. According to Hallock[7] there is no guarantee that adequate perforators are present. Consequently, standard drawing of a perforator flap based on the pectoral branch is impossible, the pedicle length is indeterminate, and perforators located too caudally require muscle dissection that can cause partial denervation of the pectoralis major muscle. Although these fears are justified, we believe that drawing of the flap is possible when certain precautions are taken such as identification and use of fixed anatomical landmarks, careful dissection of the perforator branches.

Perforator flaps based on the TAA's pectoral branch and perforator flaps based on the ITA have common advantages. However, in contrast with the increasing popularity of ITA flaps, the feasibility and reliability of perforator flaps based on the TAA's pectoral branch has been questioned.[4–6,16] The size of the perforator artery arising from the TAA and the small diameter of its perforators are not often compatible with flap surgery. However, our work showed that perforators issued from the TAA's pectoral branch are certainly viable. The ITA perforator flap can be used in the same indications as perforator flaps based on the TAA's pectoral branch. And unlike the latter, ITA flap has been the subject of several studies.[17,20,21] For this flap, obtaining a long enough pedicle can require removal of one or more rib cartilages, which causes thorax deformity. Another contraindication to use of ITA perforator flaps are iatrogenic factors such as prior incisions from cardiovascular surgery. However, it has several other advantages such as primary closure of the donor site, possibility of cutaneous pre-expansion, along with absence of nipple asymmetry after the flap is applied.[16] As for the perforator flap based on the TAA's pectoral branch, its location limits the area than can be expanded, and while it is larger in size, it can lead to nipple asymmetry due to ipsilateral nipple elevation after application.[16] Despite these drawbacks, the donor site can be sutured in a single step, and pedicle dissection is easier and less invasive than for the ITA perforator flap. Due to the length of the pedicle and the anatomical boundaries of the flap, it is technically possible to reach large tissue defects in the head area.

Based on our experience, a perforator flap based on the TAA's pectoral branch can be raised in a laterocaudal location on the cranial part of the thorax and applied to a mediocranial recipient site in the head or neck area.

Small clinical studies have shown this perforator flap can be used to cover frontal, nuchal and even dorsal defects.[7,14,16] However, certain guidelines must be followed when raising and applying this flap: its orientation before development (caudal or slightly mediocaudal according to Salmon et al.[18]), its anatomical boundaries and average dimensions, the converg ence point (pivot point) of perforators over the middle of the deltopectoral groove, and the potential length of the pedicle. It is also important to preserve the perforator and muscular vascularization in this area. If necrosis was to occur with a TAA perforator flap, an ITA perforator flap or a flap pedicled to the pectoralis major muscle could be used as "rescue flap".

Conclusion

Our study showed that viable muscle and integument vascularization is provided by the TAA and its perforator arteries in the laterocranial regions of the anterior thoracic wall. In most cases, the pectoral branch of the TAA gives off several perforator branches, which are consistent and have dimensions compatible with perforator flap surgery. A perforator flap based on the TAA's pectoral branch is feasible when the anatomical boundaries described in this study are followed. This flap is one more weapon in the therapeutic arsenal of surgeons tasked with covering cervical, cephalic and dorsal defects while preserving the color, texture, thickness and pilosity of the site.

Acknowledgments

The authors are grateful for the contribution of the entire staff of the Lille University Anatomy Laboratory (France) to this work, along with the staff of the Radiology Department of the Lille University Hospital.

Conflict of Interest

All authors declare no conflict of interest.

Author Contributions

PMMN: protocol, project development, data collection, data analysis, and manuscript writing. CF: protocol development, data analysis, and manuscript editing. VDM: protocol development, data analysis, and manuscript editing. XD: protocol development, data analysis, and manuscript editing. AB: protocol development.

Ethics Approval

All the institutional procedures concerning cadaveric dissection were respected, as well as the ethical framework. The authors of this work thank all the donors for their contribution.

Funding

No funding.

References

1. Bakamjian VY. Total reconstruction of pharynx with medially based deltopectoral skin flap. NY State J Med 1968;68:2771–8.
2. Ariyan S. The pectoralis major myocutaneous flap: a versatile flap for reconstruction in the head and neck. Plast Reconst Surg 1979;63:73–81.
3. Morris SF, Tang M, Almutari K, Geddes C, Yang D. The anatomic basis of perforator flaps. Clin Plast Surg 2010;37:553–70.
4. Song D, Pafitanis G, Pont LEP, Yang P, Koshima I, Zhang Y, Iida T, Zhou X, Li Z. Chimeric thoracoacromial artery perforator flap for one-staged reconstruction of complex pharyngoesophageal defects: a single unit experience. Head Neck 2018;40:302–11.
5. Zhang YX, Li Z, Grassetti L, Lazzeri D, Nicoli F, Zenn MR, Zhou X, Spinelli G, Yu P. A new option with the pedicle thoracoacromial artery perforator flap for hypopharyngeal reconstructions. Laryngoscope 2016;126:1315–20.
6. Geddes CR, Tang M, Yang D, Morris SF. An assessment of the anatomical basis of the thoracoacromial artery perforator flap. Can J Plast Surg 2003;11:23–7.
7. Hallock GG. The island thoracoacromial artery muscle perforator flap. Ann Plast Surg 2011;66:168–71.
8. Reid CD, Taylor GI. The vascular territory of the acromiothoracic axis. Br J Plast Surg 1984;37:194–212.
9. Kiyokawa K, Tai Y, Tanabe HY, Inoue Y, Yamauchi T, Rikimaru H, Mori K, Nakashima T. A method that preserves circulation during preparation of the pectoralis major myocutaneous flap in head and neck reconstruction. Plast Reconstr Surg 1998;102:2336–45.
10. Rikimaru H, Kiyokawa K, Inoue Y, Tai Y. Three-dimensional anatomical vascular distribution in the pectoralis major myocutaneous flap. Plast Reconstr Surg 2005;115:1342–52.
11. Serafin D. Atlas of microsurgical composite tissue transplantation. Philadelphia (PA): WB Saunders; 1996. p. 813.
12. Wei WI, Chan YW. Pectoralis major flap. In: Wei FC, Mardini S, editors. Flaps and reconstructive surgery. 1st ed. Philadelphia (PA): WB Saunders; 2009. p. 175–92.
13. Kosutic D, Krajnc I, Pejkovic B, Anderhuber F, Solman L, Djukic E, Solinc M. Thoraco-acromial artery perforator 'propeller' flap. J Plast Reconstr Aesthet Surg 2010;63:e491–3.
14. Nishi Y, Rikimaru H, Kiyokawa K, Watanabe K, Koga N, Sakamoto A. Development of the pectoral perforator flap and the deltopectoral perforator flap pedicled with the pectoralis major muscle flap. Ann Plast Surg 2013;71:365–71.
15. Okada M, Ikeda M, Uemura T, Takada J, Nakamura H. A propeller flap based on the thoracoacromial artery for reconstruction of a skin defect in the cervical region: a case report. J Plast Reconstr Aesthet Surg 2013;66:720–2.

16. Zhang YX, Yongjie H, Messmer C, Ong YS, Li Z, Zhou X, Spinelli G, Agostini T, Levin LS, Lazzeri D. Thoracoacromial artery perforator flap: anatomical basis and clinical applications. Plast Reconstr Surg 2013;131:759e–70e.

17. Wong C, Saint-Cyr M, Rasko Y, Mojallal A, Bailey S, Myers S, Rohrich RJ. Three-and four-dimensional arterial and venous perforasomes of the internal mammary artery perforator flap. Plast Reconstr Surg 2009;124:1759–69.

18. Salmon M, Grégoire R. Artères de la peau (Vol. 4). Paris: Masson; 1936. p. 123–131.

19. Salmon M, Dor J. Les artères des muscles des membres et du tronc. Paris: Masson; 1933. p. 238.

20. Schellekens PPA, Paes EC, Hage JJ, van der Wal MBA, Bleys RLAW, Kon M. Anatomy of the vascular pedicle of the internal mammary artery perforator (IMAP) flap as applied for head and neck reconstruction. J Plast Reconstr Aesthet Surg 2011;64:53–7.

21. Vesely MJJ, Murray DJ, Novak CB, Gullane PJ, Neligan PC. The internal mammary artery perforator flap: an anatomical study and a case report. Ann Plast Surg 2007;58:156–61.

ORCID ID:
P. Manyacka Ma Nyemb 0000-0002-3339-4312;
C. Fontaine 0000-0001-9280-7546;
V. Duquennoy-Martinot 0000-0003-4296-9736;
X. Demondion 0000-0003-2418-4396

Correspondence to: Philippe Manyacka Ma Nyemb, MD, PhD, MBA
Department of Anatomy and Organogenesis, School of Medicine,
Gaston Berger University, P.O. box 234, Saint-Louis, Sénégal
Phone: +221 77 445 43 13
e-mail: phil_manyacka@yahoo.fr / philippe-manyacka.manyemb@ugb.edu.sn

Conflict of interest statement: No conflicts declared.

 How to cite this article: Manyacka Ma Nyemb P, Fontaine C, Duquennoy-Martinot V, Demondion X. Perforator flaps based on the pectoral branch of the thoracoacromial artery: anatomical basis using 24 dissections. Anatomy 2023;17(1):13–21.

anatomy
An International Journal of Experimental and Clinical Anatomy

Original Article

http://dergipark.org.tr/en/pub/anatomy
Received: January 21, 2023; Accepted: March 28, 2023
doi:10.2399/ana.23.1362687

Revisiting the obturator nerve anatomy with a nerve blocking perspective

Turan Koç[1], Orhan Beger[2], Şebnem Rumeli[3], Alev Bobuş Örs[4], Nail Can Öztürk[4]

[1]*Department of Anatomy, Kahramanmaraş Sütçü İmam University Faculty of Medicine, Kahramanmaraş, Türkiye*
[2]*Department of Anatomy, Gaziantep University Faculty of Medicine, Gaziantep, Türkiye*
[3]*Department of Anesthesiology, Mersin University Hospital, Mersin, Türkiye*
[4]*Department of Anatomy, Mersin University Faculty of Medicine, Mersin, Türkiye*

Abstract

Objectives: Accurate nerve block is important for the success of local anesthesia-assisted surgery. Failure to consider the anatomical variations of the targeted nerve anatomy can lead to failure of anesthetic interventions. Given the distinct nature of the obturator nerve, blocking the nerve during clinical procedures is one such problematic situation. The aim of this article is to revisit the anatomy of the obturator nerve in adult cadavers and fetuses in order to discuss in detail its relationship with the obturator nerve block from an anatomical perspective.

Methods: Obturator nerve and its branches were exposed at the posterior wall of the abdomen, lateral wall of the lesser pelvis and anterior aspect of the thigh region in 47 fetuses and 10 adult cadavers. Then, various anatomical variations and morphometry of the obturator nerve were evaluated and measured in detail.

Results: In adult cadavers, the anterior and posterior branches branched 40% in the obturator canal and 60% in the extra-pelvic region, with no branching in the pelvis. In fetuses, the obturator nerve divided into its main branches 8.5% in the pelvis, 33% in the canal and 58.5% distal to the canal. Regarding the muscular branching of the obturator nerve, all adult cadavers showed three fully traceable branches from the anterior and a single branch from the posterior branch.

Conclusion: Our findings regarding the variable branching pattern of the obturator nerve anatomy from the nerve block perspective may help anesthesiologists to improve the success of obturator nerve block by incorporating results from the current and limited number of anatomical data sets.

Keywords: fetal anatomy; obturator nerve; regional anesthetic techniques

Anatomy 2023;17(1):22–33

Introduction

The obturator nerve (ON) generally originates from the ventral rami of L2–L4 spinal nerves and emerges on the medial side of the psoas major muscle, then descends at the medial side of this muscle. After running at the lateral wall of the lesser pelvis, it passes through the obturator canal (OC) and reaches to the medial side of the thigh region.[1] Upon passing through the OC, it bifurcates into an anterior branch (AB) and a posterior branch (PB) to innervate adductor muscles, hip and knee joints.[1–3]

There are many studies in the literature suggesting that branching of the ON can exhibit variability[2–4] and have distinct variations from the originally described anatomy.[1] Primarily, there are three known AB/PB bifurcation pattern in terms of its location: 1) in the pelvic region proximal to the OC; 2) inside the OC; 3) after leaving the OC (extra-pelvic).[2–5] This branching variability can become crucial for a successful ONB during many clinical applications such as hip and knee amputations, preventing the obturator reflex during transurethral bladder tumor resections,[6–9] relieving the thigh adductor spasms in patients suffering from multiple sclerosis, paraplegia or cerebral palsy and treatment of chronic hip pain.[10,11] It is also important to know the variations of the femoral and lateral cutaneous femoral nerves in order to provide a complete anesthesia in this region. femoral and lateral cutaneous femoral nerves.[10–12]

Since successful blockade of this nerve is crucial for the mentioned clinical procedures, efforts to develop selective ONB have been ongoing for almost a century. From a historical perspective, the first selective ONB trial dates back to the 1920s.[13] Either recognized as Labat's or Pubic approach, this classical procedure was designed to target ONB based on anatomical landmarks and applied 1.5 cm lateral and caudal to the pubic tubercle.[7,13,14] Long after, in 1973, namely as 3-in-1, a newer concept, targeting the simultaneous blockage of multiple nerves (ON, FN and lateral cutaneous nerve) was described by Winnie et al.[15] However, it is not surprising that strong arguments against this approach have accumulated, because with this technique, inadequate or weak nerve blocking was seen as well as unexpected results.[16] Almost two decades after 3-in-1 technique appeared, technological progresses brought nerve stimulated assisted inter-adductor approach into the arena as described by Wassef.[17] Then, relatively recently, in 2005, Choquet et al.[18] described a nerve stimulation-assisted blockade procedure, termed the "inguinal approach", also based on standard anatomical landmarks, applied through the midpoint of the inguinal fold between the femoral artery and the adductor longus muscle tendon. Compared to its older alternative the “pubic approach”, the “inguinal approach” provides a significantly more effective blockade, given better patient comfort and higher blockade efficacy.[18,19] Rapid advances in medical technology have created even newer approaches for anesthesiologists. A few years after the Choquet approach, ultrasound-guided fascia iliaca block with selective ONB, a new generation method using ultrasound technology, was introduced.[20] Although efforts towards better ONB performance are still evident, in this study we wanted to focus on the relation of ON anatomy to ONB procedures. Therefore, the aim of this study is to revisit the anatomy of the obturator nerve in adult cadavers and fetuses in order to discuss in detail its relationship with the ONB from an anatomical perspective.

Materials and Methods

This study was conducted on 94 sides of 47 fetuses (mean gestational week: 22.85±3.35) and 20 sides of 10 formalin-fixed male cadavers (mean age 80±18.022) without any external pathology or anomaly. The cadavers were available in the inventory of Anatomy Department of Mersin University, Faculty of Medicine. The fetus and adult cadavers were preserved with 10% formalin solution. All the dissections were performed in the supine position under a surgical microscope (Carl Zeiss f170 surgical microscope, Oberkochen, Germany) and photographed with a digital camera. Additionally, morphometric distances were measured by using a digital caliper with ± 0.01 mm precision. All measurements were repeated three times independently by two researchers (TK and OB). Mean-standard deviation was used for descriptive statistics of all parameters used.

The posterior abdominal wall and pelvic regions were dissected in order to identify the roots of the ON, the 3–4th lumbar vertebrae and psoas major muscle (PM). The ON coursing with the obturator artery and vein on the lateral pelvic wall was followed proximally and blunt dissection was performed in this region. The initial parts of the PM were carefully dissected to identify the roots of this nerve, which runs medial to the PM.

In order to visualize the passage of the ON from the pelvis to the thigh, the entrance and exit of the OC was exposed by shaving the superior pubic ramus (SPR). Dissection was then continued on the anterior aspect of the thigh.

Anterior superior iliac spine (ASIS), inguinale ligament (IL), pubic tubercle (PT), femoral vein (FV), femoral artery (FA), femoral nerve (FN), SPR, branches of ON and adductor muscles are chosen as anatomical landmarks. The inguinal ligament was exposed by blunt dissection from proximal to distal through the anterior abdominal wall in the supine position. The great saphenous vein running under the skin was identified and hiatus saphenous was exposed. The femoral sheath surrounding the FV and FA was carefully dissected and the vascular lacuna was identified. The muscular lacuna on the lateral side was also carefully opened and the iliopsoas muscle and the FN were exposed. In order not to disrupt the position of the structures, only the fascial sheaths adherent to the anterior side of the structures were opened. Then, after removal of the skin and subcutaneous tissues of the anterior and inner thigh, the sartorius, pectineus and adductor longus muscles were dissected free from the anterior fascia and a transverse incision line was created to expose the adductor brevis and external obturator muscles at a deeper level. The ON and its AB was identified in the connective tissue surrounding the adductor brevis muscle. After cutting and removing the adductor brevis muscle anterolaterally, the course of the PB of the ON was revealed. Both branches of the ON were followed cranially and caudally.

Thereafter, to provide a descriptive and convenient map of the anatomical relations given above, a sum of

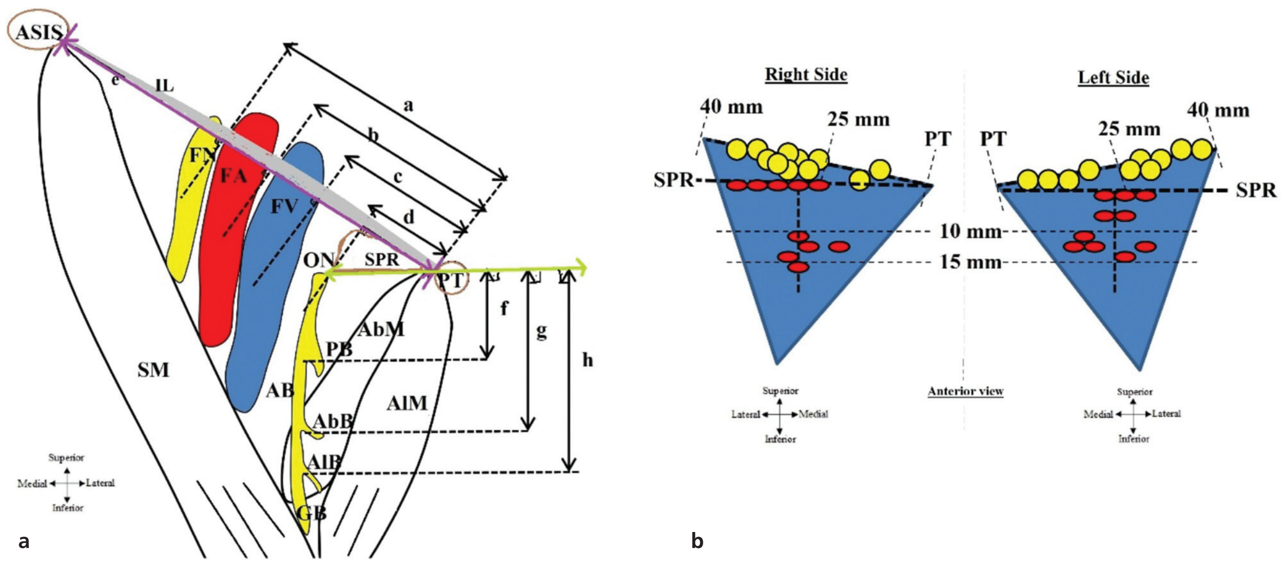

Figure 1. Schematic drawing of the anterior view of the femoral triangle showing (**a**) the measurements of the parameters related with obturator nerve and (**b**) description of its location and branching points. **a–h:** measurements of distances. **AB:** anterior branch of the obturator nerve; **AbB:** adductor brevis branch; **AbM:** adductor brevis muscle; **AlB:** adductor longus branch; **AlM:** adductor longus muscle; **ASIS:** anterior superior iliac spine; **FA:** femoral artery; **FN:** femoral nerve; **FV:** femoral vein; **GB:** gracilis branch; **IL:** inguinal ligament; **ON:** obturator nerve; **PB:** posterior branch of the obturator nerve; **PT:** pubic tubercle; **SPR:** superior pubic ramus; **SM:** sartorius muscle. **Green line:** The line passing through the lower edge of the SPR. **Purple line:** line extending between the lateral edge of PT and the medial edge of ASIS, passing through the lower edge of the IL. **Red circle** exhibits the branching point of the AB and PB on the vertical line. **Yellow circle** exhibits location of the obturator nerve on the oblique line.

eight distance parameters between the neuro-vascular structures and certain landmarks (**Figure 1**). The locations of the ON, FV, FA and FN along the lower edge of the IL were recorded. For this purpose, measurements were made by considering the vertical and oblique lines. Oblique line was extending between the lateral edge of PT and the medial edge of the ASIS. Vertical line was passing through the medial edges of the neurovascular structures. The projections of the structures on the oblique line were recorded, considering the 90-degree angle between both lines as (**Figure 1**):

(a) Distance between the PT–FN; (b) Distance between the PT–FA; (c) Distance between the PT–FV; (d) Distance between the PT–ON.

In order to define the exit points of the branches of the ON, the vertical line passing through the intersection of the lower edge of the SPR and the medial edge of the ON was taken as landmark. The distance of each branch separated along this line was recorded as:

(e) Distance between the ASIS–PT; (f) Distance between the SPR and AB/PB diverging point; (g) Distance between the SPR and AB/branch to adductor brevis muscle (AbB) diverging point; (h) Distance between the SPR and AB/branch to gracilis muscle (GB) diverging point.

Following parameters were measured via digital caliper in adult cadavers. Respective data was presented based on descriptive statistics. Lastly, foot lengths of fetuses were measured to estimate the gestational ages (in weeks/months) of the fetuses (**Table 1**).

Results

In all cases in the study, both in fetuses and adult cadavers, ON originated from the L2–L4 spinal nerves and emerged on the medial side of the psoas major muscle. In fetuses, 8.5% (8/94) of the AB and PB branched from ON in the pelvic region (**Figures 2a** and **3a**), 33% (33/94 cases) in the OC (**Figures 2b** and **3b**) and 58.5% (53/94 cases) in the extra-pelvic region (**Figures 2c** and **3c**).

On the other hand, in adult cadavers, the OB branched into the AB and PB in its own canal in 40% (8/20) of the specimens (**Figures 2d** and **4a**), whereas in the remainder (60%, 12/20) it branched after leaving the canal (**Figures 2e** and **4b**). When the ON branching was examined on the lateral wall of the pelvic region, a branch to the hip joint was found proximal to the OC entrance in 35% (7/20) of adult cadavers (**Figures 5a**, **c** and **d**), whereas in the remaining cases this branch diverged from the AB (65–13/20%) (**Figures 5b** and **e**). On the other hand, distance of ON to PT was 26.61±

Table 1
Demographic data belonging to fetuses.

Gestational age		Foot length (mm)	Number of sides	Number of cases	
Months	Weeks			Male	Female
V	18	25.55±0.70	6	2	1
	19	27.98±0.76	8	2	2
	20	30.72±0.99	14	1	6
VI	21	32.80±0.65	10	2	3
	22	34.50±1.06	12	5	1
	23	38.44±1.09	10	2	3
	24	40.71±1.03	8	3	1
VII	25	41.34±1.11	4	2	0
	26	45.56±0.89	6	1	2
	27	48.23±1.36	6	2	1
	28	52.14±0.90	2	1	0
VIII	29	53.30±0.15	2	1	0
	30	54.48±0.83	6	0	3
Total	22.85±3.35	37.48±8.32	94	24	23

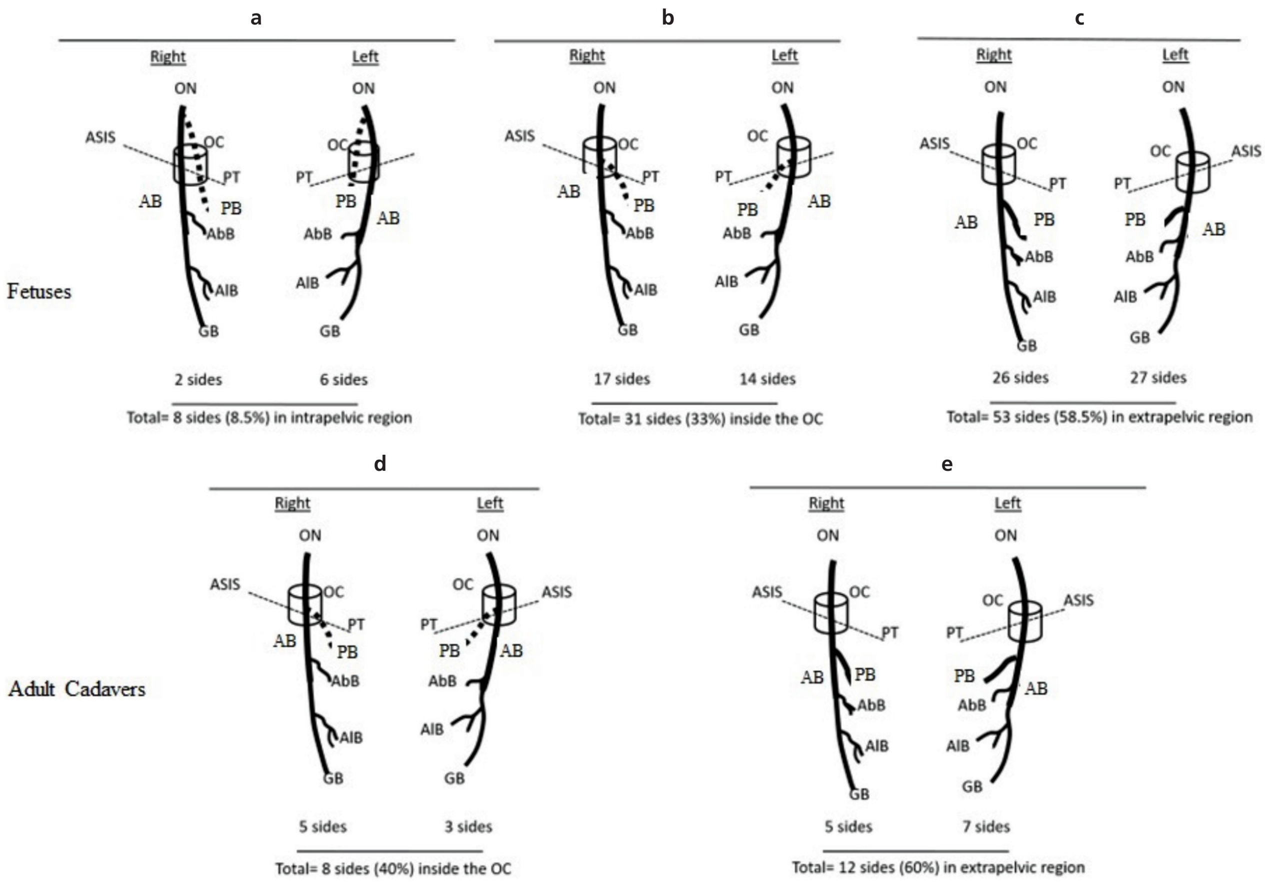

Figure 2. Schematic drawings of the branching pattern of the obturator nerve in fetuses (**a**–**c**) and in adult cadavers (**d**–**e**). AB: anterior branch of the obturator nerve; AbB: adductor brevis branch; AlB: adductor longus branch; ASIS: anterior superior iliac spine; GB: gracilis branch; OC: obturator channel; ON: obturator nerve; PB: posterior branch of the obturator nerve; PT: pubic tubercle.

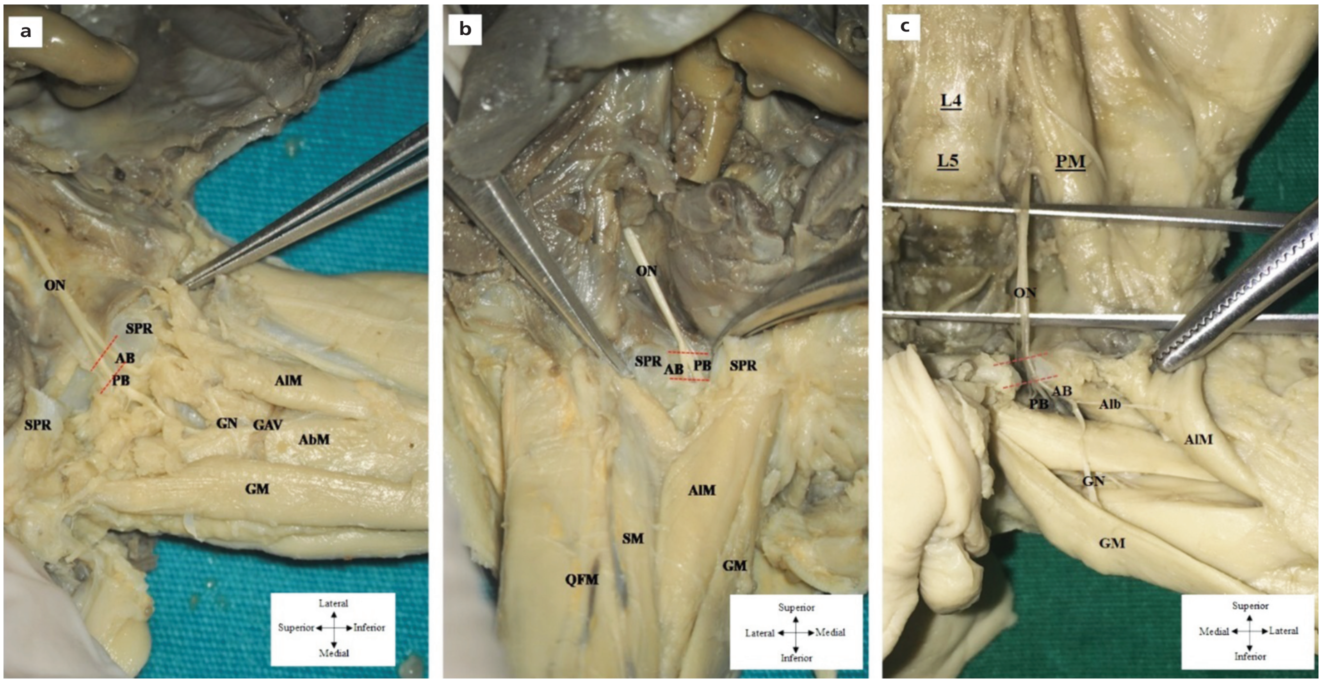

Figure 3. Anterior view of the pelvic and thigh regions showing bifurcation pattern of the obturator nerve in fetuses: (**a**) intrapelvic; (**b**) inside the obturator canal; (**c**) extrapelvic. **AB:** anterior branch of the obturator nerve; **AlM:** adductor longus muscle; **GAV:** artery and vein of gracilis muscle; **GN:** gracilis branch; **GM:** gracilis muscle; **L4:** 4th lumbar vertebra; **L5:** 5th lumbar vertebra; **ON:** obturator nerve; **PB:** posterior branch of the obturator nerve; **PM:** psoas major muscle; **QFM:** Quadriceps muscle; **SM:** sartorius muscle; **SN:** saphenous nerve, **SPR:** superior pubic ramus. **Red dashed lines** illustrate the obturator channel fold.

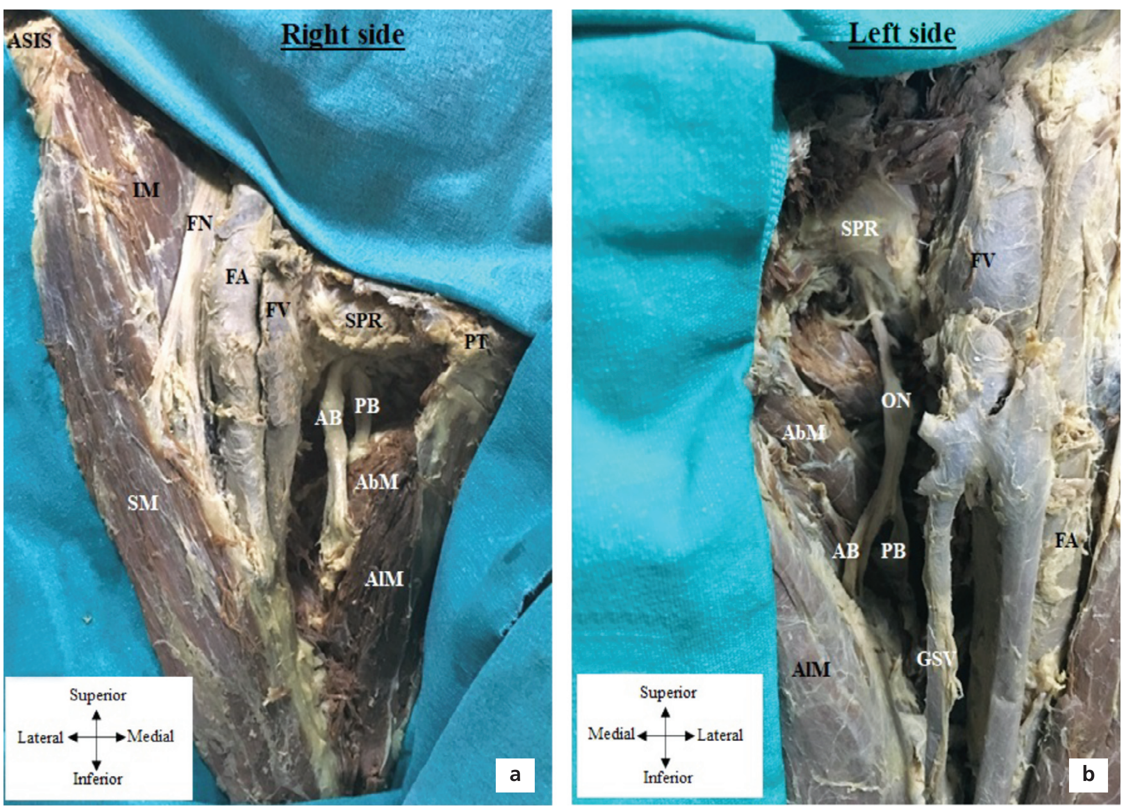

Figure 4. Anterior view of the pelvic and thigh regions showing bifurcation pattern of the obturator nerve in adult cadavers: (**a**) intrapelvic; (**b**) extrapelvic. **AB:** anterior branch of the obturator nerve; **AbM:** adductor brevis muscle, **AlM:** adductor longus muscle; **ASIS:** anterior superior iliac spine; **FA:** femoral artery, **FN:** femoral nerve; **FV:** femoral vein; **GSV:** great saphenous vein, **IM:** iliopsoas muscle; **ON:** obturator nerve; **PB:** posterior branch of the obturator nerve; **PT:** pubic tubercle; **SM:** sartorius muscle; **SPR:** superior pubic ramus.

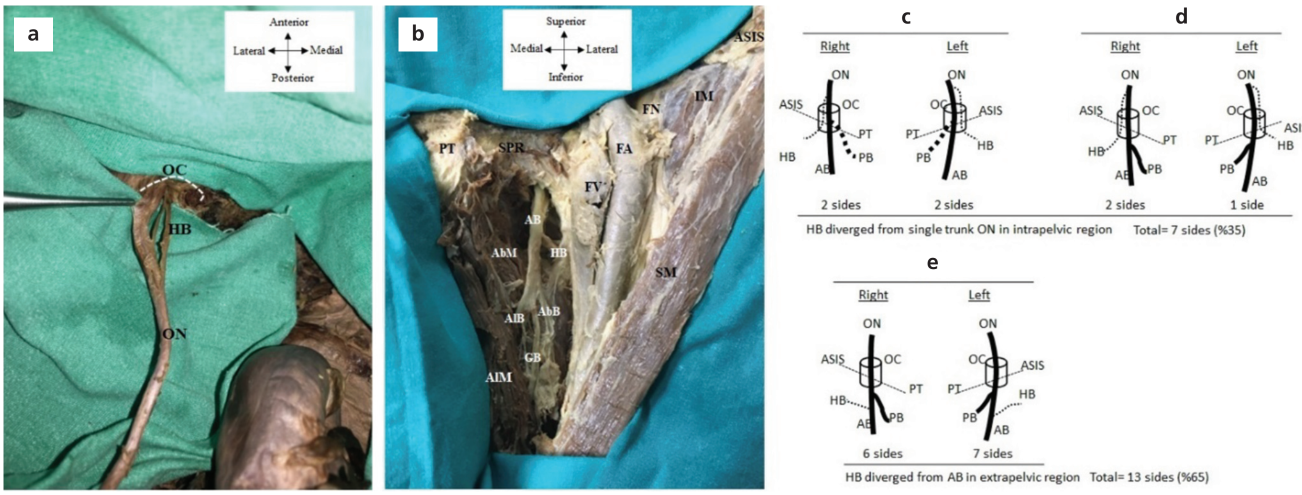

Figure 5. Hip branching patterns of the obturator nerve (**a**–**e**). (**a**) Superior view of pelvic region; (**b**) anterior view of the thigh. **AB:** anterior branch of the obturator nerve; **AbB:** adductor brevis branch; **AbM:** adductor brevis muscle, **AlB:** adductor longus branch; **AlM:** adductor longus muscle; **ASIS:** anterior superior iliac spine; **FA:** femoral artery; **FN:** femoral nerve; **FV:** femoral vein; **GB:** gracilis branch; **HB:** hip branch; **IM:** iliopsoas muscle, **OC:** obturator canal; **PB:** posterior branch of the obturator nerve; **PT:** pubic tubercle; **SM:** sartorius muscle; **SPR:** superior pubic ramus.

3.94 mm (**Figure 6** and **Table 2**). The mean distance from SPR to the AB and PB diverging point was 12.48±2.27 mm (**Figure 6** and **Table 2**). In addition to these findings, in one of the fetuses, unilateral accessory obturator nerve (AON) was passing superior to the SPR and connected with AB (**Figure 6**).

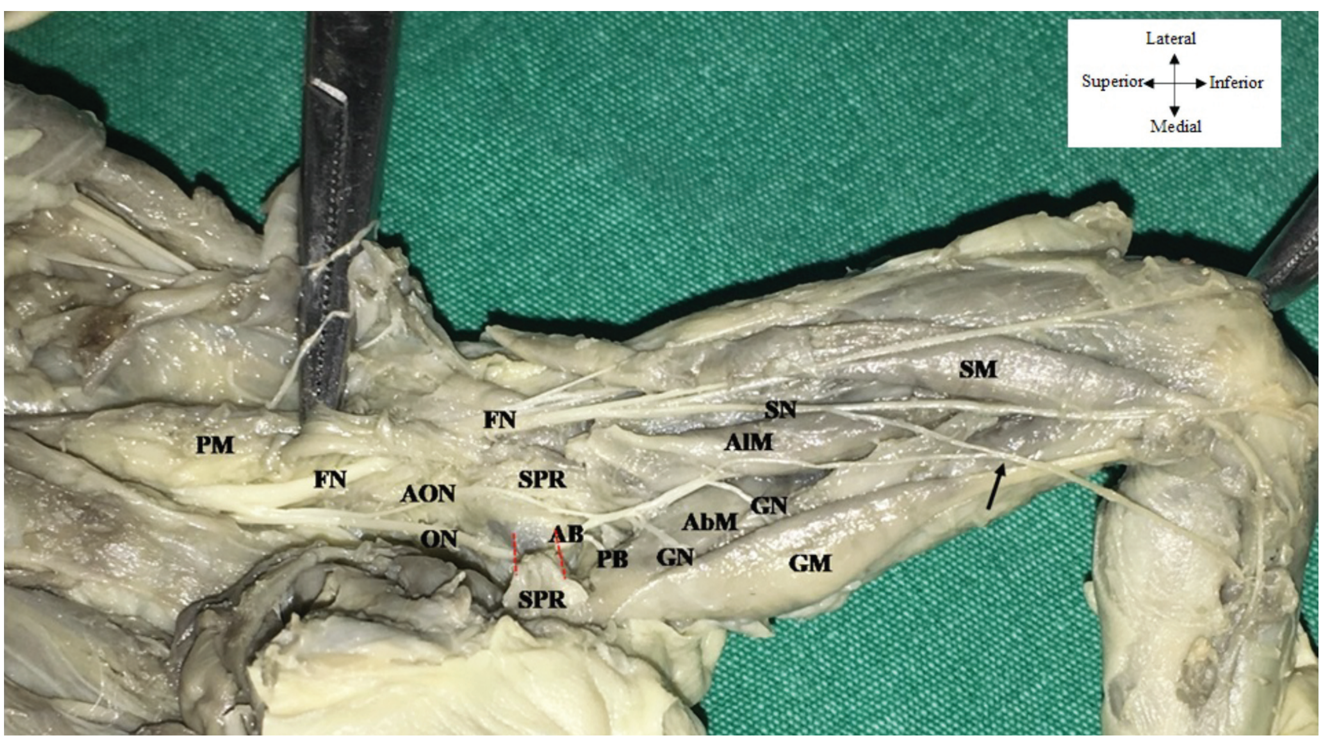

Figure 6. Anterior view of the pelvic and thigh regions of a fetus showing communication between obturator nerve and accessory obturator nerve. **AB:** Anterior branch of the obturator nerve; **AlM:** adductor longus muscle; **AON:** accessory obturator nerve; **GM:** gracilis muscle; **GN:** gracilis nerve; **ON:** obturator nerve; **PB:** posterior branch of the ON; **PM:** psoas major muscle; **QFM:** quadriceps muscle; **SM:** sartorius muscle; **SN:** saphenous nerve; **SPR:** superior pubic ramus. **Black arrow** indicates the connection between saphenous and obturator nerves; **red dashed lines** illustrate the obturator channel fold.

Discussion

The origin of ON can be quite diverse. For example, whilst ON often arise from the L2–L4 level,[21–23] it can emergence from L3–L4[21,22] or even T12–L5[21,22] levels. In this context, our findings seem to be consistent with the anatomical origin reported by Anloague et al.[23] On the other hand, revisiting its branching pattern (where the AB/PB diverges from the ON; sub-branches of the AB and PB; branching origin and pattern of nerves to the hip joint and muscles) is necessary to discuss its fundamental relevance to anesthetic interventions.

From an anesthesia perspective, a successful ONB can be defined as achieving the desired level of anesthesia on the relevant anatomical structures (e.g. hip joint capsule, medial side of the thigh, adductor group muscles, etc.) and completing the procedure in the least amount of time, with the least amount of puncture and the least amount of anesthetic substance volume while achieving maximum patient comfort with no or minimal complications. For this purpose, of course, the success of the procedure may vary depending on the target anatomical structure to be anesthetized. For example, to secure blockade of the hip articular branches, the chosen blockade approach should act on the most favorable proximal levels to guarantee blockade of the main ON closer to the AB and/or PB. Otherwise, the success of the anesthetic intervention may be insufficient or even fail due to possible variations, for example, hip joint branching. Since the list of anatomical structures innervated by the ON is long and it travels over a wide anatomical territory, successful access to selected structures can be problematic even with currently used anesthetic techniques (e.g. inguinal and pubic approach) (**Table 3**).

While efforts to improve methods for better ONB seem to be ongoing, these improvements will be aided by a focus on detailed anatomy, particularly the variations that can be seen in the branching and course of the nerve. The results of different anatomical studies on the main divergence point of the common ON are important in this regard. Any kind of ON branching within the pelvic region may result in inadequate anesthesia in clinical practice. Previous studies on adult cadavers and fetuses have shown that the ON branching point can be

Table 2
Position and location of neurovascular structures according to oblique and vertical lines.

Parameters	Mean±SD (mm)
Distance between ASIS–PT	118.92±8.43
Distance between PT–ON	26.61±3.94
Distance between PT–FV	38.66±4.18
Distance between PT–FA	49.13±4.48
Distance between PT–FN	64.33±5.16
Distance between SPR–AB/PB diverging point	12.48±8.27
Distance between SPR–AbB diverging point	24.65±8.77
Distance between SPR–GB diverging point	33.77±14.13

ASIS: anterior superior iliac spine; **AB:** anterior branch; **AbB:** adductor brevis branch; **FA:** femoral artery; **FN:** femoral nerve; **FV:** femoral vein; **GB:** gracilis branch; **PB:** posterior branch; **PT:** pubic tubercle; **SPR:** superior pubic ramus.

Table 3
Success rate based on the anesthetic approach.

Anesthetic approach	Targeted nerves and branches	Success rate (%)	Applied surgeries	Reference
3 in 1		16%	Above-below knee amputation, various knee surgeries	Atanassoff et al.[29]
		50%		Wallace et al.[30]
	Sensorial branches of femoral and lateral cutaneous femoral nerves	52% for sensorial branches		Capdevilla et al.[31]
	Sensorial and motor branches of obturator nerve	32% for motor branches		
Labat's classic	Common ON	84%	Transurethral resection surgery	Jo et al.[9]
		84%		Moningi et al.[7]
		78%		Macalou et al.[14]
		74.1%		Aghamohammadi et al.[8]
Inguinal	Common ON or separately anterior and posterior branches	97.2%		Thallaj et al.[6]
		80%		Anagnostopoulou et al.[3]
		96.1%		Jo et al.[9]
		98%		Moningi et al.[7]
		97.1%		Aghamohammadi et al.[6]

Table 4
Bifurcation pattern of the obturator nerve (sides and %).

Study	Specimens	N (sides)	Branching pattern of the obturator nerve (sides and %)		
			Intrapelvic	Inside the channel	Extrapelvic
Anagnostopoulou et al.[3]	Adult cadavers	168	39 (23.22%)	87 (51.78%)	42 (25%)
Tshabalala[4]	Adult cadavers	201	4 (2%)	187 (93%)	10(5%)
Current study	Adult cadavers	20	0 (0%)	8 (40%)	12 (60%)
	Fetuses	94	8 (8.5%)	31 (33%)	55 (58.5%)
		Total: 114	8 (7%)	39 (34%)	67 (59%)

located in the pelvic region, and this branching pattern may exhibit a wide range of prevalence (0–23%) (**Table 4**). Although the studies of Anagnostopoulou et al.[3] and Tshabalala[4] included impressive numbers of adult cadavers being 168 and 201, respectively, the bifurcation pattern of ON within the pelvis was distributed quite differently between the studies (23%–39/168 vs. 2%–4/201) (**Table 4**). Furthermore, based on our observations in adult cadavers, no ON bifurcation is found in the pelvic region (0/20), whereas in fetuses (24–26 weeks) 8.5% (8/94) of nerve bifurcations occur in the intrapelvic region (**Table 4**). Considering that peripheral nerve development is no longer progressing at this fetal age, this 8.5% intrapelvic occurrence can probably be included in the adult rate. To our knowledge, our study is the first in the literature to illustrate the fetal anatomy of the ON. These three separate data set clearly show that the division of the ON into anterior and posterior branches can vary greatly.

All these data indicate that the variations of the ON bifurcation should be well known. An example of such an anatomical-anesthetic relationship is given in the study by Yoshida et al.[24] in which they aimed to perform obturator nerve blockade at the proximal level. These researchers clearly observed that with a single injection of blue dye into the thick fascia between the pectineus and obturator externus muscles of a cadaver, the dye traveled retrograde along the obturator canal. With this method, the AB and PB were stained both proximal and distal to the canal.[24] They called this procedure the US-guided pubic approach and also achieved 100% success using this approach in twenty patients undergoing transurethral bladder tumor resection.[20] However, this procedure was only tested in transurethral bladder tumor resection. Therefore, further studies are needed to examine whether this method is reproducible for other indications, such as blocking the hip joint branches for the treatment of hip pain. In this sense, new anatomical studies with dye injection trials may be useful to test the efficacy of different ONB techniques (e.g. different landmarks and needle position, etc.).

The second important issue in ON anatomy is the origin and number of hip joint branches. Variations in hip branches may complicate nerve blockade to provide hip anesthesia. Therefore, knowledge of variations in hip joint branching can be crucial for anesthesiologists. Although we have not observed any cadavers with more than one hip joint branch, Anagnostopoulou et al.[3] encountered up to three branches. The prevalence of articular branches emerging from the main ON in the presence of a single articular branch was reported to be 35% and 47% in two studies, including ours (**Table 5**). Interestingly, when the number of articular branches is more than single, the origin of the branch is also multiply distributed, e.g. this branch can diverge from ON and PB or AB and PB as shown by Anagnostopoulou et al.[3] However, what is even more interesting is that the bifurcation of AB and PB has a highly variative state discussed in the paragraph above. For example, if the bifurcation of ON occurs in the pelvic region, the question of how the variability of hip branching occurs is unknown. Therefore, the co-occurrence of two variable factors (the site where the bifurcation of the ON and the hip branch from the ON and the AB/PB arise) may create even greater variability, which is clearly undesirable for anesthesiologists aiming at blocking the hip branches.

Regarding the use of ONB when targeting blockade of sensory innervation in the hip joint capsule (hip surgery, pain management), no matter how wide the anatomical variability, the chosen ONB method should have the ability to affect these dual-source hip joint branches, especially the main ON and PB at more proximal levels. Furthermore, while it remains unclear whether ONB alone can relieve acute postoperative

Table 5
Distribution of hip articular branch of the obturator nerve.

Study	Specimens	N (sides)	Number and origin of hip articular branchese		
Anagnostopoulou et al.[3]	Adult cadavers	168	Single branch *Total:* 104 sides (61.9%) ON (80 sides) (76.92%) AB (20 sides) (19.24%) PB (4 sides) (3.84%)	2 branches *Total:* 34 sides (20.24%) ON (16 sides) (47.05%) PB (14 sides) (41.17%) Both ON and PB (4 sides) (11.76%)	3 branches *Total:* 30 sides (17.86%) ON (16 sides (53.34%) Both ON and PB (8 sides) (26.66%) Both AB and PB (6 sides) (20%)
Current study	Adult cadavers	20	Single branch 20 sides (100%) ON (7 sides (35%) AB (13 sides) (65%)	$\bar{\chi}$	$\bar{\chi}$

pain, lateral femoral cutaneous nerve blockade in combination with ONB has been suggested to be beneficial.[25] However, it is clear that ONB is a vital component for indications related to the hip joint. Although ONB interventions have not been performed for indication of hip joint anesthesia, Taha et al.[20] demonstrated 100% successful blockade of both the AB and PB in all patients through a single application of local anesthetic to the interfacial plane between the pectineus and obturator externus muscles, combined with an ultrasound-guided proximal approach. Based on the high blockade rates of the AB and PB from Taha's[20] findings, it can be concluded that the proximal approach is also useful when blocking sensation in the hip joint capsule.

Since the occurrence of sudden thigh reflex during tumor resection in bladder is high and constituting complications,[16] desired level of temporary relief of adductor reflex via ONB is another important matter. In this regard, origin and the number of the muscular ramification of ON also bear importance to the selected ONB approach. Limited to just a few studies, a highly diverse state of the muscular ramification of ON was evident (**Table 6**). In our study, both cadaveric (20) and fetal sides (94) showed that in each side, AB gives triple muscular branches, while PB gave only single muscular branch. When tracing the course for respective innervation targets, those triplets arising from AB were reaching to adductor longus, brevis and gracilis muscles as well as the only muscular branch from PB was reaching to adductor magnus muscle in all the cases (**Table 6**). Commonly observed in three of the studies, when AB shows triple motif, they reached adductor longus, brevis and gracilis muscles (66.7–100%) (**Table 6**). PB motif was also evident. One distinct feature of our PB data was that it was giving single muscular branch (adductor magnus muscle), whereas in other two studies, PB was sourcing multiple muscular branches (to adductor brevis, longus and external obturator muscles) (**Table 6**).

Since the occurrence of sudden thigh reflex is high and can be a complication during tumor resection in the bladder,[16] temporary relief of the adductor reflex at the desired level via ONB is another important issue. In this context, the origin and number of muscle branching of the ON is also important for the chosen ONB approach. Limited to only a few studies, it has been observed that the muscle branching of the ON shows considerable variation (**Table 6**). In our study, in both adult cadavers and fetal cadavers, it was shown that the AB gave three muscle branches on both sides, whereas the PB gave only one muscle branch. When the muscles to which these muscle branches went were examined, it was observed that the three branches from the AB reached the adductor longus, brevis and gracilis muscles, while the single muscle branch from the PB reached the adductor magnus muscle in all cases (**Table 6**). Commonly, in three of the studies, when the AB gave three muscle branches, these branches reached the adductor longus, brevis and gracilis muscles (66.7–100%) (**Table 6**). PB branching pattern was also evident. A distinctive feature of our PB data was that it gave a single muscle branch (adductor magnus muscle), whereas in the other two studies, PB gave multiple muscle branches (adductor brevis, longus and external obturator muscles) (**Table 6**).

After Taha et al.[20] showed promising results on the use of US-guided proximal approach to block the adductor muscle, different strategies for US-guided fascia iliac approach have been described and tested. The first group of studies suggested that the proximal approach was superior to the distal approach.[16] Thus, the distal

Table 6
Distribution of muscular branching of the obturator nerve.

Study	Specimens	N (sides)	Number of muscular branches from AB	Number of muscular branches from PB
Anagnostopoulou et al.[3]	Adult cadavers	168	**2 branches:** Adductor longus and gracilis 48 sides (28.57%) **3 branches:** Adductor longus, brevis and gracilis 112 sides (66.66%) **4 branches:** Adductor longus, brevis, gracilis and external obturator 8 sides (4.76%)	**Single branch:** Adductor magnus 23 sides (13.69%) **2 branches:** Adductor magnus and brevis 101 sides (60.11%) **3 branches:** Adductor magnus, brevis and external obturator 31 sides (19.04%) **4 branches:** Adductor magnus, brevis, longus and external obturator 12 sides (7.14%)
Tshabalala[4]	Adult cadavers	195	**3 branches:** Adductor longus, brevis and gracilis 195 sides (99%)	**2 branches:** Adductor magnus an external obturator 184 sides (89%) **3 branches:** Adductor magnus, brevis and external obturator 10 sides (11%)
Current study	Adult cadavers & fetuses	20 94	**3 branches:** Adductor longus, brevis and gracilis 114 sides (100%)	**Single branch:** Adductor magnus 114 sides (100%)

approach is relatively less suitable for blockade of the PB compared to the proximal approach. A comprehensive discussion on the comparison of distal and proximal approaches has been included in other studies.[16] Anatomical studies indicate that the AB innervates the adductor longus, brevis and gracilis muscles. Therefore, significant adductor muscle anesthesia is possible, even in the case of AB blockade alone. Accordingly, findings from clinical studies have shown that complete adductor blockade does not always occur; moreover, partial blockade is sometimes sufficient. For example, Han et al.[19] found that US-guided proximal and distal approaches did not significantly differ in the clinical efficacy of ONB in patients undergoing transurethral bladder tumor resection, but low-grade adductor muscle spasm was still evident. Interestingly, efforts to combine two different methods can also be effective. For example, in 2016, Yoshida et al.[24] demonstrated a successful ONB with US-guided pubic approach in twenty patients undergoing transurethral bladder tumor resection. Incidentally, using the newest approaches does not always mean that the older ones are less successful. Parallel to the exciting developments in the proximal approach or others, for example Choquet's inguinal approach is still considered a cutting edge procedure even in 2019.[19] A major limitation of comparing different approaches is that different approaches cannot be tested on the same patient.

Akkaya et al.[26] defined a triangle for the ONB surrounded by the SPR, pectineus and external obturator muscles in a study performed through the inguinal approach. In our study, a similar anatomical triangle was observed with the SPR at the top, adductor longus muscle at the medial border and FV at the lateral border (**Figures 1** and **6**). In addition to variations in the branching pattern of the ON,[27–31] it has been reported that the presence of AON and possible anastomoses with the ON can be observed.[27,28] Akkaya et al.[28] interpreted the occurrence of such variations in terms of nerve blockade as AON blockade added to the ONB may increase clinical efficiency and quality of application.

Conclusion

Although there is a strong visual guidance provided by US-guided procedures, more anatomical landmarks could serve to facilitate existing approaches as well as to establish new ones. In this sense, we currently present a detailed morphometric map composed of distances between specific anatomical landmarks. In addition to those in other studies on ON anatomy, the differential branching patterns of the ON in the pelvic region presented in this article should be considered under a single roof to avoid possible anesthesia errors and increase the success rate of the clinical procedures involved. Finally, we believe that scientific collaborations of anesthesiologists with anatomists have a great potential to improve the fundamentals of anesthesiology.

Limitations

The first limitation of the study was that we did not have adult female cadavers suitable for dissection in our inventory and therefore could not discuss the differences between the sexes. However, we were able to perform evaluations for both sexes in fetuses. The second limitation is that we were not able to identify the branches to the hip joint in pelvic or thigh dissections due to the difficulty of dissection in fetuses. Another limitation is that the measurements obtained from fixed cadavers could not be scanned on patients with ultrasound support. This situation can be supported by new studies in the future.

Acknowledgement

We thank to donor of human cadavers and fetuses. Also, we thank to the Pathology and Obstetrics and Gynecology Departments of Mersin University Hospital that contributed to the acquisition of the materials in the Anatomy inventory.

Conflict of Interest

The authors declare that they have no conflict of interest.

Author Contributions

TK: project development, data collection, analysis, supervision, and manuscript writing; OB: data collection, analysis; ŞR: supervision, participated in evaluation of clinician perspective; ABÖ: supervision, participated in evaluation of anatomical perspective; NCÖ: manuscript writing and analysis, participated in evaluation of anatomical perspective. All authors reviewed the manuscript.

Ethics Approval

Whole dissections and anatomical protocol of the study were approved by Mersin University, Ethics Board of Clinical Research (2019/278). Human cadaver and postmortem human fetuses used in this study are legally registered in the educational and research gross anatomical archive of the Anatomy Department of Mersin University, Faculty of Medicine. This study accordance with recognized standards of Helsinki Declaration.

Funding

None.

References

1. Standring S. Gray's anatomy: the anatomical basis of clinical practice. 40th ed. Edinburgh (Scotland): Elsevier Churchill Livingstone; 2008. p. 1551.
2. Bergman RA, Afifi AK, Miyauchi R. Illustrated encyclopedia of human anatomic variation. Opus III: Nervous system: Plexuses [Internet]. [Retrieved on October 11, 2022]. Available from: https://www.anatomyatlases.org/AnatomicVariants/NervousSystem/Text/ObturatorNerve.shtml
3. Anagnostopoulou S, Kostopanagiotou G, Paraskeuopoulus T, Chantzi C, Lolis E, Saranteas T. Anatomic variations of the obturator nerve in the inguinal region: implications in conventional and ultrasound regional anesthesia techniques. Reg Anesth Pain Med 2009;34:33–9.
4. Tshabalala ZN. The anatomy and clinical implications of the obturator nerve and its branches (Dissertation submitted in full fulfilment of the requirements for the degree Master of Science in Anatomy, University of Pretoria) 2015. [Internet]. [Retrieved on October 11, 2022]. Available from: https://repository.up.ac.za/bitstream/handle/2263/53048/Tshabalala_Anatomy_2015.pdf?sequence=1&isAllowed=y
5. Kumka M. Critical sites of entrapment of the posterior division of the obturator nerve: anatomical considerations. J Can Chiropr Assoc 2010;54:33–42.
6. Thallaj A, Rabah D. Efficacy of ultrasound-guided obturator nerve block in transurethral surgery. Saudi J Anaesth 2011;5:42–4.
7. Moningi S, Durga P, Ramachandran G, Murthy PV, Chilumala RR. Comparison of inguinal versus classic approach for obturator nerve block in patients undergoing transurethral resection of bladder tumors under spinal anesthesia. J Anaesthesiol Clin Pharmacol 2014;30:41–5.
8. Aghamohammadi D, Gargari RM, Fakhari S, Bilehjani E, Poorsadegh S. Classic versus inguinal approach for obturator nerve block in transurethral resection of bladder cancer under spinal anesthesia: a randomized controlled trial. Iran J Med Sci 2018;43:75–80.
9. Jo YY, Choi E, Kil HK. Comparison of the success rate of inguinal approach with classical pubic approach for obturator nerve block in patients undergoing TURB. Korean J Anesthesiol 2011;61:143–7.
10. Enneking FK, Chan V, Greger J, Hadzić A, Lang SA, Horlocker TT. Lower-extremity peripheral nerve blockade: essentials of our current understanding. Reg Anesth Pain Med 2005;30:4–35.
11. McNamee DA, Parks L, Milligan KR. Post-operative analgesia following total knee replacement: an evaluation of the addition of an obturator nerve block to combined femoral and sciatic nerve block. Acta Anaesthesiol Scand 2002;46:95–9.
12. Marhofer P, Nasel C, Sitzwohl C, Kapral S. Magnetic resonance imaging of the distribution of local anesthetic during the three-in-one block. Anesth Analg 2000;90:119–24.
13. Labat G. Regional anesthesia: its technic and clinical application. 1st ed. Philadelphia (PA): WB Saunders; 1923. 496 p.
14. Macalou D, Trueck S, Meuret P, Heck M, Vial F, Ouologuem S, Capdevila X, Virion JM, Bouaziz H. Postoperative analgesia after total knee replacement: the effect of an obturator nerve block added to the femoral 3-in-1 nerve block. Anesth Analg 2004;99:251–4.
15. Winnie AP, Ramamurthy S, Durrani Z. The inguinal paravascular technic of lumbar plexus anaesthesia: the "3-in-1" block. Anesth Analg 1973;52:989–96.
16. Yoshida T, Nakamoto T, Kamibayashi T. Ultrasound-guided obturator nerve block: a focused review on anatomy and updated techniques. BioMed Res Int 2017;2017:7023750.
17. Wassef MR. Interadductor approach to obturator nerve blockade for spastic conditions of adductor thigh muscles. Reg Anesth 1993;18:13–7.
18. Choquet O, Capdevila X, Bennourine K, Feugeas JL, Bringuier-Branchereau S, Manelli JC. A new inguinal approach for the obturator nerve block: anatomical and randomized clinical studies. Anesthesiology 2005;103:1238–45.

19. Han C, Ma T, Lei D, Xie S, Ge Z. Effect of ultrasound-guided proximal and distal approach for obturator nerve block in transurethral resection of bladder cancer under spinal anesthesia. Cancer Manag Res 2019;11:2499–505.
20. Taha AM. Brief reports: ultrasound-guided obturator nerve block: a proximal interfascial technique. Anesth Analg 2012;114:236–9.
21. Horwitz MT. The anatomy of (A) the lumbosacral nerve plexus-its relation to variations of vertebral segmentation, and (B) the posterior sacral nerve plexus. Anat Rec 1939;74:91–107.
22. Arora D, Kaushal S, Singh G. Variations of lumbar plexus in 30 adult human cadavers – a unilateral prefixed plexus. The International Journal of Plant, Animal and Environmental Sciences 2014;4:225–8.
23. Anloague PA, Huijbregts P. Anatomical variations of the lumbar plexus: a descriptive anatomy study with proposed clinical implications. J Man Manip Ther 2009;17:e107–4.
24. Yoshida T, Onishi T, Furutani K, Baba H. A new ultrasound-guided pubic approach for proximal obturator nerve block: clinical study and cadaver evaluation. Anaesthesia 2016;71:291–7.
25. Rashiq S, Vandermeer B, Abou-setta AM, Beaupre LA, Jones CA, Dryden DM. Efficacy of supplemental peripheral nerve blockade for hip fracture surgery: multiple treatment comparison. Can J Anesth 2013;60:230–43.
26. Akkaya T, Ozturk E, Comert A, Ates Y, Gumus H, Ozturk H, Tekdemir I, Elhan A. Ultrasound-guided obturator nerve block: a sonoanatomic study of a new methodologic approach. Anesth Analg 2009;108:1037–41.
27. Katritsis E, Anagnostopoulou S, Papadopoulos N. Anatomical observation on the accessory obturator nerve (based on 1000 specimens). Anat Anz 1980;148:440–5.
28. Akkaya T, Comert A, Kendir S, Acar HI, Gumus H, Tekdemir I, Elhan A. Detailed anatomy of accessory obturator nerve blockade. Minerva Anestesiol 2008;74:119–22.
29. Atanassoff PG, Weiss BM, Brull SJ, Horst A, Külling D, Stein R, Theiler I. Electromyographic comparison of obturator nerve block to three-in-one block. Anesth Analg 1995;81:529–33.
30. Wallace JB, Andrade JA, Christensen JP, Osborne LA, Pellegrini JE. Comparison of fascia iliaca compartment block and 3-in-1 block in adults undergoing knee arthroscopy and meniscal repair. AANA J 2012;80:S37–44.
31. Capdevila X, Biboulet PH, Bouregba M, Barthelet Y, Rubenovitch J, d'Athis F. Comparison of the three-in-one and fascia iliaca compartment blocks in adults: clinical and radiographic analysis. Anesth Analg 1998;86:1039–44.

ORCID ID:
T. Koç 0000-0001-6970-3351; O. Berger 0000-0002-4932-8758;
Ş. Rumeli 0000-0002-7042-6934; A. Bobuş Örs 0000-0003-4026-5460;
N. C. Öztürk 0000-0001-9459-2120

deomed

Correspondence to: Turan Koç, PhD, Assist. Prof. Dr.
Department of Anatomy, Kahramanmaraş Sütçü İmam University Faculty of Medicine, Kahramanmaraş, Türkiye
Phone: +90 344 300 26 35
e-mail: turann_koc@yahoo.com

Conflict of interest statement: No conflicts declared.

 How to cite this article: Koç T, Beger O, Rumeli Ş, Bobuş Örs A, Öztürk NC. Revisiting the obturator nerve anatomy with a nerve blocking perspective. Anatomy 2023;17(1):22–33.

anatomy
An International Journal of Experimental and Clinical Anatomy
Original Article
http://dergipark.org.tr/en/pub/anatomy
Received: January 11, 2023; Accepted: March 29, 2023
doi:10.2399/ana.23.1381128

Evaluation of the morphological and morphometric characteristics of the acetabulum in the Anatolian population

Melike Taşci, Büşra Pirinç, Betül Sevindik, Nadire Ünver Doğan

Department of Anatomy, Faculty of Medicine, Selçuk University, Konya, Türkiye

Abstract

Objectives: The aim of our study was to investigate the shape, variations and dimensions of the acetabulum, which has an important place in the structure of the hip joint and is of great importance in terms of surgical interventions and compliance with hip joint prostheses, in the Anatolian population.

Methods: A total of 45 coxal bones, 24 right-sided and 21 left-sided, were evaluated. The anterior ridge of the acetabulum was classified into four types: straight, curved, angular and irregular. The transverse diameter (TD), posteroinferior-vertical diameter (VD), acetabular depth (AD) and width of the acetabular notch (WAN) were measured using a digital caliper.

Results: Seven (15.6%) acetabula had straight, 23 (51.1%) had curved, 9 (20%) had angular and 6 (13.3%) had an irregular anterior ridge. The measurements were as follows; TD: 52.3±4.7 mm; VD: 54±4.4 mm; WAN: 26.3±3.6 mm; and AD: 25.3±3 mm. There was no significant difference between the right and left sides for any of the morphometric measurements.

Conclusion: Our study revealed that the most common anterior acetabular ridge shape was curved on both sides of the coxal bone and showed that acetabular morphometry did not vary by side.

Keywords: acetabulum; dry bone; morphology; morphometry

Anatomy 2023;17(1):34–40

Introduction

The acetabulum is a structure formed at the junction of the ilium, ischium and pubis in the coxal bone. It articulates with the femoral head to form hip joint. Thus, it plays a role in the connection and force transmission between the pelvis and lower limbs.[1,2]

Knowing the morphometric properties of the acetabulum is important for radiologists and orthopedic surgeons in diagnosis and surgical planning.[2] Antevert and shallow orientation of the acetabulum is associated with acetabular dysplasia, while increased depth may be associated with femoroacetabular impingement and other orthopedic problems.[3] Even small anatomical incongruities in the structure of the acetabulum can increase susceptibility to degenerative changes in the joint.[4]

During preoperative planning for total hip arthroplasty (THA), differences in bone structure between individuals make it difficult to use uniform materials and standardized methods.[5] Knowledge of variations in the diameter and depth of the acetabulum is also important in the surgical treatment of acetabular fractures.[6] In this context, it is important to know the acetabular morphometry to ensure an optimal fit between the femoral head and acetabulum.

Another clinically important factor in THA is the degree of anteversion, which is necessary for proper implant placement and prevention of dislocation. The morphology of the anterior ridge of the acetabulum also affects the degree of anteversion and therefore its variations are considered important. Since the posterior margin of the acetabulum is usually a simple semicircle, only the anterior margin types have been classified.[7,8]

With our study, we aimed to contribute to the literature on the morphology and morphometric characteristics of the acetabulum in Anatolian population.

Materials and Methods

The study included 45 dry coxal bones from our anatomy laboratory with unknown sex and age. The bones were unilateral from different individuals and did not belong to the pelvis as a whole. There were 24 coxal bones from the right side and 21 from the left side, and the bones reflected the Anatolian population in terms of their origin. The morphology of the anterior margin of the acetabulum was classified into four groups: straight, curved, angular and irregular, in accordance with the literature (**Figure 1**).[9]

For manual morphometric measurements, a digital caliper with a measurement range of 0–150 mm and a

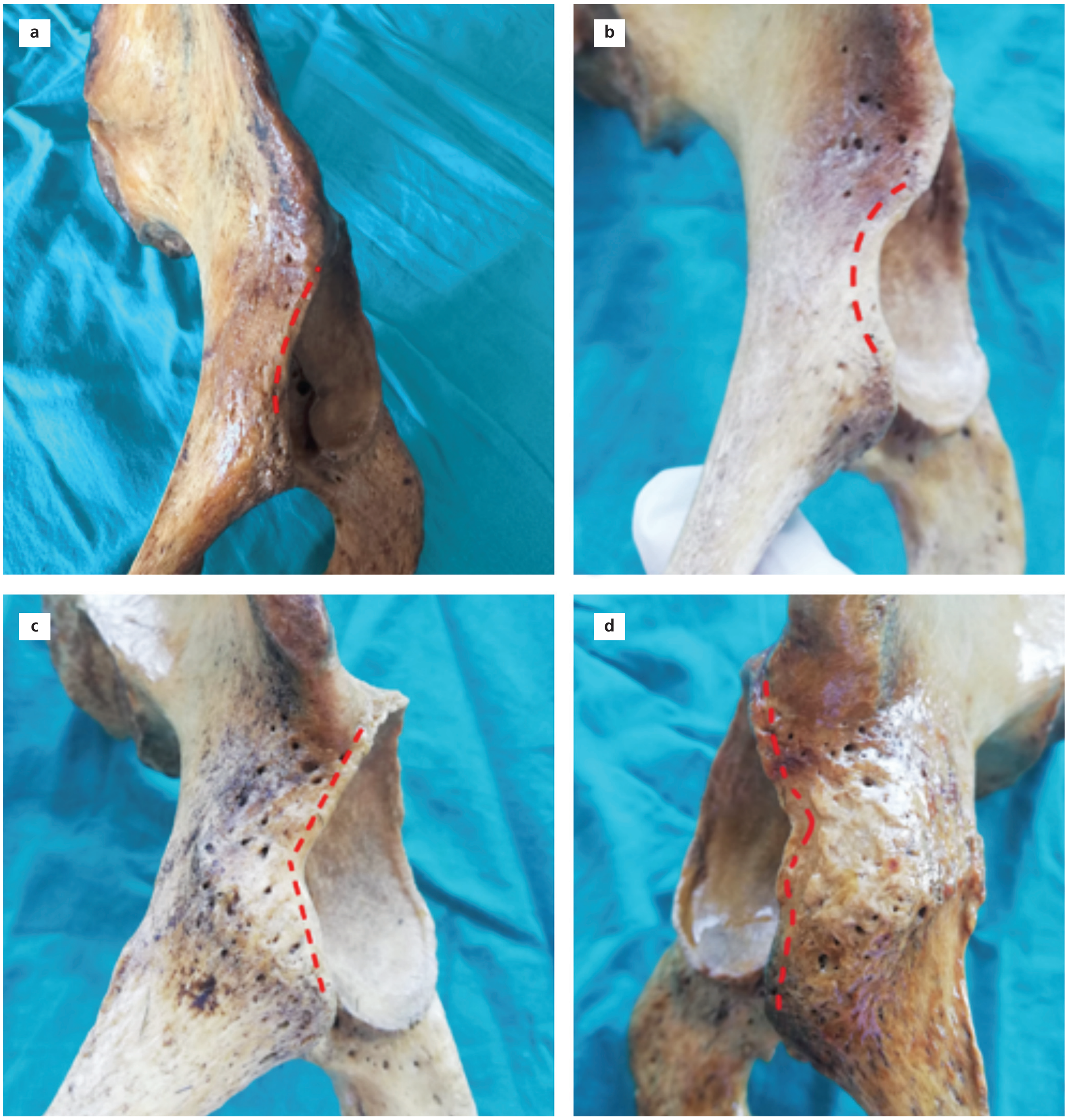

Figure 1. Acetabular anterior ridge types. (**a**) straight; (**b**) curved; (**c**) angular; (**d**) irregular.

precision of 0.03 mm was used. The measurements were repeated twice by the same researcher and the average of the measurements was given as the result. Following parameters were evaluated by measurements:

- Vertical (posteroinferior) diameter (VD) was measured along the axis passing through the anterior superior iliac spine and ischial tuberosity (**Figure 2a**).[10]
- The transverse diameter (TD) of the acetabulum is measured as the maximum distance between the anterior and posterior edges of the acetabular cavity (**Figure 2b**).[2]
- The width of the acetabular notch (WAN) is measured as the distance between the two edges of the lunate surface (**Figure 2c**).[7]
- Acetabular depth (AD) is measured as the perpendicular distance from the deepest point of the acetabular fossa to the horizontal plane passing through the sides of the acetabulum (**Figure 2d**).[6]

Statistical analyses were performed using BM SPSS Statistics Standard Concurrent User v. 22 (IBM Corp., Armonk, NY, USA). Whether the data conformed to the normal distribution was evaluated according to the kurtosis and skewness values. Independent sample t-test was applied for the comparison between right and left sides. A p-value of <0.05 was considered statistically significant.

Results

Of the 45 bones evaluated, 24 were right and 21 were left. Regarding the evaluation of the anterior acetabular ridge types: in the right coxae there were 4 straight (16.6%), 12 curved (50%), 3 angular (12.5%) and 5 irregular types (20.8%). The bones on the left side had 3 flat (14.2%), 11 curved (52.3%), 6 angular types (28.5%) and 1 irregular type (4.7%). In the whole sample, there were 7 flat types (15.6%), 23 curved types (51.1%), 9 angular types (20%) and 6 irregular types (13.3%) (**Table 1**).

When the average values of all bones were considered, TD was 52.3±4.7 mm; VD was 54±4.4 mm; WAN was 26.3±3.6 mm; AD was 25.3±3 mm. TD was 51.8±3.8 mm on the right and 52.9±5.5 mm on the left. VD was 54.1±3.5 mm on the right and 53.9±5.4 mm on the left. WAN was 26.1±3.4 mm on the right and 26.6±3.9 mm on the left. AD was 24.9±3.07 mm on the right and 25.8±3 mm on the left (**Table 2**). No significant differences were found for any of the morphometric assess-

Table 1
Frequencies of morphological types of anterior acetabular ridge.

Ridge type	Right	Left	Total
Straight	4 (16.6%)	3 (14.2%)	7 (15.6%)
Curved	12 (50%)	11 (52.3%)	23 (51.1%)
Angular	3 (12.5%)	6 (28.5%)	9 (20%)
Irregular	5 (20.8%)	1 (4.7%)	6 (13.3%)
Total	24 (100%)	21 (100%)	45 (100%)

Table 2
Mean acetabular morphometric measurements according to side.

	Side	Mean±SD (mm)	p-value
TD	Right	51.8±3.8	0.42
	Left	52.9±5.5	
VD	Right	54.1±3.5	0.86
	Left	53.9±5.4	
WAN	Right	26.1±3.4	0.66
	Left	26.6±3.9	
AD	Right	24.9±3.1	0.33
	Left	25.8±3.0	

AD: acetabular depth; SD: standart deviation; TD: transverse acetabular diameter; VD: vertical (posteroinferior) acetabular diameter; WAN: width of the acetabular notch.

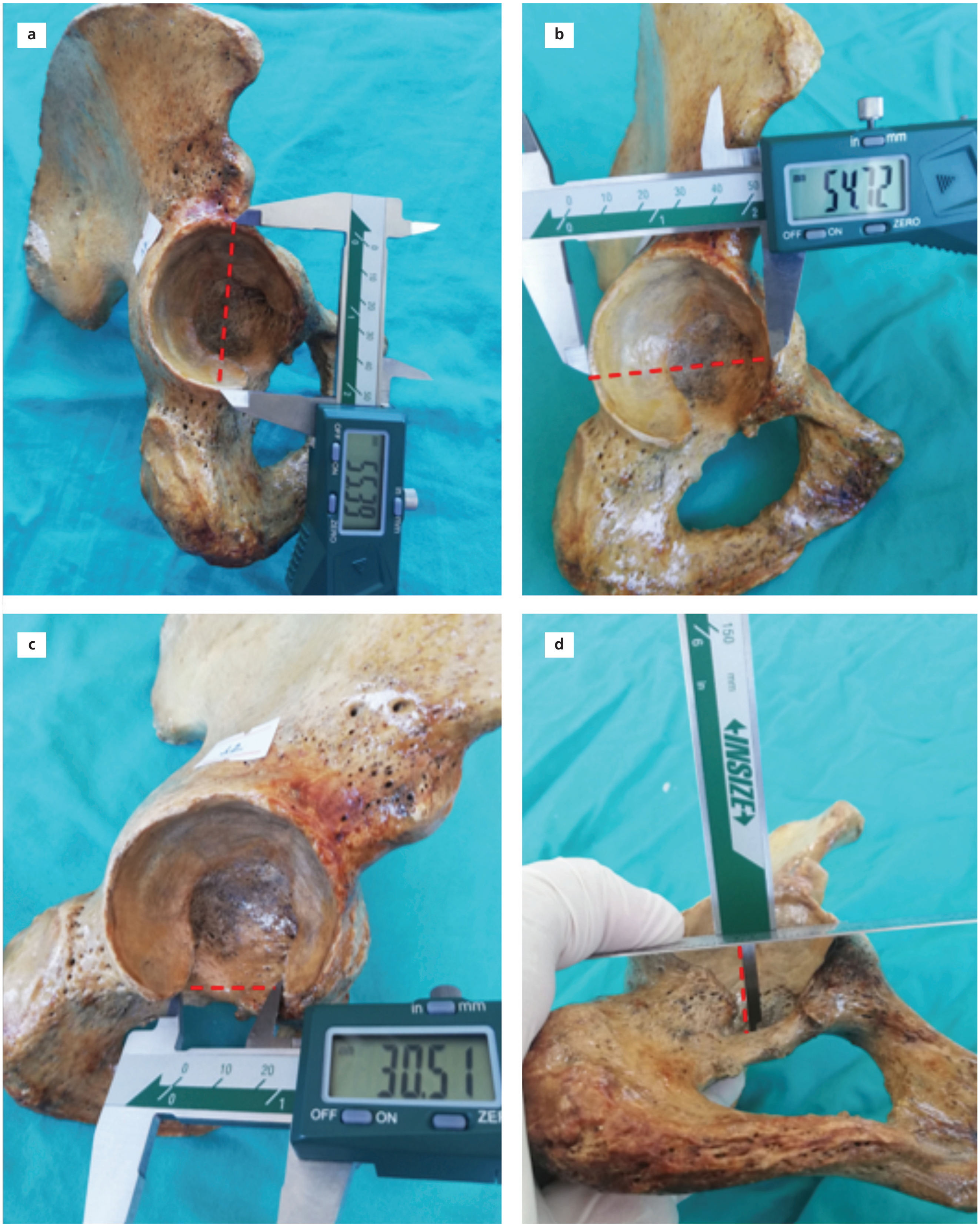

Figure 2. Measurements taken with a digital caliper. (**a**) vertical (posteroinferior) acetabular diameter (VD); (**b**) transverse acetabular diameter (TD); (**c**) width of the acetabular notch (WAN); (**d**) acetabular depth (AD).

ments between the right and left sides (for TD p=0.42, for VD p=0.86, for WAN p=0.66, and for AD p=0.33).

Discussion

In our study, we evaluated the morphologic features of the acetabulum on right and left sides. And no significant difference was found between the right and left sides in terms of TD, VD, WAN and AD. When other studies on this subject were examined; in a dry bone study conducted by Ukoha et al.[2] no significant difference was found between the right and left sides in terms of TD, VD and AD. Likewise, Sreedevi et al.[7] reported that there was no significant difference between right and left sides in terms of VD, AD and WAN in a dry bone study on Indian population. In another the dry bone study conducted by Vyas et al.[4] on Indian population, no significant difference was found between right and left sides in terms of TD and AD. In the study of Yugesh et al.[11] on dry bones in Indian population, no statistically significant relationship was found between right and left sides for TD, WAN and AD. Both our study and results of other studies emphasize that the morphometric properties of the acetabulum do not differ significantly between the sides.

Both the studies of Vyas et al.[4] and Yugesh et al.[11] were conducted on the Indian population; however, it is noteworthy that they found significantly different values for WAN, 22.2±2.9 mm and 30.8±0.42 mm, respectively (**Table 3**). The different results in the studies conducted on the same population and using the same method may be attributed not only to ethnicity but also to factors such as age, sex and body weight of the individuals to which the bones belonged. Furthermore, different results may also be related to ethnic diversity among individuals living in the same country.

In our study, the gender of the individuals to whom the bones belonged is not known. However, there are some studies in the literature evaluating according to gender: Indurjeeth et al.[10] in South Africa reported that acetabular diameter, acetabular depth and acetabular notch width were significantly higher in males than females. In a study conducted by Chauhan et al.[12] in India on a total of 48 cadavers (36 males and 12 females) aged 50–70 years in India, acetabular diameter was larger in males (right: 47.10±2.90 mm, left: 47.48±3.05) compared to females (right: 44.38±3.01 mm, left: 46.0±2.28 mm) and there was a significant difference between genders. Zeng et al.[3] performed a CT study on 50 men and 50 women in a Chinese population with a mean age of 48.2±8.47 years and did not show a significant difference between the sexes. However, acetabular width (for male; right 55.2±3.11 mm, left 56.0±3.33 mm- for female; right 51.4±2.38 mm, left 51.4±2.07 mm) and depth (for male; right 19.3±2.48 mm, left 19.4±2.21 mm- for female; right 17.3±1.68 mm, left 17.4±1.58 mm) were significantly lower in women. In studies conducted in various populations, there are findings showing that acetabular parameters are larger in men.

Table 3
Results of studies in the literature on acetabular morphometrics.

Study	Ethnic origin	Side	Number of bones	TD (mm)	VD (mm)	WAN (mm)	AD (mm)
Ukoha et al.[2]	Nigerian	Right	44	53.9±0.3	55.8±0.3		29.7±0.3
		Left	56	53.2±0.3	54.6±0.3		30.2±0.3
Indurjeeth et al.[10]	South African (black race)	Right	44		54.84±4.18	21.72±2.98	31.30±3.18
		Left	56				
Sreedevi et al.[7]	Indian	Right	39		49.4±3.5	22.2±2.9	24.0±2.6
		Left	41		48±5.6	22.5±2.4	25.1±2.8
Vyas et al.[4]	Indian	Right	74	47.9±3.5			27.1±2.7
		Left	78	48.3±3.1			26.5±3.4
Yugesh et al.[11]	Indian	Right	60	47.4±0.27		30.8±0.42	29.9±0.21
		Left		48.0±0.37		31.1±0.72	29.7±0.23
Aksu et al.[6]	Anatolian		154		54.29±3.8		29.49±4.2
Uzun et al.[1]	Anatolian	Right	50	50.57		18.08	24.87
		Left	46	51.44		20.25	22.85
Currentstudy	Anatolian	Right	24	51.8±3.8	54.1±3.5	26.1±3.4	24.9±3.07
		Left	21	52.9±5.5	53.9±5.4	26.6±3.9	25.8±3.0

AD: acetabular depth; **SD:** standart deviation; **TD:** transverse acetabular diameter; **VD:** vertical (posteroinferior) acetabular diameter; **WAN:** width of the acetabular notch.

When the results of the study conducted by Uzun et al.[1] on Anatolian population were compared with the results of our study, very similar results were obtained for TD and AD. However, our study showed larger values for WAN. In terms of VD, our present study presented similar values to Aksu et al.[6] Although there is a difference in the mean value for AD, the standard deviation values show that the results are not significantly different (**Table 3**). The study of Uzun et al.[1] was performed with 96 bones without specifying gender and age characteristics, while the study of Aksu et al.[6] was performed with 154 bones without specifying gender and age characteristics. Despite similar limitations in our study, both studies had larger sample sizes compared to ours.

When the morphometric findings of our study were compared with the mean and standard deviation values of other populations, it was observed that our measurements were similar for TD and VD. However, in terms of WAN, we found higher values compared to both the study by Indurjeeth et al.[10] in a South African population and the study by Uzun et al.[1] in an Anatolian population, and lower values compared to the study by Yugesh et al.[11] in an Indian population. The differences observed in studies in the same population may be related not only to race but also to parameters such as gender and age that may affect morphometry.

In our study, in terms of the shape of the acetabular anterior margin, 7 of 45 coxal bones were classified as straight type (15.6%), 9 as angular type (20%) and 6 as irregular type (13.3%). The most common type was the curved type observed in 23 bones (51.1%). Among other studies conducted in Anatolian population, Aksu et al.[6] found curved type in 46.1% of their samples, Govsa et al.[9] found it in 43.3% samples and curved type was the most common type in these studies. In the study by Uzun et al.[1] the curved type was seen with a frequency of 28.1%, while the straight type was found to be 42.7%. The type of anterior prominence may be a parameter influenced by the observer, and the higher prevalence of the straight type in the study of Uzun et al.[1] compared to our study and other studies may indicate a discrepancy related to the bones included in the study and the observer. The effect of age and gender characteristics of the bones was not evaluated in our study and related studies, so their effect on ridge type could not be evaluated.

In studies conducted on the Indian population, the curved type was the most common type with a rate of 37.5% in the study by Vyas et al.,[4] 43.7% in the study by Sreedevi et al.[7] and 61% in the study by Parmara et al.[13] The higher rate in the Indian population in the study of Parmara et al.[13] compared to other studies may be due to the fact that angular type was not included in their classification. In the study conducted by Ukoha et al.[2] in the Nigerian population, the curved type was the most common type with a rate of 35%. Maruyama et al.[8] also found that the curved type was the most common with a rate of 60.5%. In a study conducted by Indurjeeth et al.[10] in Africa, the angular type was found to be the most common type with a rate of 41%. Considering that the study was conducted on black population, it can be assumed that the angular type is relatively higher in this population. In addition, although types were defined for genders in the study, a gender-based comparison was not made (**Table 4**).

Limitations of our study include the limited number of bones in our sample and the lack of information on

Table 4

A comparison of frequencies of anterior acetabular ridge shapes among various studies in the literature (%).

	Ethnic Origin	Number of Bones	Straight (%)	Curved (%)	Angular (%)	Irregular (%)
Ukoha et al.[2]	Nigerian	100	23	35	33	9
Indurjeeth et al.[10]	South African (black race)	100	14	22	41	23
Maruyama et al.[8]	American/ African-American	200	9 (4.5%)	121 (60.5%)	51 (25.5%)	19 (9.5%)
Sreedevi et al.[7]	Indian	80	22	35	18	5
Parmara et al.[13]	Indian	100	20	61		19
Vyas et al.[4]	Indian	152	48	57	19	28
Govsa et al.[9]	Anatolian	226	27	98	64	37
Aksu et al.[6]	Anatolian	154	36	71	26	21
Uzun et al.[1]	Anatolian	96	41	27	20	8
Current study	Anatolian	45	7	23	9	6

the sex, age and body weight of the individuals to whom the bones belonged. Also, the demographic characteristics of the bones are not known. Therefore, the study data are reported to reflect the characteristics of the Anatolian population according to their origin.

Conclusion

Understanding the morphologic and morphometric properties of the acetabulum is very important because of its contribution to the structure of the hip joint. Our study emphasized that the morphometric characteristics of the acetabulum did not differ significantly between the parties. It also showed that the most common shape of the anterior acetabular margin is the curved type. Therefore, our study contributes to the literature on the characteristics of the acetabulum in Anatolian population.

Conflict of Interest

The authors declare that they have no conflict of interest.

Author Contributions

MT: data collection, data analysis, manuscript writing; BP: project development, manuscript writing and editing; BS: project development, manuscript editing; NUD: project development, manuscript editing.

Ethics Approval

All procedures performed in this study involving human participants were in accordance with the ethical standards of the institutional and/or national research committee and with the 1964 Helsinki declaration and its later amendments or comparable ethical standards. Ethical approval was given by the Non-Intervention Clinical Research Ethics Committee of the Medical Faculty (Approval No: 2023/372).

Funding

This research did not receive any specific grant from funding agencies in the public, commercial, or not-for-profit sectors.

References

1. Uzun GB, Değermenci M, İlyas U, Arslan A, Nisari M. Morphometric evaluation of acetabulum. Journal of Surgery and Medicine 2020;4:555–7.
2. Ukoha UU, Umeasalugo KE, Okafor JI, Ndukwe GU, Nzeakor HC, Ekwunife DO. Morphology and morphometry of dry adult acetabula in Nigeria. Revista Argentina Anatomia Clinica 2014;6:150–5.
3. Zeng Y, Wang Y, Zhu Z, Tang T, Dai K, Qiu S. Differences in acetabular morphology related to side and sex in a Chinese population. J Anat 2012;220:256–62.
4. Vyas K, Shroff B, Zanzrukiya K. An osseous study of morphological aspect of acetabulum of hip bone. International Journal of Research in Medicine 2013;2:78–82.
5. Solomon LB, Howie DW, Henneberg M. The Variability of the volume of os coxae and linear pelvic morphometry. considerations for total hip arthroplasty. J Arthroplasty 2014;29:769–76.
6. Aksu FT, Çeri NG, Arman C, Tetik S. Morphology and morphometry of the acetabulum. Dokuz Eylül Üniversitesi Tıp Fakültesi Dergisi 2006;20:143–8.
7. Sreedevi G, Sangam MR. The study of morphology and morphometry of acetabulum on dry bones. International Journal of Anatomy and Research 2017;5:4558–62.
8. Maruyama M, Feinberg JR, Capello WN, D'Antonio JA. Morphologic features of the acetabulum and femur: anteversion angle and implant positioning. Clin Orthop Relat Res 2001;(393):52–65.
9. Govsa F, Ozer MA, Ozgur Z. Morphologic features of the acetabulum. Arch Orthop Trauma Surg 2005;125:453–61.
10. Indurjeeth K, Ishwarkumar S, De Gama BZ, Ndlazi Z, Pillay P. Morphometry and morphology of the acetabulum within the black African population of South Africa. Int J Morphol 2019;37:971–6.
11. Yugesh K, Kumar SS. Morphometric analysis of acetabulum and its clinical correlation in South Indian population. International Journal of Advanced Research 2016;2:1011–4.
12. Chauhan R, Paul S, Dhaon B. Anatomical parameters of North Indian hip joints: cadaveric study. J Anat Soc India 2002;51:39–42.
13. Parmara G, Rupareliab S, Patelc S, Patelb S, Jethvaa N. Morphology and morphometry of acetabulum. International Journal of Biological and Medical Research 2013;4:2924–6.

ORCID ID:
M. Taşci 0000-0001-9428-1189;
B. Pirinç 0000-0002-6927-1306;
B. Sevindik 0000-0003-1287-5544;
N. Ünver Doğan 0000-0001-5696-5547

Correspondence to: Büşra Pirinç, PhD
Department of Anatomy, Faculty of Medicine,
Selçuk University, 42130, Konya, Türkiye
Phone: +90 332 224 38 49
e-mail: busrapirinc2016@gmail.com

Conflict of interest statement: No conflicts declared.

Case Report

http://dergipark.org.tr/en/pub/anatomy
Received: January 28, 2023; Accepted: March 18, 2023
doi:10.2399/ana.23.1273366

anatomy
An International Journal of Experimental and Clinical Anatomy

A rare cadaveric report of the azygos lobe of the right lung

Aditya Srinivasan, Robert-Louis Hollingsworth, Natalia Lowry, Jeffrey Fahl, Michael P. Smith, Amanda S. Khan

Division of Anatomy, Albany Medical College, Albany, NY, USA

Abstract

Variations in the vessels of the mediastinum may cause unexpected complications during thoracic procedures. In this report, we show a rare variation of the azygos vein resulting in an azygos lobe of the right lung in a female cadaver. During routine dissection of the superior mediastinum in a white female cadaver, a variation in the venous anatomy was observed and documented. Further dissection of the middle and posterior mediastinum was performed to follow the course of the anomalous vein, and the right lung was removed. The observed anomalous vein was discovered to be a variation of the azygos vein which arched around the superior lobe of the right lung to unite with the superior vena cava resulting in an azygos lobe of the right lung. Variations in the anatomy of the azygos venous system are not uncommon, and azygos lobes of the right lung are commonly reported as incidental findings on imaging, but not often in cadavers. While individuals with this type of variation are unlikely to present clinically, documenting unusual vascular anatomy of the mediastinum is of interest to avoid unnecessary procedures and unexpected complications during thoracic surgery.

Keywords: anatomical variation; azygos lobe; azygos vein; posterior mediastinum

Anatomy 2023;17(1):41–44 ©2023 Turkish Society of Anatomy and Clinical Anatomy (TSACA)

Introduction

The azygos vein drains the upper abdomen, back, vertebrae, vertebral canal, and the mediastinal viscera, and forms a pathway for collateral circulation between the superior and inferior vena cavae. The azygos vein typically arises from the union of a branch from the posterior aspect of the inferior vena cava (IVC) and right ascending lumbar vein. The azygos vein ascends in the posterior mediastinum either along the right border of the T4–T12 thoracic vertebrae or midline along the T4–T12 vertebral bodies. The azygos vein then arches over the superior aspect of the root of the right lung to join the superior vena cava (SVC). Along its course, the azygos vein receives multiple tributaries including the posterior intercostal veins, the pericardial, mediastinal, esophageal, and bronchial veins, the hemiazygos and accessory hemiazygos veins, and communicating branches from the vertebral venous plexuses that drain the vertebrae and vertebral canal.[1]

Clinically, the azygos vein is typically only affected by hemodynamic changes or mediastinal lesions. Changes in the shape and contour of the azygos vein, observed via imaging of the thorax, often provide insight into possible hemodynamic changes. For example, enlargement of the azygos vein is indicative of increased right mean atrial pressure which can be suggestive of constrictive pericarditis, cardiac tamponade, pulmonary hypertension, or portal hypertension.[2]

Discovering variations in venous anatomy through dissection is not unusual. Variations in the azygos vein course have been previously reported after medical imaging,[3] but less frequently in cadavers.[4] These variations included an azygos vein which arches laterally through the right lung to join the SVC forming an azygos lobe of the lung[5] or an azygos vein that continues directly as the IVC.[6] Here, we present a rare report of an abnormal azygos vein in a female cadaver which resulted in an azygos lobe.

Case Report

During a routine dissection of the anterior and superior mediastinum in a 70-year-old white female cadaver, an anomalous vein that split the superior lobe of the right lung into a superior and inferior portion was observed. The middle and posterior mediastinum were then dissected to visualize the course of the abnormal vein. Images of the full venous course were then taken.

Upon removal of the anterior portion of the thoracic cage to access the superior and anterior mediastinum, an anomalous vein that divided the superior lobe of the right lung into two portions was observed (**Figure 1a**). After removal of the right lung, the anomalous vein was found to receive contributions from the posterior intercostal veins and the IVC and followed a course along the midline of the thoracic vertebrae posterior to the descending thoracic aorta and esophagus (**Figure 1b**), consistent with descriptions of the azygos vein.

The right lung had a superior, middle, and inferior lobe separated by the horizontal and oblique fissures, respectively (**Figure 1c**). The superior lobe of the right lung contained an additional fissure where the anomalous azygos vein passed through the superior lobe dividing the lobe into lateral and medial segments (**Figure 1d**). The medial segment of the divided superior lobe did not have an associated secondary bronchus (**Figure 1e**), consistent with descriptions of an azygos lobe of the right lung.

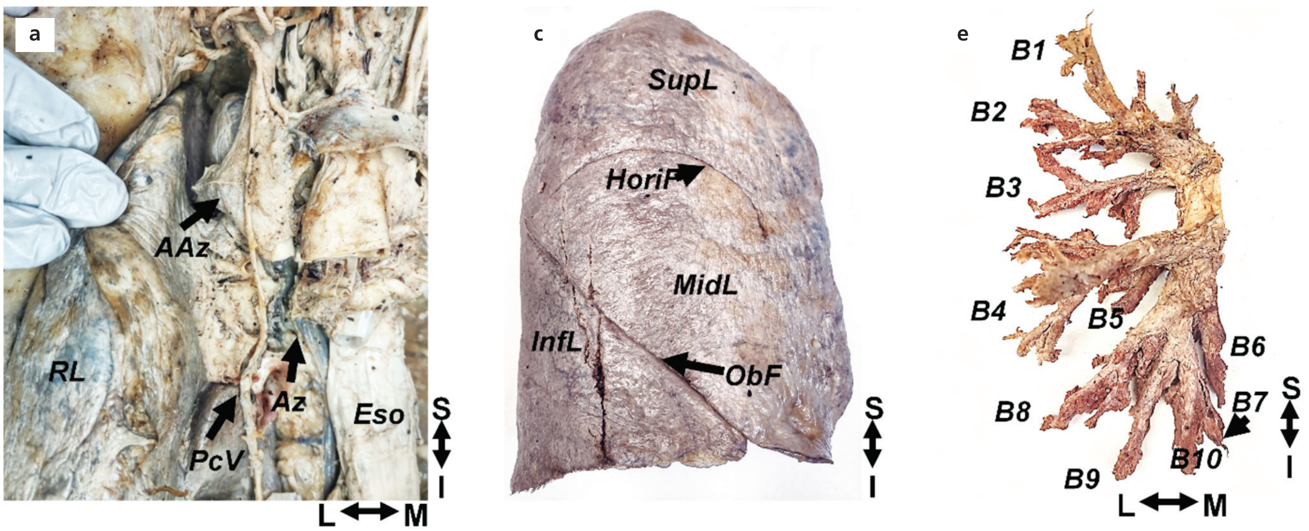

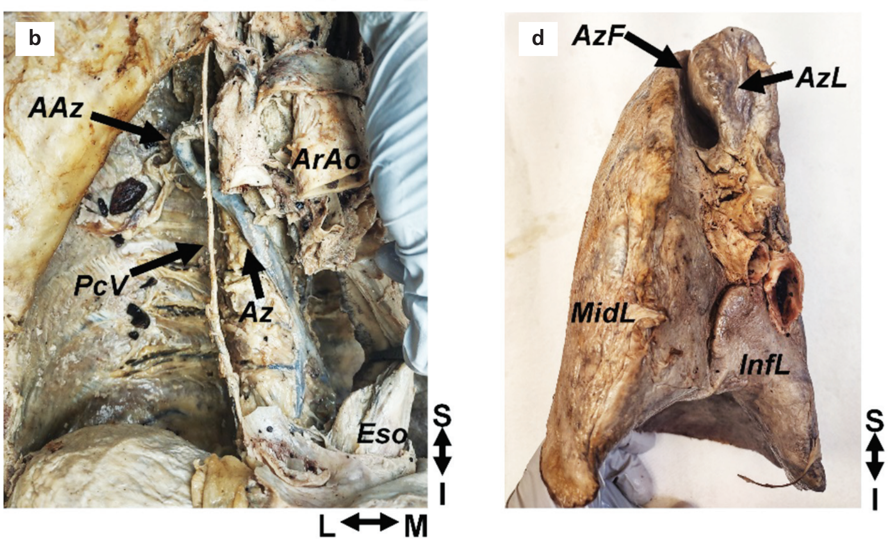

Figure 1. Azygos vein variant and azygos lobe of the right lung. (**a**–**b**) The arch of the azygos vein passes through the superior lobe of the right lung dividing it into two segments. (**c**) The right lung has a superior, middle, and inferior lobe divided by the horizontal and oblique fissures, respectively. (**d**) The superior lobe of the right lung is divided by the azygos vein in the azygos fissure causing the superior lobe of the right lung to have a medial azygos lobe of the right lung. (**e**) A separate secondary bronchus traveling to the azygos lobe was not observed. **AAz:** arch of the azygos vein; **ArAo:** arch of the aorta; **Az:** azygos vein; **AzF:** azygos fissure; **AzL:** azygos lobe of the right lung; **B1:** apical bronchus of superior lobe; **B2:** posterior bronchus of superior lobe; **B3:** anterior bronchus of superior lobe; **B4:** lateral bronchus of middle lobe; **B5:** medial bronchus of middle lobe; **B6:** superior bronchus of inferior lobe; **B7:** medial basal bronchus; **B8:** anterior basal bronchus; **B9:** lateral basal bronchus; **B10:** posterior basal bronchus; **Eso:** esophagus; **HoriF:** horizontal fissure; **I:** inferior; **InfL:** inferior lobe of the right lung; **L:** lateral; **M:** medial; **MidL:** middle lobe of the right lung; **ObF:** oblique fissure; **PcV:** pericardiophrenic vessels; **RL:** right lung; **S:** superior; **SupL:** superior lobe of the right lung.

Discussion

We discovered a rare variation of the azygos vein and its associated azygos lobe of the right lung. Typically, the azygos vein branches from the posterior aspect of the IVC and the right ascending lumbar vein. The azygos vein ascends along the right border or the midline of the inferior eight thoracic vertebrae in the posterior mediastinum before arching over the root of the right lung to drain into the superior vena cava.[1] The azygos venous system is known to vary significantly and rarer variants include an inferior vena cava that underwent agenesis with the drainage of the abdomen and lower limbs instead being routed through the azygos vein.[6] Additionally, an azygos vein passing through the superior lobe of the right lung has been observed on imaging,[5] but less frequently in cadavers,[4,7,8] and far less commonly in females, 0.25%, than in males, 1.17%.[9] Despite the azygos system varying significantly,[10,11] variations in the azygos venous system that affect the lungs are likely due to abnormalities during development.

During the fifth week of development, the main veins of the embryo are the vitelline, umbilical, and anterior and posterior cardinal veins. During the fifth to seventh weeks of development, the subcardinal, sacrocardinal, and supracardinal veins form. At this time, the body walls drain into the posterior cardinal vein, and then drain into longitudinal veins on either side of the body, the early azygos venous system, which still ultimately drains into the posterior cardinal vein. Over time, the left common cardinal vein regresses shunting blood from the veins of the left azygos line into the right azygos line. The azygos vein forms from the veins of the right azygos line and the most cranial part of the right posterior cardinal vein. As the left cardinal vein regresses, the cranial portion of the right posterior cardinal vein migrates from lateral to medial to its final position wrapping around the root of the right lung.[12,13] Incomplete migration of the posterior cardinal vein medially can cause it to pierce the developing superior lobe of the right lung resulting in the formation of an azygos lobe, as observed here. As the azygos lobe lacks an associated secondary bronchus, it is not considered to be a true lobe of the right lung.[5]

The azygos venous system itself is usually not affected by clinical pathologies. However, changes in the shape and contours of the veins of the azygos venous system, especially the azygos vein, often signify an underlying pathology: constrictive pericarditis, cardiac tamponade, pulmonary hypertension, or portal hypertension.[2] Furthermore, the abnormal course of the azygos vein which results in an azygos lobe of the right lung leads to abnormal paratracheal opacities being observed on chest X-ray. These are often treated as a mediastinal lesion leading to unnecessary surgical procedures of the thorax.[5] Additionally, the azygos lobe may be unaffected by pathological processes occurring in the rest of the lung such as disseminated pulmonary tuberculosis,[14] and pathologies of the azygos lobe often remain confined to the lobe making identification and treatment more difficult. For example, carcinomas of the azygos lobe are not associated with the involvement of the regional mediastinal lymph nodes.[15] Knowledge of the anatomy of the azygos vein and its influence on associated structures such as the lungs are important to understand when interpreting imaging of the chest and during surgical procedures within the thoracic cage.

Conclusion

The azygos vein can pierce the superior lobe of the right lung forming an azygos lobe of the right lung which can be mistaken for mediastinal pathology. Documenting the presence and course of this variation in the azygos vein and its associated abnormal lung anatomy is important to avoid unnecessary procedures of the mediastinum and thorax.

Acknowledgements

The authors would like to thank the donors to the Anatomical Gift Program at Albany Medical College so that anatomical research can be conducted.

Conflict of Interest

The authors have no conflicts of interests to declare.

Author Contributions

AS: project development, data collection, manuscript writing/editing; RLH: data collection, manuscript writing/editing; NL: manuscript writing/editing; JF: manuscript writing/editing; MS: project development, manuscript writing/editing; AK: project development, manuscript writing/editing.

Ethics Approval

Ethics approval was received through the Anatomical Gift Program at Albany Medical College.

Funding

None.

References

1. Piciucchi S, Barone D, Sanna S, Dubini A, Goodman LR, Oboldi D, Bertocco M, Ciccotosto C, Gavelli G, Carloni A, Poletti V. The azygos vein pathway: an overview from anatomical variations to pathological changes. Insights Imaging 2014;5:619–28.

2. Shin MS, Ho KJ. Clinical significance of azygos vein enlargement: radiographic recognition and etiologic analysis. Clin Imaging 1999; 23:236–41.
3. Al-Mnayyis A, Al-Alami Z, Altamimi N, Alawneh KZ, Aleshawi A. Azygos lobe: prevalence of an anatomical variant and its recognition among postgraduate physicians. Diagnostics (Basel) 2020;10: 470.
4. Bostanci K, Ozyurtkan MO, Polat MO, Batirel H, Lacin T, Yuksel M, Stamenovic D. Variations in pulmonary fissural anatomy: a medicolegal autopsy study of 256 cases. ANZ J Surg 2020;90:608–11.
5. Akhtar J, Lal A, Martin KB, Popkin J. Azygos lobe: a rare cause of right paratracheal opacity. Respir Med Case Rep 2018;23:136–7.
6. Liu Y, Guo D, Li J, Zhang X, He J, Huang M, Dai J, Cai H. Radiological features of azygos and hemiazygos continuation of inferior vena cava: a case report. Medicine (Baltimore) 2018;97:e0546.
7. Sudikshya K, Shrestha P, Shah AK, Jha AK. Variations in human pulmonary fissures and lobes: a study conducted in Nepalese cadavers. Anat Cell Biol 2018;51:85–92.
8. Rauf A, Rauf WUN, Navsa N, Ashraf KTA. Azygos lobe in a South African cadaveric population. Clin Anat 2012;25:386–90.
9. Yurasakpong L, Yammine K, Limpanuparb T, Janta S, Chaiyamoon A, Kruepunga N, Meemon K, Suwannakhan A. The prevalence of the azygos lobe: a meta-analysis of 1,033,083 subjects. Clin Anat 2021;34: 872–83.
10. Quraishi MB, Mufti O, Wase A. Absent left and right superior vena cava and azygos continuation of inferior vena cava: a rare anomaly of systemic venous return. J Invasive Cardiol 2010;22:159–61.
11. Badagabettu SN, Shetty P, D'Souza MR. A unique variation of azygos system of veins. J Cardiovasc Echogr 2016;26):61–4.
12. Petrenko VM. Development of the ascending lumbar and azygos veins in human embryogenesis. [Article in Russian] Arkh Anat Gistol Embriol 1990;98: 65–70.
13. Dudiak CM, Olson MC, Posniak HV. CT evaluation of congenital and acquired abnormalities of the azygos system. Radiographics 1991; 11:233–46.
14. Denega T, Alkul S, Islam E, Alalawi R. Recurrent hemoptysis – a complication associated with an azygos lobe. The Southwest Respiratory and Critical Care Chronicles 2015;3:44–7.
15. Darlong LM, Ram D, Sharma A, Sharma AK, Iqbal SA, Nagar A, Hazarika D. The azygous lobe of the lung: in the case of lung cancer. Indian J Surg Oncol 2017;8:195–7.

ORCID ID:
A. Srinivasan 0000-0002-8498-4136; R. L. Hollingsworth 0000-0001-6653-1355; N. Lowry 0009-0006-8962-7820; J. Fahl 0009-0009-5929-3999; M. P. Smith 0009-0004-3425-230X; A. S. Khan 0009-0001-1449-1846

Correspondence to: Amanda S. Khan, MS, PhD
47 New Scotland Avenue Mail Code 135, Albany,
NY 12208, USA
Phone: +1 518 2626422
e-mail: khana18@amc.edu

Conflict of interest statement: No conflicts declared.

Case Report

http://dergipark.org.tr/en/pub/anatomy
Received: January 28, 2023; Accepted: March 31, 2023
doi:10.2399/ana.23.3230650

http://dergipark.org.tr/en/pub/anatomy
anatomy
An International Journal of Experimental and Clinical Anatomy

A rare variation of the sternocleidomastoid muscle in a Turkish male cadaver: a case report of four clavicular heads on sternal head and an accessory head

Zehra Çelik, **Shanzeda Khan**, **Mehmet Ülkir**, **Burcu Erçakmak Güneş**

Department of Anatomy, Faculty of Medicine, Hacettepe University, Ankara, Türkiye

Abstract

During a routine dissection at Hacettepe University Department of Anatomy a variation of the sternocleidomastoid muscle was found unilaterally on the left side, in a 75-year-old Turkish male cadaver. At first the skin was removed, then the superficial cervical fascia along with the platysma muscle. Four clavicular heads (CH1, 2, 3, 4) and an accessory head of sternal part were observed on the left side along with one typical sternal head. The length, width and distance from the anterior border of the trapezius muscle, the acromioclavicularjoint and the sternoclavicular joint of each muscle were measured twice by two investigators using a digital caliper. Surgeons need to study thoroughly about the variations before any neck surgeries. For a successful muscle flap harvesting, central venous catheterization, cervical examination and many other procedures involving the neck region, we need to aware of all kind of variation of the sternocleidomastoid muscle.

Keywords: anatomy; dissection; neck surgery; sternocleidomastoid muscle

Anatomy 2023;17(1):45–48

Introduction

The sternocleidomastoid muscle (SCM) is a superficial neck muscle which descends diagonally along the edge of the neck. The lower part of the muscle generally separates into 2 heads at its point of attachment. Embryologically, the SCM shares a common origin with the trapezius muscle from the sixth branchial arc.[1] Between the 4th and 5th months of embryologic developmental period, the muscle attachments significantly increase.[2] In an adult, the sternal head begins from the anterior surface of the manubrium sterni and extends posterolaterally. The clavicular head originates above the middle 1/3 of the clavicle and extends vertically. The sternocleidomastoid muscle is attached by a strong tendon to the lateral aspect of the mastoid process and to the superior nuchal line by a thin aponeurosis. Clavicular fibers extend more to the mastoid process, while sternal fibers extend transversely and superficially to the occiput.[3]

The sternocleidomastoid muscle has usually 5 heads consisting of two layers. It is often divided into cleidomastoid and sternomastoid parts. In addition, it consists of a superficial layer; namely the superficial sternomastoid, sterno-occipital, cleido-occipital and a deep layer; the deep sternomastoid and cleidomastoid. A sixth part has been seen in addition to these five parts which has been described as sternomastoideus profundus.[4]

Case Report

During a routine dissection at Hacettepe University Department of Anatomy, a variation of the SCM was found unilaterally on the left side, in a 75-year-old Turkish male cadaver. At first, the skin was removed, then the superficial cervical fascia along with the platysma muscle. Four clavicular heads (CH1, 2, 3, 4) and an accessory head of sternal part (AH) was observed on the left side along with on typical sternal head (SH) (**Figures 1** and **2**). The length, width and distance from the anterior border of the trapezius muscle, the acromioclavicular joint and the sternoclavicular joint of each muscle part was measured twice by two investigators using a digital caliper. The average values were given as result.

The SH originated from the anterior and superior part of manubrium sterni. The AH originated from the superolateral part of manubrium sterni and sternoclavicular joint capsule. They both terminated at the mastoid process. The AH length was 171.77 mm and width was 1.83 mm. The SH had a length of 194.21 mm and width of 18.92 mm. The length of CH1 was 167.43 and width was 15.52 mm. CH muscle length was 162.41 mm and width was 15.52 mm. CH3 muscle had a length of 152.47 mm and width of 3.10 mm. The length of CH4 was 148.05 mm and width was 4.67 mm. The distance from the sternoclavicular joint to the CH, CH2, CH3, CH4 was 21.06, 23.74, 31.81, 44.42 mm respectively. The distance from the acromioclavicular joint to the SH, AH, CH1, CH2, CH3, CH4 was 152.31, 153.69, 129.46, 139.46, 130.49, 119.23 mm respectively. The distance from the anterior border of the trapezius muscle to the SH, AH, CH1, CH2, CH3, CH4 was 116.23, 110.58, 101.43, 91.62, 76.84, 65.70 mm respectively.

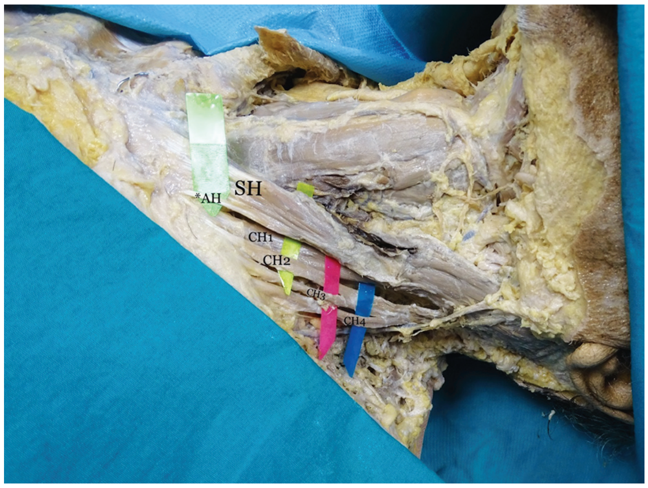

Figure 1. Left lateral view of the neck region showing variation of the sternocleidomastoid muscle with four clavicular heads, one sternal and one accessory head. **AH:** accessory head; **CH:** clavicular head, **SH:** sternal head.

Discussion

The sternocleidomastoid muscle typically originates from the manubrium sterni and medial aspect of the clavicle and attaches to the mastoid process of the temporal bone and superior nuchal line.[5]

Variations in the SCM muscle are diverse. Nayak et al.[6] reported a case with an additional sternal head arising from the capsule of the sternoclavicular joint and the superolateral border of the manubrium sterni in both sides of a cadaver. The width of this additional sternal head was 1.2 cm on the left and 0.7 cm on the right side. The clavicular part was joining the muscle at a distance of 5.2 cm on the left and 6 cm on the right from its origin.

Kim et al.[7] reported bilateral four-bellied sternocleidomastoid muscles in a 67-year-old Korean male cadaver. On the right side; there were 2 sternomastoids, 1 cleidomastoid, 1 cleido-occipital and on the left, 1 sternomastoid, 1 cleido-occipital, 2 cleidomastoids.

Another case of a 60 year-old male cadaver reported by Surendran et al.[8] the clavicular head of the right sternocleidomastoid muscle was revealed to had 4 bellies. The most medial belly of the clavicular head had 3 tendons, the 2nd belly had 3 tendons, the 3rd belly had 4 tendons, and the 4th belly had 2 tendons.

Heo et al.[9] revealed a multiheaded sternocleidomastoid muscle on the left side of a 85-year-old Korean male cadaver. The authors noted three heads and an accessory belly on the sternal head. One of these three parts has

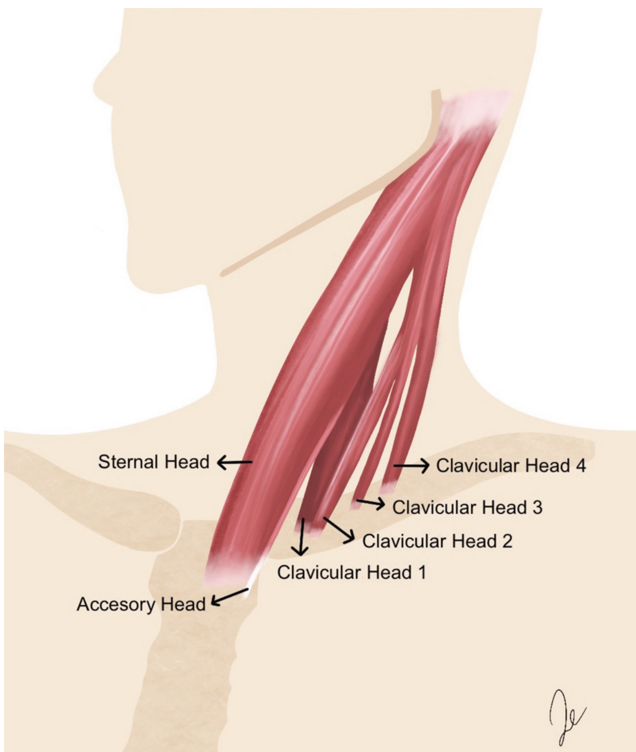

Figure 2. Illustration of the left lateral view of the neck region showing variation of the sternocleidomastoid muscle with four clavicular heads, one sternal and one accessory head.

been reported as the sternal head, the others as the medial clavicular and lateral clavicular head. The width of th sternal head was 12.8 mm and the length was 189.4 mm. The accessory head was located lateral to the sternal head and was 77.6 mm in length and 3.7 mm in width. The length of the lateral clavicular head was 137.8 mm and the medial clavicular head length was 143.6 mm. Its insertion has been reported to be corresponding to the normal anatomy (mastoid process and superior nuchal line). Being aware of variations in the SCM is important for surgeons to plan ahead in case they suddenly encounter any anatomical variations during invasive neck procedures such as central venous catheterization (CVC).[9] For example, Dupont et al.[10] reported an 81-year-old fresh-frozen male cadaver with 2 separate headed SCM connected bilaterally to the occiput and mastoid and showed 6 tendon insertions on the occiput. As seen in the case report of Dupont et al.[10] the variability of the attachment points of the SCM should be well known before planning interventions to the neck.

The SCM has proven to be important in many areas of medical education and clinical pathologies, so its variations need to be known and studied. Examination of the sternocleidomastoid muscle forms part of the examination of the cranial nerves. It can be felt on both sides of the neck when a person moves their head to the opposite side.[11]

The triangle formed by the sternal and clavicular heads of the clavicle and sternocleidomastoid muscle is used as a landmark to determine the correct location for CVC. Correct CVC placement prevents serious complications, especially intracardiac implamentation, which can be fatal. As seen in a study by Chen et al.[12] both the length of the SCM muscle and the body height are statistically significant for predicting the depth of CVC placement. In their study on the standardization of botulinum toxin injection into the SCM, Torun et al.[13] emphasized the significance of considering the lower part of the muscle, particularly for toxin administration in cases of torticollis. They highlighted that this region, which is thinner and in close proximity to the structures beneath the jugular vein, should be avoided. Similarly, in our study, we have identified variations in the lower part of the SCM, underscoring the importance of taking these variations into account in clinical practice.

Conclusion

The SCM is a large, superficial muscle located in the anterior part of the neck. Due to its anatomical movements and structure, it plays an important role in many areas of medicine. Surgeons need to make a thorough study of the variations of this muscle before any neck surgery. The SCM muscle also acts as a landmark and a useful flap during head and neck dissections.[14] For a successful muscle flap harvest, central venous catheterization, cervical examination and many other procedures involving the neck region, we need to be aware of all possible variations of the SCM.

Acknowledgements

The authors would like to thank the donors to the Anatomical Gift Program at Hacattepe University Faculty of Medicine so that anatomical research can be conducted.

Conflict of Interest

The authors have no conflicts of interest to disclose.

Author Contributions

ZÇ: cadaver dissection, manuscript writing, data collection, drawing the illustration; SK: cadaver dissection, manuscript writing, data collection; MÜ: cadaver dissection, manuscript editing, approval of the fina version; BEG: manuscript editing, data management, approval of the final version.

Ethics Approval

This study has been prepared in accordance with the Helsinki Declaration. There were no ethical violations in the creation of this work.

Funding

The authors received no financial support for this study.

References

1. Cherian SB, Satheesha N. A rare case of unilateral third head of sternocleidomastoid muscle. Int J Morphol 2008; 26:99–101.
2. Marecki B, Lewandowski J, Jakubowicz M. Anthropomorphology of sternocleidomastoid muscle. Gegenbaurs Morphol Jahrb 1989;135: 491–503.
3. Standring S. Gray's anatomy: the anatomical basis of clinical practice. 41st ed. London: Elsevier; 2016. p. 448–9.
4. Bergman R, Afifi A, Miyauchi R. Illustrated encyclopedia of human anatomic variation: Opus I: Muscular System: Alphabetical listing of muscles: [Internet]. [Retrieved on January 13, 2023]. Available from: https://www.anatomyatlases.org/AnatomicVariants/MuscularSystem/Text/S/28Sternocleidomastoideus.shtml.
5. Kohan EJ, Wirth GA. Anatomy of the neck. Clin Plast Surg 2014;41: 1–6.
6. Nayak SR, Krishnamurthy A, Kumar Sj M, Pai MM, Prabhu LV, Jetti R. A rare case of bilateral sternocleidomastoid muscle variation. Morphologie 2006;90:203–4.
7. Kim SY, Jang HB, Kim J, Yoon SP. Bilateral four heads of the sternocleidomastoid muscle. Surg Radiol Anat 2015;37:871–3.

8. Surendran S, Nayak SB, Reghunathan D, Nelluri VM. Sternocleiodomastoid muscle with five fleshy bellies and thirteen heads of origin. Online Journal of Health and Allied Sciences 2016;3:11.
9. Heo YR, Kim JW, Lee J-H. Variation of the sternocleidomastoid muscle: a case report of three heads and an accessory head. Surg Radiol Anat 2020;42:711–3.
10. Dupont G, Iwanaga J, Altafulla JJ, Lachkar S, Oskouian RJ, Tubbs RS. Bilateral sternocleidomastoid variant with six distinct insertions along the superior nuchal line. Anat Cell Biol 2018;51:305–8.
11. Fehrenbach MJ, Herring SW. Illustrated anatomy of the head and neck. Philadelphia (PA): Elsevier; 2012. p. 87.
12. Chen CK, Tan PP, Lee HC. Sternocleoidomastoid muscle length predicts depth of central venous catheter insertion. Acta Anaesthesiol Taiwan 2007;45:211–5.
13. Torun Bİ, Kendir S, Aysun U. Standardization of sternocleidomastoid for botulinum toxin applications. Anatomy 2017;11:128–32.
14. Rao TR, Vishnumaya G, Prakashchandra S, Suresh R, Ramesh R, Vishnumaya G. Variation in the origin of sternocleidomastoid muscle. Int J Morphol 2007;25:621–3.

ORCID ID:
Z. Çelik 0000-0001-6386-2204;
S. Khan 0000-0001-9519-4191;
M. Ülkir 0000-0001-5615-8913;
B. Erçakmak Güneş 0000-0001-6936-0766

deomed

Correspondence to: Zehra Çelik, MD
Department of Anatomy, Faculty of Medicine,
Hacettepe University, Ankara, Türkiye
Phone: +90 312 305 21 01
e-mail: drcelikzehra@gmail.com

Conflict of interest statement: No conflicts declared.

 How to cite this article: Çelik Z, Khan S, Ülkir M, Erçakmak Güneş B. A rare variation of the sternocleidomastoid muscle in a Turkish male cadaver: a case report of four clavicular heads on sternal head and an accessory head. Anatomy 2023;17(1):45–48.

Table of Contents

Volume **17** / Issue **1** / April **2023** *(Continued from back cover)*

Case Reports

On the Front Cover:

Azygos vein variant and azygos lobe of the right lung. (**a–b**) The arch of the azygos vein passes through the superior lobe of the right lung dividing it into two segments. (**c**) The right lung has a superior, middle, and inferior lobe divided by the horizontal and oblique fissures, respectively. (**d**) The superior lobe of the right lung is divided by the azygos vein in the azygos fissure causing the superior lobe of the right lung to have a medial azygos lobe of the right lung. (**e**) A separate secondary bronchus traveling to the azygos lobe was not observed. **AAz:** arch of the azygos vein; **ArAo:** arch of the aorta; **Az:** azygos vein; **AzF:** azygos fissure; **AzL:** azygos lobe of the right lung; **B1:** apical bronchus of superior lobe; **B2:** posterior bronchus of superior lobe; **B3:** anterior bronchus of superior lobe; **B4:** lateral bronchus of middle lobe; **B5:** medial bronchus of middle lobe; **B6:** superior bronchus of inferior lobe; **B7:** medial basal bronchus; **B8:** anterior basal bronchus; **B9:** lateral basal bronchus; **B10:** posterior basal bronchus; **Eso:** esophagus; **HoriF:** horizontal fissure; **I:** inferior; **InfL:** inferior lobe of the right lung; **L:** lateral; **M:** medial; **MidL:** middle lobe of the right lung; **ObF:** oblique fissure; **PcV:** pericardiophrenic vessels; **RL:** right lung; **S:** superior; **SupL:** superior lobe of the right lung. From Srinivasan A, Hollingsworth RL, Lowry N, Fahl J, Smith MP, Khan AS. A rare cadaveric report of the azygos lobe of the right lung. *Anatomy* 2023;17(1):41–44.

http://dergipark.org.tr/en/pub/anatomy

anatomy

An International Journal of Experimental and Clinical Anatomy

Table of Contents

Volume **17** / Issue **1** / April **2023**

Original Articles

(Contents continued on inside back cover)

deomed®